

**OSTEOPONTIN-MEDIATED NEUTROPHILIC INFILTRATION AND
HIGHER LIVER INJURY IN A FEMALE RODENT ALCOHOLIC
STEATOHEPATITIS MODEL**

A Dissertation

by

ATRAYEE BANERJEE

Submitted to the Office of Graduate Studies of
Texas A&M University
in partial fulfillment of the requirements for the degree of

DOCTOR OF PHILOSOPHY

May 2008

Major Subject: Toxicology

**OSTEOPONTIN-MEDIATED NEUTROPHILIC INFILTRATION AND
HIGHER LIVER INJURY IN A FEMALE RODENT ALCOHOLIC
STEATOHEPATITIS MODEL**

A Dissertation

by

ATRAYEE BANERJEE

Submitted to the Office of Graduate Studies of
Texas A&M University
in partial fulfillment of the requirements for the degree of

DOCTOR OF PHILOSOPHY

Approved by:

Chair of Committee,
Committee Members,

Chair of Toxicology Faculty,

Shashi K. Ramaiah
Timothy Phillips
Gregory A. Johnson
Weston W. Porter
Robert C. Burghardt

May 2008

Major Subject: Toxicology

ABSTRACT

Osteopontin-mediated Neutrophilic Infiltration and Higher Liver Injury in a Female
Rodent Alcoholic Steatohepatitis Model.

(May 2008)

Atrayee Banerjee, B.S, University of Calcutta;

M.S., University of Calcutta

Chair of Advisory Committee: Dr. Shashi K. Ramaiah

Females are known to be more susceptible to alcoholic liver disease (ALD), but the precise mechanism behind this increased susceptibility is not well understood. The objective of this study was to identify the molecular mechanism behind the increased susceptibility of females to alcoholic steatohepatitis (ASH). Female rats in ASH model were found to have significantly higher neutrophilic infiltration in the liver as compared to the males. Osteopontin (OPN), a member of the SIBLING family of proteins was also found to be induced in females. Neutralizing OPN antibody experiments provided further evidence that OPN acts as a chemokine in attracting neutrophils into the liver making females more susceptible to ASH.

Since neutrophil transmigration in the liver is mediated by integrins, the mechanism for OPN-mediated neutrophil infiltration was tested. Females in ASH had significantly higher expression of $\alpha_4\beta_1$ and $\alpha_9\beta_1$ integrins, and animals treated with neutralizing OPN antibody had significantly lower expression of these integrins, wherein

hepatic neutrophilic infiltration was also decreased by 50% compared to the untreated group. Immunoprecipitation experiments suggested the binding of OPN to $\alpha_4\beta_1$ and $\alpha_9\beta_1$ integrins. OPN-mediated neutrophilic infiltration was further confirmed using Boyden chamber assays. Antibodies directed against α_4 , β_1 integrins and SLAYGLR sequence was also found to significantly inhibit neutrophilic migration in vitro, suggesting that higher hepatic neutrophil chemokinesis in the female ASH appears to be mediated through both $\alpha_4\beta_1$ and $\alpha_9\beta_1$ integrin signaling.

In addition, higher liver injury and higher expression of OPN in females were also found to be regulated by estrogen in a biphasic pattern; ovariectomy resulted in significantly increased liver injury compared to intact rats. Depending on dose, estradiol supplementation in the ovariectomized rats fed ethanol resulted in both a protective and damaging effect on liver.

Besides OPN, several other oxidative stress related proteins like Ferritin H Chain, ER60, HSP60, Peroxiredoxin 6 were identified by proteomics approach. Females in ASH were found to have differentially regulated levels of these proteins as compared to their male counterparts, highlighting the potential novel mechanisms associated with higher liver injury noted in our female rat ASH model.

ACKNOWLEDGEMENTS

I would like to thank my research advisor, Dr. Shashi K. Ramaiah, for his guidance, support and advice during the course of this work. I also thank my committee members: Dr. Timothy Phillips, Dr. Gregory A. Johnson and Dr. Weston W. Porter for all their advice and help. Sincere thanks are also due to Dr. Stephen Safe, Dr. Robert Burghardt and Dr. Arul Jayaraman for all their time, help and advice.

I also like to thank Dr. Robert Rose for helping me with my animal studies, without which I would not have managed to get everything done. Special thanks are also due to Kim Daniel for her administrative support. In addition, I would also like to thank Society of Toxicology for providing me with the Novartis Fellowship and Texas Research Society of Alcoholism for the Mc Govern Fellowship, which provided a part of the financial support of this work.

Finally, my heartfelt appreciation goes to my parents and sister for giving me the love and encouragement over the years; and motivating me in getting a doctoral degree. Special thanks, love and appreciation are also due to my husband, Arindam, for his love, patience, encouragement, support and being a part of this roller coaster life of a graduate student. I am also thankful to my parents-in-law for being supportive over the years. Lastly, I would like to thank my brother-in-law and all other family members for their help and advice in time of need.

NOMENCLATURE

α	Alpha
β	Beta
2-D	2 dimensional
ADH	Alcohol dehydrogenase
ALD	Alcoholic liver disease
ALDH	Acetaldehyde dehydrogenase
ALT	Alanine aminotranferase
AP-1	Activated protein 1
AS	Alcoholic steatosis
ASH	Alcoholic steatohepatitis
AST	Aspartate aminotransferase
C+L	Control+LPS
CCl ₄	Carbon tetrachloride
CINC-1	Cytokine induced neutrophils chemoattractant 1
cOPN	Cleaved osteopontin
Ctrl.	Control
CXC	Chemokines
CYP2E1	Cytochrome P450 2E1
E+L	Ethanol+LPS
E2	Estradiol

ER	Estrogen receptor
EtOH	Ethanol
FFA	Free fatty acid
FLIP	Fas associated death domain like interleukin beta converting enzyme
GAPDH	Glyceraldehyde 3-phosphate dehydrogenase
H&E	Hematoxylin and Eosin
Hrs	Hours
ICAM-1	Intercellular adhesion molecule 1
IL-6	Interleukin 6
IL-8	Interleukin 8
IL-R6 α	Interlukin 6 receptor alpha
LBP	Lipopolysaccharide binding protein
LPS	Lipopolysaccharide
Mg/dl	milligram/deciliter
MIP-2	Macrophage inflammatory protein 2
NAD	Nicotinamide adenine dinucleotide
NADH	Reduced Nicotinamide adenine dinucleotide phosphate
NAFLD	Non alcoholic fatty liver disease
NF- κ B	Nuclear factor kappa B
nOPN	Neutralizing osteopontin
OPN	Osteopontin
OPN-KO	Osteopontin knock out

OVX	Ovariectomized
PAF	Platelet activating factor
PMN	Polymorphonuclear leukocyte
<i>p</i> NP	<i>para</i> nitrophenol hydroxylase
PPAR α	Perxisome proliferator activated receptor alpha
PrX6	Peroxiredoxin6
RGD	Arginine Glycine Aspartate
RNS	Reactive nitrogen species
ROS	Reactive oxygen species
SFRE	Steroidogenic factor responsive element
SREBP-1	Steroid response element binding protein 1
TEN	Total enteral nutrition
TLR4	Toll like receptor 4
TNF α	Tumor necrosis factor alpha
USF	Upstream stimulatory factor
VCAM-1	Vascular cell adhesion molecule 1
VDR	Vitamin D receptor
VDRE	Vitamin D responsive element

TABLE OF CONTENTS

	Page
ABSTRACT	iii
ACKNOWLEDGEMENTS	v
NOMENCLATURE	vi
TABLE OF CONTENTS	ix
LIST OF FIGURES	xii
LIST OF TABLES	xvi
 CHAPTER	
I INTRODUCTION	1
Mechanisms of higher female susceptibility to ALD.....	2
Alcoholic liver disease - pathological stages	6
Metabolism of alcohol.....	10
Animal models to study ALD	12
Mechanisms of hepatic neutrophil transmigration	15
Osteopontin - structure and function.....	20
Contribution of OPN to hepatic inflammation and toxicity.....	24
Mechanisms for OPN transcriptional gene activation.....	27
Objective of the study	30
 II MATERIALS AND METHODS	 31
Chemicals	31
Animals and treatment	31
Assessment of estrous cycle.....	34
Sample collection and processing	34
Evaluation of the liver injury	35
Assessment of steatohepatitis.....	35

CHAPTER	Page
Estimation of plasma levels of endotoxin, GRO/CINC-1, and IL-6 by ELISA.....	36
Western blot analysis	39
Immunohistochemical analysis of OPN in the liver.....	42
Immunohistochemical analysis of Ferritin Heavy chain (Ferritin H) in the liver.....	43
Assessment of mRNA from liver samples	43
In-situ hybridization analysis	46
Analysis of neutrophil activation by OPN in vitro using FACS Calibur flow cytometer.....	48
OPN-mediated neutrophil chemotactic response in an experimental rat peritoneal model.....	49
Neutralizing OPN antibody experiment.....	50
Immunoprecipitation	51
Expression and purification of recombinant native and mutated N-terminal osteopontin fragments.....	51
Neutrophil isolation from blood.....	52
Boyden chamber assay	52
2-D gel electrophoresis.....	53
Statistics	58
III RESULTS.....	59
Rat alcoholic steatohepatitis model.....	59
Role of osteopontin in neutrophil mediated integrin signaling.....	78
Influence of estrogen on osteopontin and hepatic neutrophil infiltration in females	86
Proteomics approach to study differential protein expression between male and females in alcoholic steatohepatitis.....	94
Development of the mouse alcoholic steatohepatitis model	102
IV DISCUSSION, SUMMARY AND CONCLUSIONS.....	109
Females are susceptible to ALD.....	109
Osteopontin as a mediator of hepatic neutrophil infiltration.....	111
Involvement of β_1 and β_2 integrins in OPN-mediated neutrophil chemotaxis.....	113

	Page
Potential therapeutic strategies to inhibit OPN in alcoholic liver disease	117
Application of proteomics to detect unique proteins in female susceptibility to ALD	119
REFERENCES	125
VITA	159

LIST OF FIGURES

FIGURE	Page
1 Relative risk of alcohol consumption & incidence of cirrhosis of the liver in men and women	2
2 Schematic representation of endotoxin mediated alcoholic liver injury.....	5
3 Schematic representation of the progression of ALD	9
4 Oxidative pathways of alcohol metabolism	11
5 Representative scheme showing the by-products of EtOH metabolism... ..	11
6 Simplified schematic representation of the mechanism of neutrophil transmigration in the liver	16
7 Schematic representation of the structure of osteopontin (OPN) protein	22
8 ALT (A) and AST (B) activities in plasma of male and female rats fed either control or EtOH-containing Lieber DeCarli diet followed by a single dose of LPS injection	61
9 Representative photomicrographs of H&E sections of male and female rats fed either control or an EtOH-containing Lieber De-Carli liquid diet for 6 weeks	62
10 Neutrophil infiltration in the liver in alcoholic stetaohepatitis.....	64
11 Endotoxin level in plasma of male and female rats fed either control or EtOH-containing Lieber DeCarli diet followed by a single dose of LPS injection.....	65
12 GRO/CINC-1 (A) and IL-6 (B) levels in plasma of male and female rats fed either control or EtOH-containing Lieber DeCarli diet followed by a single dose of LPS injection	66
13 Hepatic microsomal CYP2E1 protein and activity in rats fed either control or EtOH-containing Lieber DeCarli diet for a period of six weeks	67

FIGURE	Page
14 Osteopontin protein expression in alcoholic steatosis.....	68
15 Osteopontin protein expression in alcoholic steatohepatitis	69
16 Representative photomicrograph of liver sections stained for OPN in male and female rats fed EtOH-containing Lieber DeCarli diet for a period of six weeks	70
17 Real time PCR analysis of OPN mRNA in liver of rats fed either control or EtOH-containing Lieber DeCarli diet for a period of six weeks, followed by a single injection of LPS	71
18 In-situ hybridization analysis of OPN mRNA in the liver of male and female rats.	73
19 Peritonitis experiment in a rat model.	75
20 Enumeration of hepatic neutrophils following nOPN administration in the LPS hepatitis model	76
21 Flow cytometric analysis of CD11b expression.....	77
22 Representative Western blots showing α_4 , α_9 and β_1 integrin protein expression in rats fed either control or EtOH-containing Lieber-DeCarli liquid diet for six weeks followed by a single dose of LPS.	79
23 Real time PCR analysis of α_4 (A), α_9 (B), β_1 (C) mRNA in the liver of rats fed either control or EtOH containing Lieber-DeCarli diet for a period of six weeks, followed by a single dose of LPS	80
24 Immunoprecipitation assay to detect the binding of OPN to $\alpha_4\beta_1$ and $\alpha_9\beta_1$ integrin in EtOH+LPS treated male and female rat	81
25 Representative Western blotting showing α_4 , α_9 and β_1 integrin protein expression in rats injected with either LPS or nOPN+LPS.....	82
26 Boyden chamber experiment to test migration of neutrophils toward OPN and c-OPN.	84

FIGURE	Page
27 Boyden chamber experiment to assess the role of α_4 , β_1 and SLAYGLR sequence in migration of neutrophils towards OPN.....	85
28 Schematic representation of the different stages of the estrous cycle of the representative rat before (A) and after (B) ethanol treatment.	86
29 Liver injury in normal and ovariectomized rats	87
30 Effect of estrogen on liver injury	89
31 OPN protein expression in ovariectomized rats	91
32 Representative photomicrograph of liver sections stained for OPN in ovariectomized female rats fed EtOH-containing Lieber-DeCarli diet.....	92
33 In-situ hybridization analysis of OPN mRNA in the liver of female ovariectomized rats fed EtOH-Containing Lieber DeCarli diet followed by a single dose of LPS injection.	93
34 2-D gel analysis of osteopontin protein from liver of female rats.....	94
35 Representative cropped 2D gel image of liver protein in male (A) and female (B) rat in alcoholic steatohepatitis group.	95
36 2D master gel indicating proteins identified as potential inflammatory markers in alcoholic steatohepatitis	99
37 Representative Western blot showing Ferritin H chain, HSP60, ER60 and PrX6 protein expression in male and female rats fed either control or EtOH-containing Lieber DeCarli diet followed by a single dose of LPS injection.	100
38 Representative photomicrographs of Ferritin stained sections of male and female rats fed either control or EtOH-containing Lieber-DeCarli diet for 6 weeks.	100
39 Liver injury in mice alcoholic steatohepatitis model	103

FIGURE	Page
40 Quantitation of (A) steatosis and (B) neutrophils as an index of inflammation in the livers of mice fed either control or EtOH-containing Lieber-DeCarli diet for 6 weeks.	105
41 Osteopontin protein expression in mice alcoholic steatohepatitis model	106
42 Representative photomicrograph of liver sections stained for OPN in male and female mice fed alcoholic steatohepatitis model.	107
43 Representative Western blotting showing OPN isolated from neutrophils in mice fed EtOH-containing Lieber-DeCarli diet for 6 weeks.	107
44 Osteopontin mRNA expression in mice alcoholic steatohepatitis model	108
45 Scheme to explain the mechanism of involvement of OPN in higher liver injury in females in alcoholic liver disease.....	116
46 Potential therapeutic strategies to target OPN and inhibit its inflammatory activities in alcoholic liver disease.	118

LIST OF TABLES

TABLE	Page
1	Different models used to study alcoholic liver disease, their advantages, disadvantages and references.....13
2	Members of proinflammatory cytokines, chemokines, adhesion molecules and other potential candidates implicated in the pathogenesis of neutrophilic alcoholic steatohepatitis.....18
3	Energy distribution of Lieber De Carli diet (Control and EtOH).....32
4	Ingredients for making Lieber DeCarli liquid diets (control and ethanol).....33
5	List of primary and secondary antibodies employed for Western blot.....41
6	The volume and concentrations of individual components used for 1 step real time PCR.....45
7	List of primers used for RT-PCR.....45
8	Treatment and doses employed in an in vivo rat peritonitis model.....50
9	Table showing number of samples and replicate groups used for running 2-D gel electrophoresis in male and females alcoholic steatosis and steatohepatitis model.....54
10	Comparison of the body weight of control and EtOH – fed male and female rats.....59
11	Steatosis and neutrophilic inflammation in male and female rats in the alcoholic steatohepatitis model.....63
12	Differentially altered proteins between males and females in a rat alcoholic steatohepatitis model.....97

CHAPTER I

INTRODUCTION*

Alcoholic liver disease (ALD) is a major public health problem in the United States, accounting for more than 150,000 deaths and costing about \$116 billion per year (Tsukomoto, 2007). According to the World Health Report (2002), of the ten leading risk factors that serve as major burden of disease in developed countries, alcohol is ranked as the third most important risk factor, whereas it is the top most risk factor in the developing countries. In recent years, a three-fold increase in ALD has been reported worldwide (Mandayam et al., 2004). Epidemiological evidence points to the greater susceptibility of females to ALD than males (Nanji et al., 2001; 2002; Gallucci et al., 2004). At any given level of alcohol consumption, women have a higher likelihood of developing cirrhosis than males (Fig 1). Studies have shown that females consuming lower concentration of alcohol than males produce similar pathological symptoms as males (Ashley et al., 1977; Loft et al., 1987; Schenker 1997). However, the precise mechanism behind the higher susceptibility of females to ALD is not well understood.

This dissertation follows the style of Toxicology and Applied Pharmacology.

* Reprinted with permission from “Higher neutrophil infiltration mediated by osteopontin as a likely contributing factor to the increased susceptibility of females to alcoholic liver disease” by Banerjee et al., 2006, *Journal of Pathology*, 208: 473-485, © 2006 by Wiley Interscience.

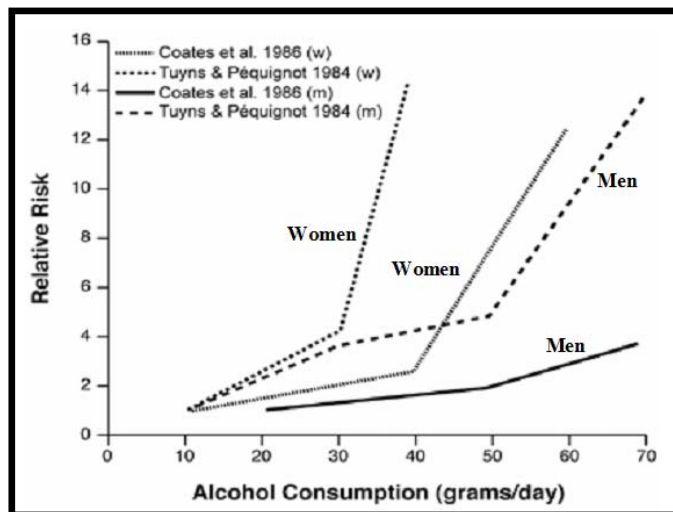


Fig. 1. Relative risk of alcohol consumption & incidence of cirrhosis of the liver in men and women. (Adapted from Mann et al., Am J Drug Alcohol Abuse, 2001).

Mechanisms of higher female susceptibility to ALD

Several theories that have been proposed to explain the higher susceptibility of females to ALD include differences in ethanol (EtOH) pharmacokinetics (Julkunen et al., 1985; Frezza et al., 1990; Chrostek et al., 2003), endotoxin (Kono et al., 2000, Yin et al., 2000) and cytokines (Colantoni et al., 2003; Gallucci et al., 2004).

Role of EtOH pharmacokinetics and metabolism

When consuming an equal amount of alcohol intake, women are reported to have higher blood alcohol level than males (Jones and Jones 1976). Higher bioavailability of alcohol in females (Baraona et al., 2001) have also been associated with the differences in alcohol metabolism between gender. In general, alcohol metabolism takes place in the liver, where EtOH is oxidized to acetaldehyde by the enzyme alcohol dehydrogenase (ADH). The acetaldehyde formed is further oxidized to acetate by acetaldehyde dehydrogenase (ALDH). ADH is believed to be the rate-limiting enzyme in the

metabolism of EtOH. Studies have shown that females have lower levels of the enzyme alcohol dehydrogenase (ADH) as compared to their male counterparts (Frezza et al., 1990; Seitz et al., 1993; Pozzato et al., 1995). In the liver, ADH consists of five different classes (Edenberg et al., 1994) of which, ADH I and II are known to play an important role in EtOH metabolism (Chrostek et al., 2003). It was found that ADH is dimorphically expressed with higher activity in males as compared to females (Frezza et al., 1990; Seitz et al., 1993; Pozzato et al., 1995). Lower ADH in females results in higher bioavailability of EtOH and higher alcohol concentration in the blood. Alcohol levels are also influenced by the elimination rate of EtOH in the liver. Females have a higher elimination rate as compared to males. Higher elimination rate results in higher concentration of toxic products like acetaldehyde in the liver leading to higher injury (Kwo et al., 1998). In addition to this, gender difference has also been reported to be due to impaired hepatic lipid-metabolism resulting in accumulation of potentially toxic fatty acids (Shevchuk et al., 1991). Alcohol feeding has been reported to inhibit the mitochondrial β oxidation of fatty acid and increase their microsomal esterification and ω oxidation (Ma et al., 1993). Dicarboxylic acid a product of ω oxidation is known to regulate the hepatic disposition of nonesterified fatty acids. Chronic alcohol administration has been found to increase ω oxidation more effectively in males than in female rats (Ma et al., 1993), resulting in higher accumulation of deleterious monocarboxylic fatty acids in females as compared to males. Further studies by Ma et al., (1999) have reported similar gender differences in humans, where females have

lower excretion of dicarboxylic acid than males indicating higher accumulation of fatty acids or steatosis in females (Iimuro et al., 1997).

Role of endotoxin and cytokines

In living organisms, the gut wall provides a protective barrier against the release of large amounts of gram-negative bacteria and endotoxin into the systemic circulation. However, in alcoholics, ethanol exposure damages the intestinal villi, allowing the endotoxin to escape into the blood, where it is removed by both circulating and fixed mononuclear phagocytes or Kupffer cells (Fig 2). Kupffer cells have been implicated in higher liver injury in ALD, and studies have shown that depletion or inactivation of Kupffer cells diminished hepatic steatosis, inflammation and necrosis in alcoholic steatohepatitis (ASH) (Adachi et al., 1994; Iimuro et al., 1996). Kupffer cells have also been shown to produce cytokines like TNF- α causing more liver injury in ALD (Iimuro et al, 1997). Studies by Iimuro et al., (1997) and Nanji et al., (2001) have shown that female rats fed EtOH have higher level of endotoxin in plasma than their male counterparts. Because estrogen receptors exist in the intestinal epithelium, estrogen has also been reported to affect the permeability of the gut leading to higher endotoxin levels in females (Kono et al., 2000, Yin et al., 2000). From the gut, the blood empties directly into the portal vein, where Kupffer cells are primarily responsible for endotoxin clearance (Wisse, 1977). In addition to Kupffer cells, endotoxin clearance can also take place by other receptors like CD14 (Gegner et al., 1995). CD14 is a glycoprotein receptor involved in macrophage activation (Schumann et al., 1990). This receptor mediates uptake of endotoxin by cells that do not express membrane bound CD 14

(Pugin et al., 1993), like Toll-like receptor 4 (TLR4) on the macrophage and Lipopolysaccharide-binding protein (LBP) in the serum (Thurman et al., 1998). Studies by Kono et al., (2000) have shown that alcohol treated females have higher levels of CD14 and LBP as compared to the males. The increase in expression of lipopolysaccharide receptor CD14 on Kupffer cells leads to production of reactive oxygen species (ROS) in liver, leading to NF- κ B activation. This causes increased proinflammatory cytokine production leading to higher liver injury in females (Fig 2).

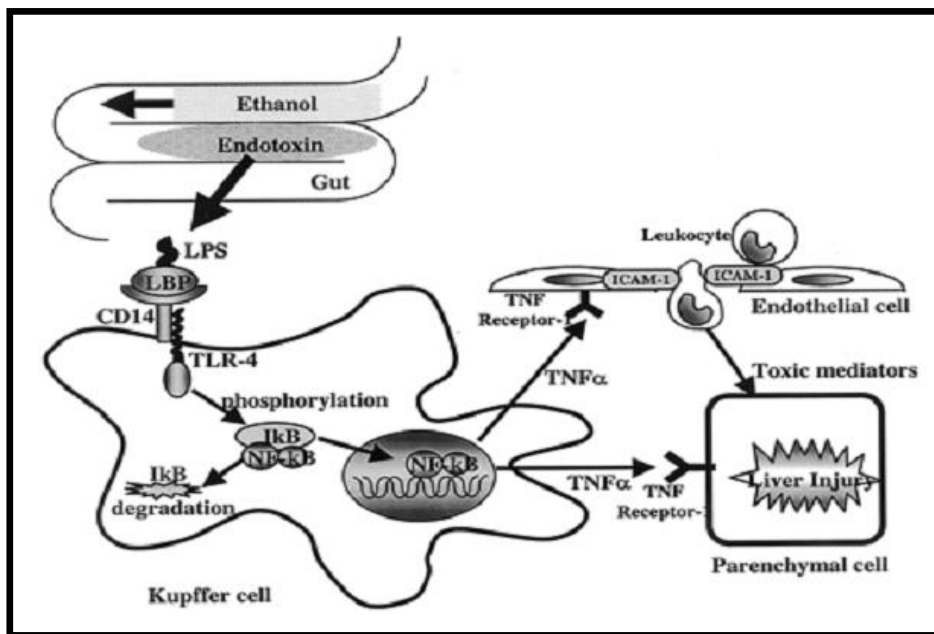


Fig. 2. Schematic representation of endotoxin mediated alcoholic liver injury. Alcohol consumption increases the gut permeability resulting in increase in blood endotoxin levels. This leads to higher levels of lipopolysaccharide receptor on Kupffer cells. The LPS or endotoxin binds to the LPS binding protein and the CD14 receptor on the Kupffer cells. In the activated Kupffer cells NF- κ B activation takes place leading to increased production of proinflammatory cytokines, which leads to higher inflammation and liver injury (Adapted from Kono et al., 2000).

Lower levels of cytokine IL-6 has also been reported to play a role in higher susceptibility of females to ALD. Ethanol-fed males are reported to have higher levels of IL-6 as compared to the females, which protect the liver from EtOH induced apoptosis (Colantoni et al., 2003). IL-6 has been reported to function as an antiapoptotic factor in the liver by helping maintain an adequate level of FLIP (FLICE [Fas-associated death-domain-like IL- β converting enzyme] inhibitory protein) and downstream antiapoptotic factors (Kovalovich et al., 2001). Lower expression of IL-6 in females is also reported to cause lower hepatocyte regeneration and higher liver injury. Further studies by Gallucci et al., (2004), have reported that significantly higher circulating levels of IL-6R α leads to increased severity of inflammation and damage observed in female EtOH-consuming rats. In addition to the role of cytokines and chemokines, higher lipid peroxidation leading to the production of higher reactive oxygen species (ROS) has also been known to play a role in higher liver injury in females (Nanji et al., 2002).

Alcoholic liver disease - pathological stages

To investigate the mechanistic and molecular basis for alcohol-mediated liver damage, different pathological stages have been investigated. EtOH consumption in humans is characterized by four distinct pathological stages ranging from fatty liver or steatosis, to steatohepatitis, fibrosis and cirrhosis (Lieber and DeCarli, 1982; MacSween and Burt, 1986; Diehl, 2002; Maher, 2002, Nanji, 2002; Ramaiah et al., 2004). Steatosis and steatohepatitis represents the early phase of ALD. In the rodent models of ALD, pathological alterations such as steatosis, oncotic necrosis, hepatocellular neutrophilic infiltration has been observed similar to that seen in early phase of human ALD

(MacSween and Burt, 1986; Diehl, 2002); however, several other histopathological changes noted in human alcoholics as Mallory bodies are rarely seen in these experimental animal models.

Alcoholic steatosis (AS)

Alcoholic steatosis, the initial stage of ALD is characterized by extensive fat accumulation in the liver along with mild to moderate liver injury (Galambos, 1972; Macsween and Burt, 1986; Maher, 2002). It is a common occurrence in alcoholics, with reported incidences ranging from 10% to 90%. Metabolic disturbances such as decreased fatty acid oxidation, increased triglyceride synthesis, reduced fat export and mobilization of extra hepatic fat stores are thought to be few of the reasons for accumulation of fat in the liver (Lieber, 1993; Maher 2002; Zhao et al., 2002). Fatty acid oxidation and synthesis are controlled by two major regulatory molecules, the peroxisome proliferators-activated receptor α (PPAR α) and the steroid response element-binding protein-1 (SREBP-1) respectively. PPAR α is reported to control transcription of many genes involved in free fatty acid (FFA) transport and oxidation. PPAR α knock out animals develop fatty liver (Costet et al., 1998), when fed high fat diet, and are particularly sensitive to the development of steatohepatitis when fed on a methionine-choline deficient diet (Ip et al., 2003). In addition to PPAR α , SREBP-1 is also known to play a role in the development of alcoholic fatty liver. Studies on transgenic mice over-expressing the mature form of SREBPs (Shimano et al., 1996) suggest that SREBP-1 regulates genes involved in hepatic triglyceride synthesis. Livers from mice over-expressing SREBP-1a or 1c have massive accumulation of cholesteryl esters and

triglycerides. In alcoholics, the effect of EtOH on lipid metabolism has been reported to result from inhibition of PPAR α and stimulation of SREBP-1, resulting in remodeling of the liver towards a fat storing, rather than fat oxidizing organ (Crabb et al., 2004).

The infiltration of fat in the liver has been reported to be both macrovesicular (one large fat droplet per hepatocyte and lateral displacement of the nucleus) and microvesicular (several small droplets per hepatocyte). Although steatosis was largely considered benign, recent investigations have revealed that AS leaves the hepatocytes highly sensitive to injury (Teli et al., 1995; Galli et al., 2001; Bathgate and Simpson, 2002; Baykov et al., 2003; Fisher et al., 2003;), suggesting that the more fat in the liver, the higher susceptibility to severe damage (Day and James, 1998). Some of the mechanisms behind such increased susceptibility to steatotic liver has been reported to be cellular changes due to metamorphosis (Teli et al., 1995; Bathgate and Simpson, 2002), increased oxidative stress (Yang et al., 1997; Colell et al., 1998; Baykov et al., 2003), decreased regenerative ability (Apte et al., 2004), and decreased expression of peroxisome proliferators-activated receptors (Everett et al., 2000; Galli et al., 2001; Fischer et al., 2003).

Alcoholic steatohepatitis (ASH)

ASH, the second stage of the disease, is the rate-limiting step in the course of ALD and is characterized by steatosis accompanied by neutrophil infiltration, liver injury and hepatic necrosis. ASH seldom (<10% cases) reverts to normal hepatic histology, even when the precipitating condition is removed (French, 2002), and a substantial population of the patients is reported to develop hepatic fibrosis and cirrhosis

with the passage of time (Fig 3). In ASH, the presence of fat seems to be a prerequisite for the development of inflammation, possibly because a fatty liver seems to be more vulnerable to various factors that trigger inflammation (Day and James, 1998). Various mechanisms of ASH have been studied, including increased ROS/RNS production (Reinke et al., 1987; Lieber, 1990; Arteel, 2003), nutritional deficit in carbohydrates (Korourian et al., 1999), enhanced proinflammatory cytokine and chemokine levels (Wheeler et al., 2001; Hoek and Pastrino, 2002), and highly circulating levels of bacterial endotoxin or lipopolysaccharide (LPS) in patients with ASH (Enomoto et al., 1999; Uesugi et al., 2001; Hoek and Pastrino, 2002; Arteel, 2003). Irrespective of the mechanisms of ASH, one of the most common findings is the presence of neutrophils in the hepatic parenchyma.

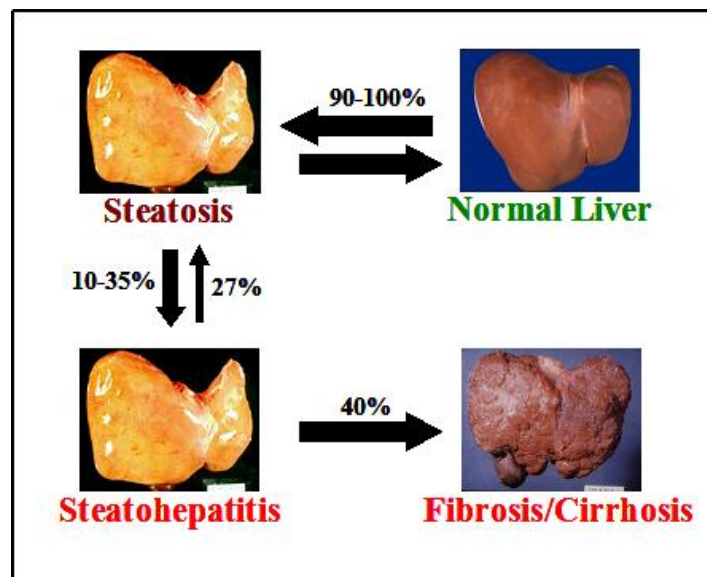


Fig. 3. Schematic representation of the progression of ALD. Consumption of EtOH produces hepatic pathology ranging from steatosis to steatohepatitis, fibrosis and cirrhosis. Steatohepatitis is reported to be the rate-limiting step in the progression of ALD (Adapted from Ramaiah et al., 2004)

Alcoholic fibrosis and cirrhosis

Fibrosis is considered the first irreversible step in ALD progressing severe fibrotic changes and eventually cirrhosis (MacSween and Burt, 1986; Teli et al., 1995). The fibrotic process is characterized by proliferation of hepatic stellate cells and their transformation into myofibroblasts. Cirrhosis the final stage of ALD is marked by the formation of scars and nodules in the liver (Fig 3). The scar tissue replaces the normal tissue, disrupting blood flow through the liver (Anand, 1999), resulting in liver failure and death.

Metabolism of alcohol

The liver is the main organ responsible for metabolizing the ingested alcohol; however, alcohol is also metabolized in extrahepatic tissues like brain (Zakhari et al, 2006). In general, the alcohol metabolism takes place mainly by the oxidative pathways involving the enzymes alcohol dehydrogenase (ADH), cytochrome P450 2E1 (CYP 2E1) and catalases. All of these enzymes produce acetaldehyde as their by-products (Fig 4).

Acetaldehyde is finally oxidized to acetate which metabolizes into water and carbon dioxide. However, the reaction by which acetaldehyde which is oxidized to acetate by aldehyde dehydrogenases (ALDHs) is extremely slow, and results in increase in acetaldehyde accumulation in the liver, leading to toxicity. Acetaldehyde forms adducts with proteins and small molecules at reactive residues (e.g. cysteines). Chemical alteration of these molecules can change or interfere with normal biological processes and can directly be toxic to the cell (Fig 5). Such modified biological molecules may also stimulate the immune response and cause autoimmune-like diseases.

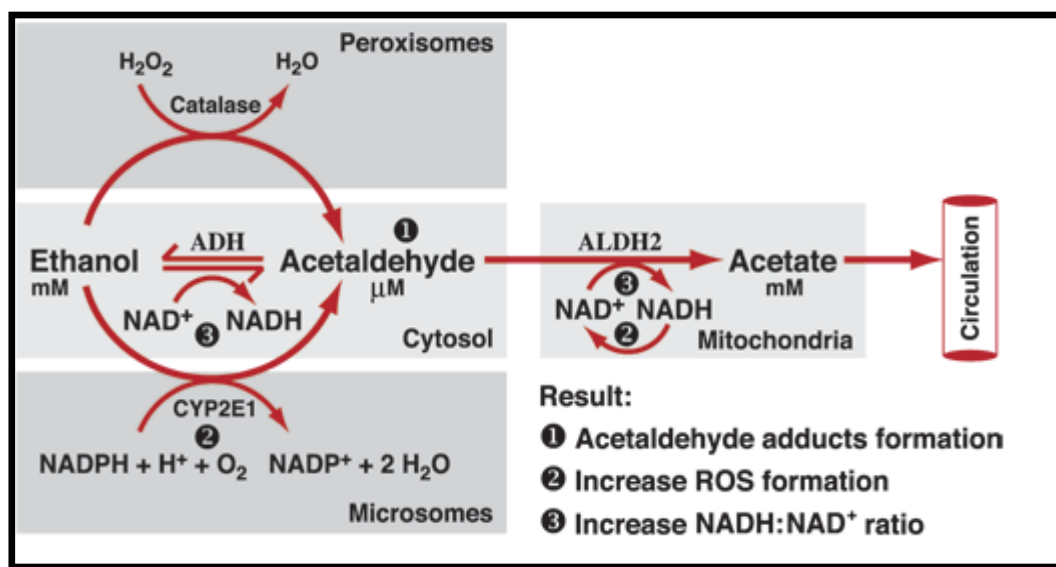


Fig. 4. Oxidative pathways of alcohol metabolism. The enzymes ADH, CYP2E1, and catalase all contribute to oxidative metabolism of alcohol. ADH, converts EtOH to acetaldehyde. In this reaction, NAD^+ , an intermediate carrier of electrons is reduced by two electrons to form NADH. Catalase requires hydrogen peroxide (H_2O_2) to oxidize EtOH. CYP2E1, also metabolizes EtOH to acetaldehyde at elevated EtOH concentrations. Acetaldehyde is metabolized mainly by ALDH2 to form acetate and NADH. ROS: reactive oxygen species (Adapted from Zakhari et al., 2006).

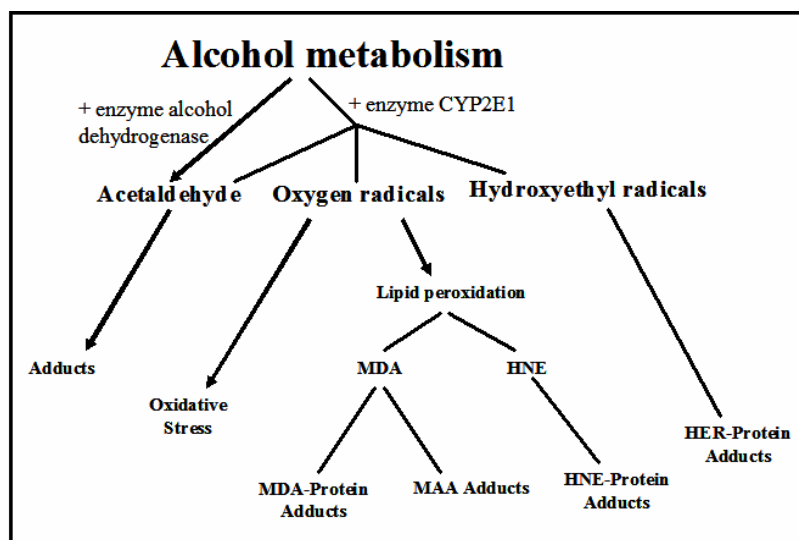


Fig. 5. Representative scheme showing the by-products of EtOH metabolism. EtOH metabolism takes place with the help of two major enzymes, alcohol dehydrogenase and CYP2E1. Both these enzymes convert EtOH to acetaldehyde. In addition to producing acetaldehyde, CYP2E1 also produces oxygen and hydroxyl radicals as by-products. Acetaldehyde and oxygen and hydroxyl radicals further react to produce various adducts, which reacts with proteins and interferes with the biological function of these molecules leading to hepatic injury (Adapted from Zakhari et al., 2006).

Several oxidized modified proteins like hybrid adduct of malondialdehyde and acetaldehyde unique to alcohol exposure have been reported in both animal and human models of ALD (see Fig 5, Klassen et al., 1995; Niemela, 2001, Thiele et al., 2001).

In addition to acetaldehyde and ADH, the isoenzyme CYP2E1 has also been known to be a major player in ALD. Studies by Bardag-Gorce and coworkers (2000) have shown that this enzyme is a major source of reactive oxygen species and contributes significantly to oxidative stress in ALD. Further studies have also shown that inhibitors of CYP2E1 partially block hepatic pathology caused by EtOH in experimental animal models (Bardag-Gorce et al., 2000).

The metabolism of EtOH has been reported to form cytotoxic by-products and also alter the cellular redox state. The oxidation of EtOH to acetaldehyde and acetate, utilizes NAD^+ as the electron acceptor, shifting the $\text{NADH}:\text{NAD}^+$ ratio to a more reduced state. This shift in the pyridine nucleotide redox state has been shown to impair normal carbohydrate and lipid metabolism, which has multiple effects, including decreased supply of ATP to the cells (Lieber, 2000). The increased reduced state of pyridine nucleotides have been reported to be responsible for the accumulation of lipids leading to progression of ALD (Day and James, 1998).

Animal models to study ALD

The use of animal models has contributed significantly to greater understanding of the progression of ALD. Although significant variations in these models have been reported, each model have been found to emphasize some aspect of our understanding of the pathogenesis of ALD (Table 1). Well-established models to investigate ALD include.

Table 1
Different models used to study alcoholic liver disease, their advantages, disadvantages and references.

Model	Advantage	Disadvantage	References
Lieber DeCarli Diet model	Rats consume EtOH in a balanced diet containing water and all sufficient nutrients. No surgery needed, relatively easy to implement.	No fibrotic changes observed in rats, after 9months of feeding the ad-libitum diet.	Lieber ,1963. Lieber and DeCarli, 1970a, 1982, 1986, 1989.
Intragastric EtOH feeding models: a) Tsukomoto and French model (b) Total Enteral Nutrition (TEN).	Increased circulating EtOH levels attainable.	Surgical manipulation, significant animal husbandry and higher cost associated as compared to Lieber DeCarli model.	Tsukomoto et al., 1985a,b. French et al., 1988. Badger et al., 1993. Kamimura et al., 1992. Yin et al., 1999. Kono et al., 2001a,b.
LPS sensitization model	Possible to achieve liver pathology especially neutrophil infiltration as observed in enteral feeding model and human patients.	Variations observed in animals.	Enomoto et al., 1999. Tamai et al., 2002. Apte et al., 2003.

chronic feeding model of Lieber and DeCarli (1982), the Tsukomoto and French enteral model (Tsukomoto and French 1985 a,b), the total enteral nutrition (TEN) model for dietary manipulations (Badger et al., 1993) and the rat model based on LPS sensitization (Enomoto et al., 1999).

Oral liquid diets

Lieber-DeCarli diets: Unlike humans, rats have an aversion to drinking alcohol. The incorporation of EtOH in a specialized liquid diet forces rats to consume EtOH in a balanced liquid diet that contains water and all sufficient nutrients. Control animals are pair fed an equicaloric amount of diet with EtOH replaced by carbohydrates (Lieber and

DeCarli, 1989). The improved formula consisted of casein (18% of calories), supplemented with methionine and cysteine, a mixture of dextrin and maltose (11% and 47% calories for EtOH and control diets), and fat (35% of calories: olive oil, corn oil, sunflower oil). All essential vitamins, mineral and fiber are reported to be present in this diet (Lieber and DeCarli 1986, 1989). This liquid diet popularly known as Lieber DeCarli diet has been extensively used in rodent models of ALD. Daily intake of Lieber DeCarli-EtOH diet resulted in fatty liver and six fold increase in hepatic triglycerides (Lieber and DeCarli, 1970). However, even after 9 months of feeding the Lieber DeCarli-EtOH diet, these rodents have rarely been reported to have fibrotic changes in the liver (Leo and Lieber, 1983). In addition, this diet also has other limitations. Despite partially overcoming their dislike of EtOH-containing diet, rodents on EtOH diet still consume less than control animals on carbohydrate diet. To address this issue, control animals are pair-fed isocaloric diet as the EtOH group (Lieber and DeCarli, 1989). However, there is still an inherent concern in comparing pair-fed rodents that typically consume their daily caloric allowance in a short period of time, as compared to EtOH-fed rodents that consume the same amount of calories over the course of a day (Ramaiah et al., 2004).

Intragastric EtOH feeding models

Both the Tsukamoto and French enteral model (Tsukamoto et al., 1985a) and the total enteral nutrition (TEN, Badger et al., 1993) model feeds the rodents EtOH-liquid diet through a permanent indwelling intragastric catheter. The animals in these models are monitored regularly for the blood EtOH levels, depending on which the composition and the EtOH level of the diet is titrated. As in the oral feeding model, controls are

infused with isocaloric amounts of EtOH-free diet with carbohydrates replacing EtOH. In these models, about 30-50% of the rats develop macro and micrvesicular steatosis, focal necrosis and mononuclear inflammation (Tsukomoto et al., 1985; French et al., 2005). Early perivenous fibrosis have been reported to develop in 3-6months provided a high-fat diet with 42-49% of total energy as EtOH is infused (Kamimura et al., 1992). These animals achieve an increased circulating level of EtOH (~500 mg/dl) as compared to the liquid diet, where ~100 mg/dl is rarely achieved. Although there are distinct advantages of enteral alcohol feeding like increased pathology, disadvantages of these models include the need for surgical manipulations, significant animal husbandry, and the relative cost of the model compared to ad libitum feeding (Ramaiah et al., 2004).

Simple nonsurgical LPS sensitization model

The simple, nonsurgical LPS sensitization model makes it possible to achieve liver pathology (steatosis, inflammation and necrosis) that resembles alterations that occur in the enteral feeding model (Tsukomoto et al., 1985a,b). This modified Lieber DeCarli diet has been known to enhance hepatic neutrophil infiltration resulting from enhanced endotoxin levels (Enomoto et al., 1999; Tamai et al., 2002; Apte et al., 2005).

Mechanisms of hepatic neutrophil transmigration

Neutrophil infiltration is one of the major concerns in a large number of inflammatory liver diseases like ischemia-reperfusion injury (Jaeschke et al., 1990; Ramaiah and Jaeschke, 2007), endotoxemia (Jaeschke et al., 1991; Rose et al., 2006,

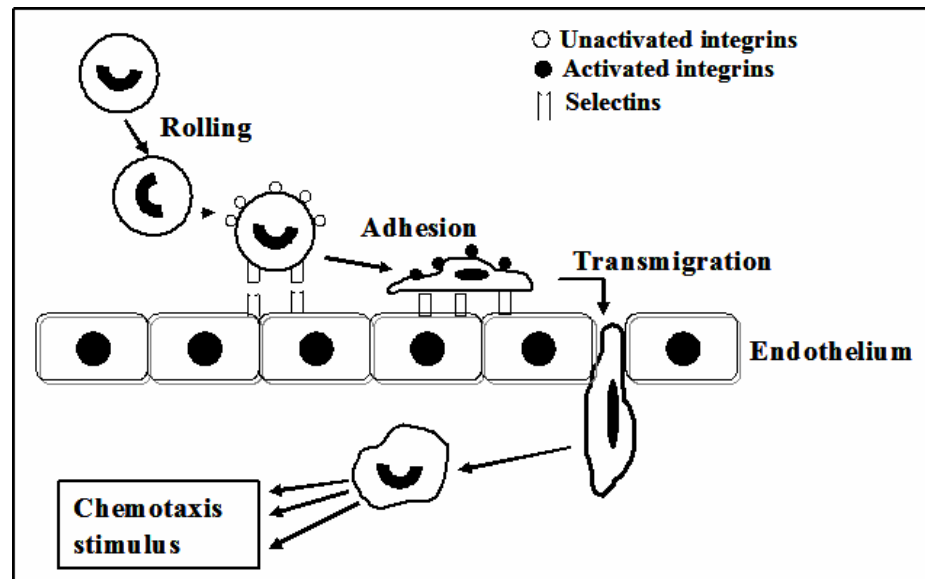


Fig. 6. Simplified schematic representation of the mechanism of neutrophil transmigration in the liver. This is a multi-step process involving rolling, adhesion and transmigration of neutrophils into the hepatic parenchyma. Rolling and adhesion takes place with the help of selectins, whereas adhesion and transmigration is mediated with the help of integrins. Up-regulation or activation of the integrins aids in adhesion and transmigration of neutrophils.

2007), and alcoholic liver disease (Ziol et al., 2001; Ramaiah et al., 2004; Apte et al., 2005). For neutrophil-mediated injury to occur and progress, neutrophils have to transmigrate into the hepatic parenchyma from the sinusoids of the liver. Transmigration of neutrophil (Fig 6) involves a sequence of events that includes neutrophil activation/accumulation within the hepatic vasculature, neutrophil transmigration/extravasation and attachment of neutrophils to hepatocytes leading to cell injury and death.

Neutrophils accumulate within hepatic sinusoids and post sinusoidal venules in response to systemic or local exposure to a variety of proinflammatory mediators such as tumor necrotic factor- α (TNF- α), CXC chemokines (IL-8, MIP-2), cytokine-induced

neutrophil chemoattractant -1 (CINC-1), activated complement factors (C5a), and platelet activating factor (PAF) (Table 2, Bautista and Spitzer 1992; Witthaut et al., 1994; Essani et al., 1995; Bajt et al., 2001). The accumulated neutrophils are at least partially activated (primed) as indicated by the up-regulation of Mac-1 ($\alpha_m\beta_2/\alpha_L\beta_2$) a member of the β_2 integrin family of adhesion molecules and by shedding of L-selectin and by their capacity to generate more reactive oxygen species in response to stimuli (Bautista et al., 1990; Bautista and Spitzer 1992; Jaeschke et al., 1993; Spitzer et al., 1994; Witthaut et al., 1994; Bajt et al., 2001). The adhesion of neutrophils in the post sinusoidal venules is initiated by the rapid expression of P-selectin on venular endothelial cells, which leads to selectin-dependent rolling of the neutrophils followed by the integrin/ICAM-1 dependent firm adhesion to endothelium (Jaeschke 1997; Wong et.al., 1997; Essani et.al., 1998). However, because of absence of rolling in the sinusoids in the liver, L-selectin is not known to play a role in sequestration and migration in the liver (Lawson et al., 1998).

Neutrophil transmigration, a prerequisite for hepatic cytotoxicity is facilitated by β_2 integrins, which are up-regulated and or activated from a constitutive low-affinity state to a high-affinity state on the neutrophil surface (Jaeschke and Hasegawa 2006). This high affinity conversion of neutrophils enables them to firmly adhere to the sinusoidal endothelium by binding to endothelial ICAM-1 and to eventually extravasate if a chemotactic signal is received from within the parenchyma. Chemotactic signals include CXC chemokines (IL-8, MIP-2, KC and CINC-1), which are potent chemoattractants for neutrophils and are produced by hepatocytes, sinusoidal

Table 2

Members of proinflammatory cytokines, chemokines, adhesion molecules and other potential candidates implicated in the pathogenesis of neutrophilic alcoholic steatohepatitis. (Adapted from Ramaiah and Jaeschke, 2007)

	Species studied	References
Proinflammatory cytokines TNF- α , IL-18, IL-18 binding protein, PAF	Rat, mice and humans	Afford et al., 1998; Bautista 2002; Spahr et al., 2004
Chemokines CXC (IL-8, CINC, KC), CC (RANTES, MIP-1, MCP-1)	Rat, mice and humans	Afford et al., 1998; Bautista 2000; 2002; Jaeschke 2002
Adhesion molecules CD-18, ICAM-1	Rats and mice	Bautista 2002; Kono et al., 2001
Apoptosis	Humans	Ziol et al., 2001
Microcirculatory disturbance eNOS, leukostasis	Rats	Karaa et al., 2005; Horie et al., 2000

endothelium, bile ductules, and Kupffer and stellate cells (Maher et al., 1997; Bajt et al., 2001; Okaya and Lentsch 2003).

Similar to neutrophil adhesion to sinusoidal endothelium during the phase of neutrophil transmigration, neutrophils use β_2 integrins to adhere to ICAM-1 on hepatocytes (Jaeschke and Hasegawa 2006). Engagement of β_2 integrins initiates a long-lasting oxidant stress through NADPH oxidase via generation of superoxide radicals (Jaeschke 2003; Gujral et al., 2004). In addition, myeloperoxidase released from neutrophils can generate hypochlorous acid resulting in the formation of chloroamines (Bilzer and Lauterburg 1991), which are potent oxidants and chlorinating agents. Similarly neutrophilic elastase can induce formation of neutrophils- and monocyte-chemoattractant chemokines in Kupffer cells (Yamaguchi et al., 2000) which can facilitate neutrophil transmigration. Thus, neutrophils serine proteases can process cytokines and chemokines, resulting in an exaggerated inflammatory response and

increased neutrophils cytotoxicity in the liver. In addition to these indirect effects, neutrophils-derived proteases may directly contribute to cell injury (Ho et al., 1996).

Although β_2 (LFA-1: $\alpha_m\beta_2$; Mac-1: $\alpha_L\beta_2$) integrins have been shown to be important for the adhesion and migration of neutrophils within the liver, it is still difficult to differentiate the specific roles of LFA-1 and Mac-1 in mediating chemotaxis in the peritoneum (Ding et al., 1999). Studies in mice deficient in LFA-1, Mac-1 and CD 18 (lacking both LFA-1 and Mac-1) have shown that neutrophils deficient in LFA-1 exhibited the same adhesion to fibrinogen as the wild type neutrophils, but adhesion to the substrate was absent in neutrophils deficient in Mac-1, indicating that LFA-1 is not required for Mac-1 on activated neutrophils to function as an adhesion molecule to its ligands (Ding et al., 1999). Further studies by Entman et al. (1992), and Nagendra et al. (1997), have shown that Mac-1 plays an important role in the adhesion of neutrophils to parenchymal cells in cardiac myocytes and hepatocytes. The marked difference in neutrophil extravasation observed in mice deficient in LFA-1 and Mac-1 in response to TNF- α demonstrates the unique role of these molecules in neutrophil extravasation; LFA-1 appears to be more important in neutrophil adhesion, while Mac-1 appears to be important in events occurring after transendothelial migration, including regulating adhesive interactions of the neutrophils as it moves through the interstitial space (Ding et al., 1999).

Surprisingly, majority of the literature on hepatic neutrophil transmigration is focused mostly on β_2 integrins. Although $\alpha_4\beta_1$ and $\alpha_9\beta_1$ have been reported to be expressed by PMN (Kubes et al., 1995; Shang et al., 1999) in the blood, there is no data

available on the role of β_1 integrins in the liver. Non- β_2 integrins such as $\alpha_v\beta_3$, $\alpha_4\beta_1$, $\alpha_5\beta_1$ are responsible for binding extra cellular matrix proteins and forming the adhesive traction forces for neutrophil migration (Gonzalez et al., 2007) In addition to the β_2 integrins, essential roles of $\alpha_4\beta_1$ (VLA4) has also been implicated in the multi-step adhesion and migration of neutrophils in the vascular endothelial cells and in patients with sepsis syndrome (Ulyanova et al., 2007; Ibbotson et al., 2001). This $\alpha_4\beta_1$ integrin has been known to be involved in all three steps of the neutrophil trafficking cascade (Kitayama et al., 1997; Chan et al., 2001). Expression of α_4 intergrins have been reported to be constitutive in all leukocytes except human neutrophils, where it is inducible (Johnson et al., 2001). Studies have reported that an initial priming event followed by multiple pro-inflammatory molecules is required for α_4 integrin expression and α_4 -integrin-dependent neutrophils binding to its ligands like VCAM-1 (Johnson et al, 2001). An increase in $\alpha_4\beta_1$ on neutrophils following transmigraton has also been reported in cardiac myocytes (Reinhardt et al., 1997). Further studies by Ulyanova et al., (2007), have shown that recruitment of neutrophils in the inflamed peritoneum, requires the presence of both α_4 and β_2 integrins. However, the interchangeable usage of the $\alpha_4\beta_1$ and β_2 integrins by neutrophils may be tissue specific, which is mediated by variations in chemokine secretion and expression of adhesion molecules in local inflammatory milieu (Ulyanova et al., 2007).

Osteopontin - structure and function

OPN an acidic member of the small integrin-binding ligand *N*-linked glycoprotein (SIBLING) family of proteins is involved in cell-to-cell and cell-to-matrix

communication (Fisher et al., 2001). This protein, a monomer of 264-301 amino acids, with a molecular mass ranging from 44-80kDa, undergoes extensive post translational modifications like phosphorylation, glycosylation and cleavage. OPN coded by a single gene (4q21-q25 in human) contains a hydrophobic leader sequence characteristic of a secreted protein that can bind to a variety of cell surface integrins (Denhardt et al., 2001a,b). The major integrin binding sites observed on OPN include the RGD-cell binding domain and the SVVYGLR domain in human (Fig 7, SLAYGLR domain in rat and mice). The RGD-cell binding domain, similar to that present in many extra cellular matrix (ECM) proteins is reported to bind to $\alpha_v\beta_3$, $\alpha_v\beta_1$, $\alpha_5\beta_1$, $\alpha_8\beta_1$ and $\alpha_v\beta_5$ integrins (Diao et al., 2004; Smith and Giachelli, 1998; Yokosaki et al., 1999, 2005). In addition to that, SVVYGLR, the second integrin binding site is reported to bind to $\alpha_9\beta_1$ and $\alpha_4\beta_1$ integrins (Moore et al., 1991; Tezuka et al., 1992; Johnson et al., 1999). Majority of the integrins appear to bind to the N-terminal thrombin cleaved fragment of OPN containing both the RGD and the SVVYGLR domain (Fig 7). The SVVYGLR domain is cryptic and the integrins bind to this domain only when OPN is cleaved at the thrombin cleavage site exposing the cryptic domain (Green et al., 2001). The thrombin cleavage motif immediately adjacent to SVVYGLR domain has a conserved sequence RSK, present in most species suggesting the requirement of OPN cleavage for some of its physiological functions (Denhardt et al., 2001a, b). The thrombin cleavage of OPN releases the SVVYGLR receptor-domain responsible to carry out distinct signaling functions. The SVVYGLR site is unusual as it lacks a critical acidic residue present in other binding motifs for integrins α_9/β_1 and α_4/β_1 . The negatively charged aspartic acid and glutamic

acid are considered to be critical acidic residues in OPN important in integrin binding ligands. It is thought that thrombin cleavage of Arginine 168 in OPN reveals a carboxylic group, enabling the SVVYGLR motif to engage these integrins. Thus the free C-terminus of SVVYGLR provides an acidic group required for its interaction with α_9/β_1 and α_4/β_1 (Green et al, 2001).

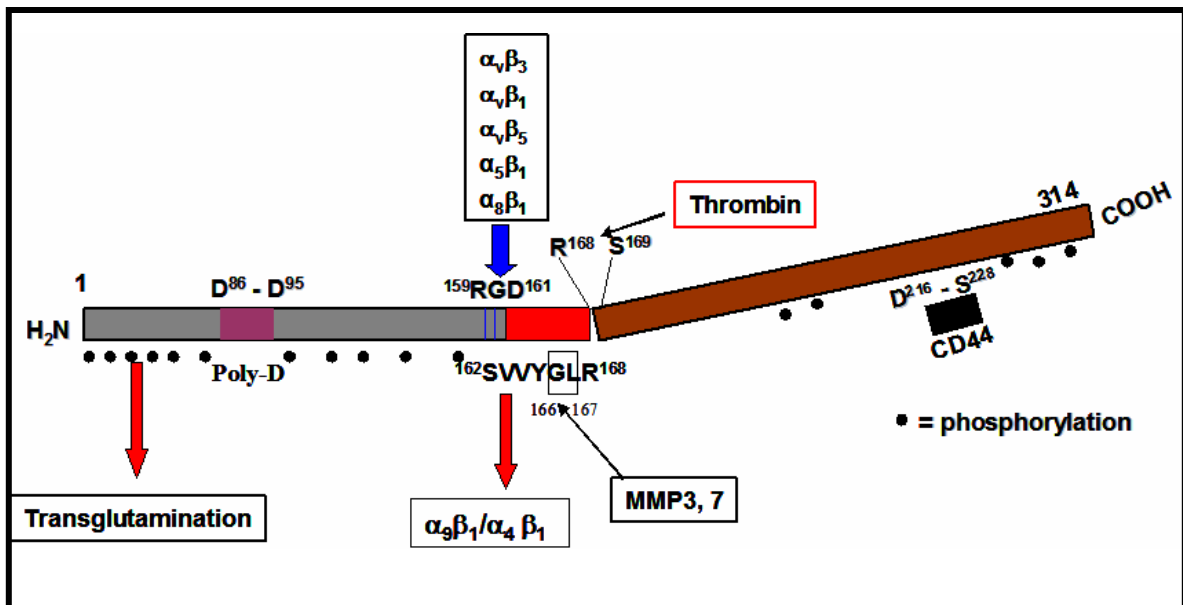


Fig. 7. Schematic representation of the structure of Osteopontin (OPN) protein. OPN undergoes extensive post translational modifications especially phosphorylation. Several binding sequence of OPN includes the RGD, SVVYGLR and the CD44. Additional motifs include the thrombin cleavage and transglutaminase binding site. The RGD-cell binding domain is reported to bind to $\alpha_v\beta_3$, $\alpha_v\beta_1$, $\alpha_5\beta_1$, $\alpha_8\beta_1$ and $\alpha_v\beta_5$ integrins, and the SVVYGLR sequence is reported to bind to $\alpha_9\beta_1$ and $\alpha_4\beta_1$ integrins (adapted from Ramaiah and Rittling, 2007).

In addition to the polymerization, OPN function is highly dependent on post-translational modification (PTM), such as phosphorylation and glycosylation (Sodek et al., 2000; Qin et al., 2004). The nature of PTMs of OPN is highly tissue- and cell

specific reflecting the diverse function of this protein in different physiological systems. Normal rat kidney cells have been reported to secrete both phosphorylated and non-phosphorylated variants of OPN (Singh et al., 1990). The regulatory roles of OPN in pathological mineralization are highly dependent on the phosphorylation status of OPN (Shiraga et al., 1992; Wada et al., 1999). Dephosphorylation of OPN hinders its ability to inhibit hydroxyapatite formation (Boskey et al., 1993), and phosphorylation is necessary for its inhibition of calcium oxalate crystallization in the urine (Hoyer et al., 2001) and calcification of vascular smooth muscle cells (Jono et al., 2000). Phosphorylation of OPN has also been shown to be essential for osteoclast attachment, and TRAP (tartarate-resistant acid phosphatase) dephosphorylation of bovine OPN resulted in a partially dephosphorylated protein that could no longer promote RGD-dependent osteoclast attachment (Ek-Rylander et al., 1994). The interaction of OPN and macrophages is also influenced by the phosphorylation state of this protein. The β_3 -integrin receptor on the macrophage has been reported to bind to the N-terminal of OPN, and secrete IL-12 only if the OPN fragment is phosphorylated (Ashkar et al., 2000). Likewise, phosphorylation is also required for OPN-mediated spreading and activation of macrophages (Weber et al., 2002). OPN has also been shown to promote trophoblastic cell migration in a process that is dependent on the level of phosphorylation of the protein (Al-Shami et al., 2005).

Although OPN protein is encoded by a single copy gene, a number of different isoforms of this protein exist mainly due to the different forms of PTM. The only OPN isoforms that have been characterized with regard to the PTM are those of bovine and

human milk, rat bone and murine ras-transformed fibroblast (FbOPN) and differentiating osteoblast (ObOPN). Bovine milk OPN contains 27 phosphoserine residues and one phosphothreonine residue (Sorensen et al., 1995). Up to 34 phosphoserines and two phosphothreonines residue (Sorensen et al., 1995) were identified in the human counterpart (Christensen et al., 2005). Studies of OPN purified from rat bone, revealed up to 29 potential phosphorylation sites (Keykhosravani et al., 2005). In addition, OPN produced by FbOPN and ObOPN contains an average of 4 and 21 phosphate groups respectively (Christensen et al., 2007). Phosphorylation sites are predominantly located at serines in the recognition motifs of the golgi kinase/ mammary gland casein kinase (Lasa-Benito et al., 1996; Lasa et al., 1997) and or casein kinase II (Lasa-Benito et al., 1996; Meggio and Pinna, 2003). In addition to phosphorylation, the characterized OPN isoforms all contain glycosylations. Bovine and human milk OPNs contain 3 and 5 O-glycosylated residues, rat bone OPN have 4, whereas FbOPN and ObOPN 5 and 1 respectively (Sorensen et al., 1995; Christensen et al., 2005; Keykhosravani et al., 2005; Christensen et al., 2007).

Contribution of OPN to hepatic inflammation and toxicity

Due to the varied structure, OPN is involved in a variety of pathophysiological conditions like cell binding, spreading, migration and tumor metastasis (Rittling and Denhardt, 1999; Denhardt et al., 2001a,b). OPN is also known to play an important role in a variety of inflammatory diseases like glomerular nephritis (Giachelli and Steitz, 2000; O'Regan and Berman, 2000; Denhardt et al., 2001a,b), inflammation during CCl₄

induced hepatotoxicity (Kawashima et al., 1999), puromycin-induced toxicity (Denhardt et al., 2001a,b) and in non-alcoholic steatohepatitis (Sahai et al., 2004).

OPN as a mediator hepatic natural killer T (NKT) cell and neutrophil infiltration

Concavalin A (Con A) mediated hepatitis is a classic example of inflammatory liver disease where in increased neutrophils and lymphocyte (NKT and T-cell) infiltration occurs followed by hepatic necrosis (Fujii et al., 2005; Zhu et al., 2007). The mechanistic link between OPN and NKT cells was recently tested in a Con A-induced hepatitis mouse model (Diao et al., 2004), where OPN-KO mice has significantly lower liver injury as compared to the wild type controls. NKT cells the major T-cell phenotype in the controls during the development of ConA-induced hepatic injury was found to significantly decrease in the OPN-deficient mice. In addition to the full-length OPN, the thrombin cleaved OPN (cOPN) was also present in the liver of the wild type mice. By in vitro migration assays, infiltrating leukocytes purified from the liver after ConA injection was found to migrate more efficiently towards the thrombin cOPN than the full-length form. Neutrophils were the predominant leukocyte population that responded to the cOPN. In summary, in this model after ConA-induced activation, NKT cells secreted OPN which is cleaved by thrombin in the liver. The interaction of cOPN with its receptors further activate NKT cells which produces MIP-2 a chemotactic factor for neutrophils. The cOPN also reacts with the α_4 and α_9 integrins on neutrophils, so that they become activated and contributes to additional liver injury (Diao et al., 2004).

OPN and non alcoholic fatty liver disease

Non alcoholic fatty liver disease (NAFLD) form a spectrum of disease from simple accumulation of fat to cirrhosis and end stage liver disease (Angulo, 2002; Diehl, 2002; Sahai et al., 2004). Recent studies by Sahai et al., (2004) have pointed out the role of OPN in an experimental dietary rodent model of NAFLD. Upregulation of OPN mRNA was noted in the early periods of treatment, when little or no pathological lesions were observed. Further in this study, the OPN-KO mice have significantly decreased liver injury and fibrosis when compared to their wild type counterparts indicating the role of OPN in the pathogenesis of NAFLD.

OPN as a mediator of the hepatic macrophage infiltration

OPN has been known to be a potent chemotactic factor for macrophages (Ramaiah and Rittling, 2007). This protein has been reported to bind to macrophages, and injection of OPN into mice resulted in inflammatory infiltrate rich in macrophages (Singh et al., 1990). Additional studies with neutralizing antibody to OPN have shown to reduce the macrophage accumulation by 60% (Giachelli et al., 1998), providing strong evidence that OPN regulates the chemotactic response of macrophages. Further studies have reported that activated macrophages themselves produce abundant OPN. This protein has also been reported to be associated with macrophage differentiation. It was identified as one of the genes most highly up regulated during differentiation of monocytes to macrophages (Krause et al., 1996). In RAW264.7 cells, down regulation of OPN expression with siRNA resulted in reduced expression of markers of macrophage

differentiation, suggesting that endogenous OPN expression supports the differentiated phenotype in these cells (Nystrom et al., 2007).

In the liver, carbon tetrachloride (CCl₄) has been reported to cause significant liver damage accompanied by increased macrophage infiltration in the tissue (Kawashima et al., 1999). OPN expression is strongly up regulated in the livers of CCl₄ treated rats, with peak expression 2 days after CCl₄ administration. Expression of OPN was highest in Kupffer cells, macrophages and hepatic stellate cells, suggesting that OPN is expressed in the macrophages and related cells at the site of hepatic injury and that the protein contributes to the host response to infection or injury. Since OPN stimulated cell migration, it may act as a chemotactic factor in the recruitment of macrophages to sites of liver injury (Kawashima et al., 1999).

Mechanisms for OPN transcriptional gene activation

Despite the many recognized functions of OPN, the mechanism by which OPN gene is up regulated in inflammation and other diseases is not well understood. This protein is known to be regulated by a variety of hormones (estrogen, progesterone, Vitamin D₃), cytokines and growth factors (Noda et al., 1988; Craig and Denhardt, 1991; Prince and Butler, 1997). Several inflammatory mediators and growth factors like interleukin-1 (IL-1), tumor necrosis factor alpha (TNF- α) and platelet growth factor (PDGF) are also known to stimulate OPN transcription via activation of protein kinase C (Denhardt and Noda, 1998). Increased OPN expression at sites of infection have also been reported to be due to release of PDGF and IL-1, that activates transcription factors like Fos and Jun, which are capable of up regulating OPN transcription. Studies by

Bonnelye et al., (1997), discovered that steroidogenic factor-responsive elements (SFREs) in the OPN promoter are targets for the estrogen-related orphan receptor ERR-1 in osteoblast cells, where ERR-1 controls ossification. In addition to this, studies by Guo et al., (2001), have shown that OPN transcription and promoter activity are significantly up regulated in response to NO in a system of endotoxin –stimulated murine macrophages, where OPN functions as a negative feedback regulatory system to down-regulate NO synthesis. Further, in the same model of RAW 264.7 murine macrophages and COS-1 cells, a transcriptional regulatory mechanism involving members of heterogeneous nuclear ribonucleoproteins have been shown to be involved in expression of OPN (Gao et al., 2005). The heterogeneous nuclear ribonucleoproteins (hnRNP) A/B and U, functions as antagonistic transcription factors for OPN expression in LPS-stimulated NO synthesis. In the presence of NO, hnRNP-A/B dissociated from the OPN promoter site with subsequent depression of OPN promoter activity, followed by binding of hnRNP-U to the same site to further augment the promoter activation.

In addition to this, transcription of OPN gene is regulated by the transactivation of cis-acting elements in the OPN gene promoter, like Activated protein-1 (AP-1), estrogen receptors (ERs) and estrogen, Vitamin D receptor (VDR) and Upstream stimulatory factor (USF).

Activated protein-1 (AP-1) is a dimeric complex that contains a heterogeneous combination of proteins from the JUN, FOS activating transcription factor families (Eferl et al., 2003). Recently, an AP-1 cis-regulating site was characterized at -76 on the rat OPN promoter (El-Tanani et al., 2004). Studies by Das et al., (2004), reported that

OPN stimulates AP-1 transcriptional activity through phosphorylation of EGFR by inducing c-Src kinase activity in breast cancer cells. OPN stimulates c-Fos expression, AP-1-DNA binding and AP-1 transactivation through the $\alpha_v\beta_3$ integrin/c-Src/ERK pathway. Thus AP-1 not only stimulates synthesis of OPN, but also stimulates its own synthesis in a positive feed back loop.

OPN expression has also been reported to be enhanced by estrogen (El-Tanani et al., 2001), and this function is postulated to be mediated by ER α and ERR α . Although an estrogen-response element is not present in the OPN promoter, there are seven steroid factor-response element (SFRE)-like sequences in this region (El-Tanani et al., 2001), that have been shown to bind ER α and ERR α , and transactivate the OPN gene.

Vitamin D receptor (VDR) a phosphoprotein member of the nuclear receptor superfamily of ligand- dependent transcription factors is known to induce OPN gene expression by binding to Vitamin D-responsive elements (VDREs). Studies by Chatterjee (2001), has shown that 1,25-dihydroxyvitamin D₃ can regulate OPN not only at the transcriptional level by VDR, but also modulate OPN's phosphorylation state independent of VDR.

Upstream stimulatory factor (USF), a basic helix-loop-helix-containing transcription factor has been shown to target a CCTCATGAC sequence in the mouse OPN promoter (-80 to -72nt) in rat aortic vascular smooth muscle cells (Bidder et al., 2002). It has been shown that USF-1 binds to a consensus E-box-response element (CAGGTG, -101 to -96nt) in the OPN promoter (Malyankar et al., 1999).

Objective of the study

The overall objective of this study was to understand the mechanism behind increased susceptibility of females to alcoholic liver disease (ALD). We hypothesize that increased hepatobiliary osteopontin (OPN) expression is the likely reason for higher neutrophilic infiltration and liver injury in female alcoholics. We anticipate increased hepatobiliary OPN secretion in females causes higher neutrophils to emigrate into hepatic parenchyma. Furthermore, it is expected that OPN mediates hepatic neutrophil infiltration via multi-integrin signaling. Understanding the role of induced OPN in the female alcoholic liver disease model to recruit neutrophils may contribute to the development of novel therapeutic strategies for treating human alcoholic liver disease patients.

CHAPTER II

MATERIALS AND METHODS*

Chemicals

All chemicals were obtained from Sigma Chemical Co. (St. Louis, MO) unless otherwise mentioned and were of the highest analytical grade. Glycine, 30% acrylamide:bis acrylamide solution, tris, tween-20, sodium dodecyl sulfate, laemelli buffer, β -mercaptoethanol and other materials related to Western blotting such as filter paper, nitrocellulose membranes were obtained from BioRad (Hercules, CA). The antibodies and primers used in this study and their vendors have been mentioned in the tables on p.41 and p.45. All the chemicals used for RT-PCR were obtained from Ambion (Austin, TX), and the primers used were obtained from IDT-DNA (Coralville, IA).

Animals and treatment

A model of alcoholic steatosis and steatohepatitis was developed based on previous reports (Enomoto et al., 1999; Deaciuc et al., 2002; Apte et al., 2005). Male and female Sprague-Dawley (SD) rats (220-250gms, purchased from Harlan, Houston, TX, US) and C57BL6 mice (19-22gms, Jackson laboratories, Barharbour, Maine, USA) were housed individually in cages in a temperature controlled animal facility with a 12hr light-dark cycle. The animals were utilized after 1-week equilibration period.

* Reprinted with permission from “Higher neutrophil infiltration mediated by osteopontin as a likely contributing factor to the increased susceptibility of females to alcoholic liver disease” by Banerjee et al., 2006, *Journal of Pathology*, 208: 473-485, © 2006 by Wiley Interscience.

Development of the alcoholic steatohepatitis (ASH) model

Weight matched male and female SD rats (n=32 each) and C57BL6 mice (n=20 each) were fed EtOH containing Lieber DeCarli liquid diet (Bio-Serv, Frenchtown, NJ, #F1697SP) for 6 weeks. An additional control group with isocaloric maltose-dextrin diet was also employed. Animals were first acclimatized to the EtOH diet for a period of 1 week. Since mice are more sensitive to alcohol diet as compared to rats, different methods of acclimatization was followed. In case of the rats, for the first day they received plain liquid diet, after which the rats in the EtOH-treated group received liquid diet containing 2% and 4% (w/v) of EtOH, for 2 days each. The 4% alcohol diet was then continued further for 6 weeks. However in case of the mice, they received plain liquid diet for the first 2 days, after which they were fed 1%, 2% and 3% diet for 3 days each. The 3% diet was then continued further for 6 weeks. The energy distribution of the control and the EtOH Liber DeCarli diet is given in Table 3.

Table 3

Energy distribution of Lieber De Carli diet (Control and EtOH). *Fat consisted of a mixture of olive oil, corn oil and sunflower oil.

	Control Diet	EtOH Diet
Protein	18%	18%
Fat*	35%	35%
Carbohydrate	47%	11.5%
EtOH	-	35.5%

Table 4
Ingredients for making Lieber DeCarli liquid diets (control and ethanol). *Bio-Serv, Frenchtown, NJ

Ingredients	
Control diet	1 bag diet* + 3560ml water + 360gms maltose dextrin
Experimental diet	1 bag diet* + 3560ml water + 268ml of 95% Ethanol

The liquid diet was prepared according to the manufacturer's protocol (Table 4). The food consumption was recorded daily for all the animals in both the groups. Calories consumed by each rat were measured daily. The control animals were pair-fed based on the food consumption of the EtOH-fed group.

After 6 weeks, the male and the female rats in the control and EtOH group were further divided into four groups, control, control+LPS, EtOH, EtOH+LPS. At the end of six weeks, rats from the control+LPS and EtOH+LPS groups were injected with a single injection of LPS or Lipopolysaccharise (*Escherchia coli* 0111:B4, 10mg/kg i.p in saline in rats, Sigma, St. Louis, MO). The animals in the control and EtOH group were injected with an equal volume of saline injection. The animals were then sacrificed 2 and 12 hrs after the LPS or saline injection by CO₂ asphyxiation. However, since mice are more sensitive, EtOH feeding alone for 6 weeks caused alcoholic steatohepatitis, and so mice were further not injected with LPS. All animals were provided humane care in compliance with the institutional guidelines (ULAAC; University Laboratory Animal Care Committee) of Texas A&M University.

Surgical technique- ovariectomy

Female Sprague-Dawley rats were anesthetized with ketamine (87mg/kg body weight) and xylazine (13mg/kg body weight) and bilateral ovariectomies were performed using a dorsal midline incision inferior to the palpated rib cage and kidneys (Jezerski and Sohrabji, 2000), and ovaries and surrounding tissues were removed. In some of the animals, a 60-day time release 17- β estradiol pellets (0.18, 0.36, 0.72 and 1.7mg, Innovative Research, FL) were inserted subcutaneously prior to closing the incision.

Assessment of estrous cycle

The estrous cycle patterns of animals were determined before and after feeding of EtOH, by daily observation of vaginal smears. Briefly, vaginal samples were taken in the morning, in between 9.00 to 11.00am, using a small wet cotton swab. The vaginal samples were then smeared on a glass slide and stained with Diff-Quik stain. The different stages of the estrous cycle were determined by microscopic visualization of the vaginal cell types as follows: (a) Proestrus: marked by the presence of clusters of round nucleated epithelial cells. (b) Estrus: keratinized cornified cells. (c) Metestrus: presence of non-cornified epithelial cells with a few leukocytes. (d) Diestrus: Predominance of leukocytes and few round epithelial cells (Long and Evans, 1922; Goldman et al., 2007).

Sample collection and processing

Blood was collected in heparinized tubes, from the dorsal aorta. Twenty micro liters of this blood was separated in gas chromatography vials (VWR, Bristol, CT) and submitted for estimation of blood alcohol content (BAC; Department of Human

Anatomy and Medical Neurobiology at the Texas A&M Health Sciences Center, College Station, TX). Liver transaminase activities were estimated from a fraction of heparinized plasma (about 0.5ml), and the remaining plasma was snap frozen in liquid N₂ and stored at –80°C. Livers were harvested, weighed and divided into two parts. Slices of the large and median lobes were fixed in 10% neutral buffered formalin, while remaining liver tissue was snap frozen in liquid N₂ and stored at –70°C for further analysis.

Evaluation of the liver injury

Liver injury was estimated by plasma transaminase activities (alanine aminotransferase; ALT and aspartate aminotransferase; AST) and corroborated by histopathology of H&E-stained liver sections. Plasma ALT and AST activities were analyzed on Vitros Chemistry Analyzer (Ortho-Clinical Diagnostics, Raritan, NJ). For histopathology, 4µM-thick paraffin-embedded liver sections were cut and stained with H&E for bright –field microscopy. Liver sections were evaluated for steatosis, hepatic cellular infiltration, oncotic necrosis and apoptosis. Hepatic steatosis was scored using a system developed for the intragastric infusion model of ALD (Nanji et al., 1989) as follows: steatosis (the percentage of hepatocytes containing fat) <25%, 1+; <50%, 2+; <75%, 3+; >75%, 4+.

Assessment of steatohepatitis

Histochemical detection of neutrophils was performed on paraffin-embedded liver sections. The H&E staining was employed to identify the neutrophils based on the segmented morphology of the nucleus followed by quantification with Naphthol AS-D Chloroacetate Esterase Staining (Sigma Diagnostics, St. Louis, MO, USA).

Assay reagents and working standards provided in the kit were prepared according to the manufacturer's protocol. Briefly, deparaffinized slides were incubated in the substrate solution (40ml warm distilled water, 1ml sodium nitrate, 1ml fast blue violet LB, 5ml of trizma 6.3 buffer concentrate, 1ml naphthol AS-D) for 30mins in a 37°C water bath. The slides were kept in dark during the incubation period, after which, they were washed in distilled water and counterstained with hematoxylin for 45secs, followed by rinsing in tap water for 4 times. The slides were then dipped 3 times in 70%, 100% alcohol and xylene. The dehydrated sections were then mounted in cytooseal and examined.

To quantitate the degree of neutrophilic inflammation (inflammation score), the number of neutrophils per five high power fields (40X) was counted. The neutrophilic foci (defined as an aggregate of ≥ 4 neutrophils) were quantitated per five-40X field.

Estimation of plasma levels of endotoxin, GRO/CINC-1, and IL-6 by ELISA

Endotoxin, GRO/CINC-1 and IL-6 levels were estimated in the plasma of Control, EtOH, Control+LPS and EtOH+LPS treated groups both in male and female rats, using rat specific Endotoxin (BioWhittaker, Walkersville, MD, USA), GRO/CINC-1 (Assay designs, Ann Arbor, MI, USA) and IL-6 kit (R&D Systems, Minneapolis, MN, USA) according to the manufactures protocol as described below. Plasma was collected from the rats as mentioned in the sample collection and processing section.

Endotoxin assay

Plasma endotoxin levels were measured using Limulus Amebocyte Lysate (LAL) Endpoint Assay Kit (BioWhittaker, Walkersville, MD, USA). Pyrogen-free procedures

were employed throughout the assay. All plasma samples were brought to room temperature prior to the assay. The plasma samples were diluted in the ratio of 1:10 with LAL reagent water and heated in a 70°C water bath for 5 mins. A pyrogen-free 96 well plate was preheated at 37°C in which the standards and plasma samples were incubated with LAL for 10mins, followed by substrate solution for 6 mins. The reaction was stopped by adding 25% acetic acid solution. The absorbance was read at 410nm using a microplate reader (Benchmark Plus, Bio-Rad, Hercules, CA), preheated at 37°C.

GRO-CINC-1 Elisa

Assay reagents and working standards provided in the kit were prepared according to the manufacturer's protocol. Briefly, to each well of the 96 well plate (GRO-CINC-1 immobilized in a microtiter plate), 100µl of standard or plasma was added, and the plate was covered with an adhesive strip and incubated at 37°C for 1 hour. After incubation, the wells were washed with 400µl of wash solution for 10 times, and 100µl of labeled antibody was added to each well. The plate was then again covered with an adhesive strip and incubated at 37°C for 30mins. After incubation, the wells were washed with 400µl of wash solution for 12 times, and 100µl of substrate solution was added to each well, and incubated for 30mins at room temperature in dark. 100µl of stop solution was added to each well, and the optical density was determined at 450nm in a microplate reader (Benchmark Plus, Bio-Rad, Hercules, CA) and the concentration of GRO-CINC-1 was read using the standard graph generated from the known concentration of GRO-CINC-1.

IL-6 Elisa

Assay reagents and working standards provided in the kit were prepared according to the manufacturer's protocol. Briefly, 50 μ l of standards and plasma were added to each well of the 96 well plate previously coated with anti-IL-6 capture antibody. The plate was then covered by an adhesive strip and incubated for 2 hrs at room temperature. After incubation, the strip was removed, contents of the plate was aspirated and washed thrice with wash buffer. To each well 100 μ l of Streptavidin-HRP conjugate was added, and incubated for another 2 hrs at room temperature. After incubation, the strip was removed, and the contents of the plate was aspirated and washed thrice with wash buffer. To each well 100 μ l of substrate solution was then added and again incubated for 30mins at room temperature in dark. 100 μ l of stop solution was then added to each well, and the optical density was determined at 450nm on microplate reader (Benchmark Plus, Bio-Rad, Hercules, CA) and the concentration of IL-6 (pg/ml of plasma) was determined based on the standard graph generated from the known concentrations of recombinant IL-6.

Para-nitrophenol hydroxylase assay

Hydroxylation of *p*-nitrophenol (*p*NP) to *p*-nitrocatechol by microsomal CYP2E1 was used as a marker to CYP2E1 enzyme activity in the *p*NP assay. 0.5mg of microsomal protein was used to measure CYP2E1 activity. Briefly, the samples were incubated with *p*NP, *p*NP assay buffer (100mM Kpi, 0.1mM EDTA, 1mM Ascorbic acid, pH 6.8) and NADPH in a water bath for 30mins. Perchloric acid (0.5ml of 0.5M) was added to each tube to stop the reaction. This mixture was incubated at room

temperature for 1hr, followed by centrifugation to precipitate the proteins. 100 μ l of the supernatant collected was pipetted in a 96-well plate followed by the addition of 14 μ l of NaOH. The optical density was determined at 546nm on a microplate reader (Benchmark Plus, Bio-Rad, Hercules, CA), and the activity of CYP2E1 was determined using the following formula:

$$\text{A.U.} \times 10,493.18 = \dots\dots\dots \text{pmol/mg/min.}$$

Where A.U.= (OD of the sample- OD of the negative control of the same sample).

Western blot analysis

Preparation of microsomes

100mg of frozen liver sections were homogenized (1:5w/v) in a buffer containing ice-cold Tris-acetate (pH 7.4) and 1.15% KCl. The homogenate was centrifuged at 10,000g for 30mins at 4°C. The supernatant was collected and further centrifuged at 100,000g for 60mins at 4°C. The microsomal pellets recovered were suspended in assay buffer (100mM KPi, 0.1mM EDTA, 1mM Ascorbic acid, pH 6.8), manually homogenized, quick-frozen and stored at -70°C. Protein concentration was estimated using a Bio-Rad protein assay kit (Bio-Rad, Hercules, CA).

Preparation of the tissue lysates

The liver samples were pulverized under liquid nitrogen, and transferred to centrifuge tubes. To 100 mg of this pulverized tissue, 5volumes of 1X homogenization buffer (1% Triton-X-100, 150mM NaCl, 10mM Tris (pH 7.4), 1mM EDTA, 1mM EGTA, 2mM NaVanadate, 0.2mM Phenylmethylsulfonylfluoride (PMSF), 1mM HEPES, 1 μ g/ml Leupeptin, 1 μ g/m Aprotinin) was added. The mixture was then

homogenized for 30-45 secs at 4°C in a Ultra-Turrax 25 homogenizer (IKA, Wilmington, NC), and the tissue lysate obtained was used for protein estimation. The protein concentration was estimated using a Bio-Rad protein assay kit (Bio-Rad, Hercules, CA).

Western blot procedures

The protein samples were solubilized in the reduced sample buffer (950µl of Laemelli Buffer, 50µl of Mercaptoethanol, Biorad-Hercules, CA), and were incubated at 100°C for 2 mins. Equal amount (50µg of protein) was loaded per lane (first lane used for dual colored molecular marker), and separated on 12% SDS-PAGE at 120 V for 1-1.5 hrs in 1x running buffer [25 mmol/L Tris-base, 192 mmol/L glycine, and 0.1% SDS (pH 8.3)], and transferred to nitrocellulose membrane (0.2µm, BioRad, Hercules, CA), 350 V for 1hr 20min at 4°C in 1x transfer buffer (48 mmol/L Tris-HCl, 39 mmol/L glycine, 0.025% SDS and methanol). The nitrocellulose membrane was blocked in TBS-Tween with 6% non-fat dry milk with gentle shaking for 3hrs (room temperature) followed by incubation overnight (4°C) in primary antibody (dissolved in TBS-Tween with 2% non- fat dry milk). (The list of primary and secondary antibodies used for Western blotting including the concentrations and time of incubation is provided in Table 5).After incubation with the primary antibody, the membranes were washed in TBS-T 3X 10 mins each at room temperature, and then incubated for 1hr with respective secondary antibodies (1:10,000 dissolved in TBS-T with 2% non-fat dry milk). The list of respective secondary antibodies used for different proteins is also given in Table 5.

Table 5
List of primary and secondary antibodies employed for Western blot.

Western blot of	Primary antibody (vendor)	Concentration of primary antibody	Secondary antibody (vendor)	Comments
CYP2E1	Goat polyclonal (458511, Gentest, Woburn, MA)	1:1000	HRP-linked anti-goat (Sigma, St. Louis, MO)	10% gel
OPN	Rabbit Polyclonal (ab 8448, Abcam, Cambridge, MA)	1:1000	HRP-linked anti-rabbit (Sigma, St. Louis, MO)	12% gel
OPN (mouse specific)	Mouse monoclonal (sc 21742, Santa Cruz Biotechnology, Santa Cruz, CA)	1:1000	HRP-linked anti mouse (Santa Cruz Biotechnology, Santa Cruz, CA)	12% gel
OPN (N-terminal)	Mouse monoclonal (Gifted by Dr. David Denhardt, Rutgers University)	1 µg/ml	HRP-linked anti mouse (Santa Cruz Biotechnology, Santa Cruz, CA)	12% gel
Alpha 4 integrin	Rabbit Polyclonal (AB 1924, Chemicon Int., Temecula, CA)	1:2000	HRP-linked anti-rabbit (Sigma, St. Louis, MO)	8% gel used for SDS-PAGE, non-reduced sample buffer used for protein Solubilization
Alpha 9 integrin	Rabbit Polyclonal (Gifted by Dr. Dean Shephard, University of California)	1:1000	HRP-linked anti-rabbit (Sigma, St. Louis, MO)	8% gel used for SDS-PAGE, non-reduced sample buffer used for protein Solubilization
Beta 1 integrin	Rabbit Polyclonal (AB 1952, Chemicon Int., Temecula, CA)	1:2000	HRP-linked anti-rabbit (Sigma, St. Louis, MO)	8% gel used for SDS-PAGE, non-reduced sample buffer used for protein Solubilization
Ferritin H	Rabbit Polyclonal (ab 16875, Abcam, Cambridge, MA)	1:1000	HRP-linked anti-rabbit (Sigma, St. Louis, MO)	12% gel
HSP 60	Rabbit Polyclonal (ab 53109, Abcam, Cambridge, MA)	1:1000	HRP-linked anti-rabbit (Sigma, St. Louis, MO)	12% gel
ER 60	Rabbit Polyclonal (Gifted by Dr. Reiko Urade, Kyoto University, Japan)	1:1000	HRP-linked anti-rabbit (Sigma, St. Louis, MO)	12% gel
PrX 6	Rabbit Polyclonal (Gifted by Dr. Aaron Fisher, University of Pennsylvania)	1:2000	HRP-linked anti-rabbit (Sigma, St. Louis, MO)	15% gel
GAPDH	Rabbit polyclonal (sc 20357, Santa Cruz Biotechnology, Santa Cruz, CA)	1:1000	HRP-linked anti-rabbit (Sigma, St. Louis, MO)	12% gel

After incubation with the secondary antibody, the membranes were washed again in TBS-T, 3X 15 mins each at room temperature. Protein visualization was done using Pierce SuperSignal West Pico Chemiluminescent Substrate (Pierce, Rockford, IL). The membranes were incubated with equal volume of Part A and B of the chemiluminescent substrate for about 2mins, and then exposed to films in a photographic dark room. The films were developed on Konica machine. (Konica Medical Imaging, Wayne, NJ). The densitometric analysis was performed using Image J software (NIH).

Immunohistochemical analysis of OPN in the liver

Hepatic OPN expression was studied by immunohistochemical analysis conducted on 4 μ m thick formalin fixed, paraffin embedded liver sections. Deparaffinized slides were quenched in 30% hydrogen peroxide for 10mins in order to quench endogenous peroxidase, and then rinsed in distilled water 3X for 2 mins each, followed by antigen retrieval using citrate buffer (10mM sodium citrate solution), after which the slides were immersed in PBS. Henceforth all the steps were performed in a humidity chamber.

The samples were blocked by using horse serum in the ratio of 1:10 for about 1hr 30mins, followed by overnight incubation with primary antibody (01-20002, mouse monoclonal, American Research Products, dilution 1:200). The slides were then rinsed with PBS and incubated with secondary antibody (biotinylated rat adsorbed anti mouse antibody, Vector Laboratories, Burlingame, CA) for 30mins in the ratio of 1:500 followed by streptavidin (Vectastain Elite ABC Kit, Vector Laboratories, Burlingame, CA) for 30 mins. After incubation with the secondary antibody, the slides were again washed with

PBS and exposed to chromogen (Diaminobenzidine reagent, Vector Laboratories, Burlingame, CA) for about 1-2mins. This reaction converts the DAB to an insoluble brown product, thus allowing for the visualization of the primary antibody antigen complex. The sections were counterstained with Gill's hematoxylin. OPN expression was identified by the brown-colored cytoplasmic staining.

Immunohistochemical analysis of Ferritin Heavy chain (Ferritin H) in the liver

Hepatic Ferritin H chain expression was studied by immunohistochemical analysis conducted on 4 μ M thick paraffin-embedded liver sections. Briefly, deparaffinized unstained liver sections were treated with 3% solution of H₂O₂ in order to quench the endogenous peroxidase activity. Sections were then incubated with 10% horse serum in PBS to block nonspecific binding sites. A Rabbit polyclonal Ferritin H antibody (ab 16875, Abcam Inc, Cambridge, MA) was employed as a primary antibody. Sections were then treated with a biotinylated anti-rabbit secondary antibody followed by streptavidin (Vector Laboratories, Burlingame, CA). The color was developed by exposing the peroxidase to diaminobenzidine reagent (Vector Laboratories, Burlingame, CA), which forms the brown reaction product. The sections were counterstained with Gill's hematoxylin. Ferritin H chain expression was identified by the brown-colored cytoplasmic staining.

Assessment of mRNA from liver samples

RNA extraction

RNA was extracted from rat liver and biliary epithelial cells using RNeasy midikit (Qiagen, Valencia, CA), according to the manufacture's protocol. All the

apparatus used were washed using RNase ZAP (Ambion, Foster city, CA) to ensure removal of RNase contamination. Briefly, samples were (frozen liver samples were ground in sterilized mortal-pestle) homogenized in 4ml of mixture of RLT + β -Mercaptoethanol buffer (10 μ l of β -Mercaptoethanol/ 1ml of RLT buffer) and the lysates were then centrifuged for 10mins at 3000-5000 x g at 4°C. The supernatant obtained was mixed with an equal volume of 70% EtOH and transferred to RNeasy column, and centrifuged at 3000-5000 x g for 5 mins 4°C. The column was thereby washed with RW1, and RPE buffer, and the RNA was eluted with 150 μ l of RNase-free water. The samples were stored at 20°C till further use.

Determination of purity and total RNA yield

To determine the concentration of RNA, 1 μ l of the sample was diluted with 199 μ l of DEPC-treated water (200-fold dilution). The absorbance of each sample was read at 260nm using DEPC water as reference.

The concentration of RNA was determined by using following formula.

$$[\text{RNA}] = (A_{260})(40 \mu\text{g/ml})D$$

where: [RNA]= total RNA concentration, A_{260} = absorption at 260nm, 40 = factor for RNA concentration, and, D = dilution factor.

Real Time RT-PCR

After extraction of the total RNA, Real Time PCR was carried out using the SYBR Green PCR Master Mix (Applied Biosystems, Foster City, CA) and Titanium One-Step RT-PCR kit (BD Biosciences Clontech, Palo Alto, CA). The reaction mixture was prepared by combining the SYBR Green Master mix, RNase inhibitor, Reverse

transcriptase, specific forward and reverse primer, and Nuclease free water (Table 6), in a MicroAmp Optical 96-Well Plates (Applied Biosystems, Foster City, CA).

Table 6
The volume and concentrations of individual components used for 1 step real time PCR.

Components	Volume (µl)	Final concentration
2X SYBR Green OCR Master Mix	6.25	1X
RNase inhibitor	0.5	
Reverse transcriptase	0.125	
Forward Primer	0.375	1µM
Reverse Primer	0.375	1µM
Template	X	100ng
Nuclease free water	Y	-
Final reaction volume	25	

Table 7
List of primers used for RT-PCR.

Name of the gene	Forward primer	Reverse primer
OPN (rat specific)	CCT CCC GCA TGA AGA G	TCA GAC GCT GGG CAA CTG
OPN (mouse specific)	TGC ACC CAG ATC CTA TAG CC	CTC CAT CGT CAT CAT CAT CG
α -4 integrin	TGA CCT CGT CTT ACG CTG TG	CTG ACC AGA GTT CAG GA
α -9 integrin	GGA GAC TCA GCA GGA ACT GG	GGT GTC TGG GAT GAG ATG CT
β -1 integrin	GGA GTC AAT GGG ACA GGA GA	TGC CAT GGC TTT GAC AAT TA
β-actin	CCG TGA AAA GAT GAC CCA GAT C	CAC AGC CTG GAT GGC TAC GT

The software Primer Express (Applied Biosystems, Foster City, CA) was used to design the primers. The primers (Table 7) were commercially obtained from Integrated DNA Technologies, Inc. (Coralville, IA). One step Real-time PCR was conducted in a Gene Amp 5700 Sequence Detection system (Applied Biosystems) using a total volume of 25 μ l containing 100ng of the RNA. The optimal assay conditions were: initial activation of AmpliTaq Gold at 95°C for 10min, followed by 40 cycles of denaturation at 95°C for 15secs and annealing and extension at 60°C for 1min. To control for DNA contamination of the RNA extracts, a no-RT reaction was run for each extract. Expression of the OPN gene relative to the housekeeping gene (beta-actin) was determined by $\Delta CT = CT_{(OPN)} - CT_{(Beta-actin)}$, and the Fold Expression was determined to be $(2)^{\Delta CT}$, where the threshold cycle (C_T) is defined as the cycle at which the fluorescence was significantly higher than the average standard deviation of the earlier cycles and the sequence detection application began to detect the increase in signal associated with an exponential growth of the PCR product (Khare et al., 2004).

In-situ hybridization analysis

Osteopontin mRNA expression in liver sections were localized by in-situ hybridization as previously described by Johnson et al., 1999. Briefly, liver sections were deparafinized in xylene and rehydrated to water through graded series of alcohol. The tissue sections were then fixed in 4% paraformaldehyde in PBS and then digested with proteinase K (20 μ g/ml) in a PK digestion buffer (50mM Tris, 5mM EDTA, pH: 8) for 8 mins at 37°C. The sections were then refixed for 5 mins in 4% paraformaldehyde, rinsed 2X for 5 mins each in PBS, and dehydrated through a series of alcohol and dried

at room temperature for 30mins. The refixed sections were then hybridized with radiolabelled antisense or sense Porcine OPN cRNA probes generated by in vitro transcription with [α -³⁵S], Uridine tri-phosphate (PerkinElmer Life Sciences, Wellesley, MA). The radiolabelled cRNA probes (5×10^6 cpm/slide) were denatured in 75 μ l hybridization buffer [50% formamide, 0.3M NaCl, 20mM Tris-HCl (pH 8), 5mM EDTA (pH 8), single strength Denhardt's solution, 10% dextran sulfate, 0.5mg/ml yeast RNA, 100mM dithiothreitol (DTT)] at 70°C for 10mins. The slides were coverslipped with the hybridization solution, and incubated in a humidified chamber containing 50% formamide/5-strength SSC (single-strength SSC is 0.15M sodium chloride, 0.015M sodium citrate) overnight at 55°C. The following day, the coverslips were floated off the slides by placement in 5-strength SSC/10mM β -Mercaptoethanol for 30mins at 55°C. The sections were then washed in (a) 50% formamide, double-strength SSC, and 50mM β -Mercaptoethanol for 20mins at 65°C. (b) single-strength TEN [0.05M NaCl, 10mM Tris (pH 8), 5M EDTA] for 10mins at room temperature, (c) 3X single-strength TEN for 10mins at 37°C, and then digested with DNase free RNase (10 μ g/ml) in single-strength TEN for 30mins at 37°C, to remove any nonspecifically bound probe and washed as follows (a) single-strength TEN for 10mins at 37°C (b) 50% formamide, double-strength SSC, 50mM β -Mercaptoethanol for 20mins at 65°C (c) double-strength SSC for 15mins at room temperature (d) 0.1 strength SSC for 12 mins at room temperature, (e) 70% ethyl alcohol, ethyl hydroxide containing ammonium acetate for 1 min at room temperature (f)

95% EtOH containing 0.03M ammonium acetate for 1 min at room temperature (g) 2X in 100% EtOH and (h) 3X in single-strength TEN for 10mins at 37°C.

Liquid film emulsion autoradiography was performed using Kodak NTB-2 liquid photographic emulsion. The slides were stored at 4°C for 5 days, developed in Kodak D-19 developer, counterstained with Harris' modified Hematoxylin in acetic acid (Fisher, Fairlawn, NJ), dehydrated through a graded series of alcohol to xylene, coverslipped and evaluated by both brightfield and darkfield microscopy with a Zeiss Photomicroscope III (Carl Zeiss Inc., Thornwood, NY).

Analysis of neutrophil activation by OPN in vitro using FACS Calibur flow cytometer

A FACS Calibur flow cytometer was employed to assess OPN-mediated neutrophil activation in vitro. Freshly drawn heparinized blood was divided into 250µl aliquots in separate glass tubes and was kept on ice unless otherwise stated. Duplicate tubes of blood were designated to control and experimental groups. Blood from each of these groups were incubated with saline, recombinant OPN (rOPN, AF808, R&D Systems, Minneapolis, MN, USA), and cOPN (rOPN incubated with thrombin for 30mins in a 37°C waterbath), and stained with fluorescein-conjugated HIS 48 (BD Biosciences, San Jose, CA, USA) and R-phycoerythrin- conjugated CD11b (Serotec Inc, Raleigh, NC, USA). Up regulation of CD-11 b indicates activation of neutrophils in the liver (Lawson et al., 1998). Following incubation, the neutrophils were treated with RBS lysis buffer and resuspended in 300µl PBS. The cells were then analyzed on a FACS Calibur (Becton Dickinson Immunocytometry Systems, San Jose, CA) flow cytometer.

Data analysis including spectral compensation was performed using FlowJo (Treestar, Inc, Ashland, OR, USA). A neutrophil gate was established based on side scatter and positive HIS48 staining, and the median fluorescence channel was determined for CD11b staining.

OPN-mediated neutrophil chemotactic response in an experimental rat peritoneal model

Sprague-Dawley (SD) rats (220-250g), purchased from Harlan, Houston, TX, USA, were housed individually in cages in a temperature controlled animal facility with a 12hr light-dark cycle. Rats were utilized after a 1-week equilibration period. Male and female rats were divided into control, zymosan, OPN and cleaved OPN (cOPN) (n=4 in each group) treated groups. All animals were injected intraperitoneally in this experiment. The treatment and doses for the animals are listed in Table 8. All solutions used in this experiment were irradiated under UV to ensure sterility. The rats were sacrificed at 4-hrs post-treatment. After sacrifice, the rats were injected with 5ml of ice-cold sterile PBS containing 20U/ml of heparin. The abdomen was massaged for 2mins and then via midline incision, free fluid was recovered from the peritoneal cavity. This fluid was centrifuged at 1000g for 5mins at 4°C to separate fluid and cellular components. Supernatants were removed and evaluated for the number of leukocytes using a Abbott Cell-dyn 3700 hematology analyzer (Abbott Labs, Abbott Park, IL) and confirmed by Beckman T543 cell counter (Beckman Coulter Inc., Brea, CA). Cytospins of the peritoneal cell were prepared by centrifugation at 500g for 5mins and these

Table 8
Treatment and doses employed in an in vivo rat peritonitis model.

Group	Treatment	Dose
Control	PBS	200µl
Positive control	Zymosan	5mg in 200µl PBS
Experimental 1	OPN	100µg of OPN in 200µl of PBS
Experimental 2	cOPN	100µg of cOPN in 200µl of PBS

cytopins were stained using Diff-Quik and the differential counts were determined by light microscopy.

Neutralizing OPN antibody experiment

The ability of OPN to mediate higher hepatic neutrophil chemotactic response was tested in the LPS-induced hepatitis model. Weight matched male and female SD rats were divided into control (n=6 each) and experimental groups (n=6 each). The control male and female group was further divided into PBS (n=3 each) and LPS groups (n=3 each). LPS alone group resulted in significant hepatic neutrophil infiltration 24 hrs post LPS injection (E. Coli 0111:B4, 20 mg/kg, ip in saline). The experimental male and female group was also further divided into neutralizing OPN antibody (nOPN, AF808, R&D Systems, Minneapolis, MN) alone (n=3 each) and nOPN+LPS (n=3 each) groups. The dose of the nOPN antibody (200µg/kg body weight) employed was based on the in vitro study (28), and was administered in two doses 6 hrs apart before administration of LPS. The rats were sacrificed 24hrs post LPS injection by CO₂ asphyxiation and neutrophils per ten high power fields were evaluated to test the role of nOPN to inhibit

hepatic neutrophil infiltration. In addition, hepatic necrosis was also evaluated on H&E stained liver sections in the different treatment groups.

Immunoprecipitation

Total liver homogenates were centrifuged for 15 min at 40,000 x g and the supernatant was used for the experiment. The supernatant was collected and protein concentrations was estimated using a Bio-Rad protein assay kit (Bio-Rad, Hercules, CA), by Bradford method. For immunoprecipitation, 1-5mg of protein was incubated with 10 μ g of OPN antibody (ab 8448, Abcam Inc, Cambridge, MA) overnight with rocking at 4°C. The antibody protein mixture was then incubated with 20 μ l of Protein A/G plus beads (Santa Cruz sc-2003) and incubated for 3 hrs with rocking at 4°C, after which the beads were pelleted. For washing, the beads were centrifuged at 400xg for 3mins, supernatant was removed and 1 ml of ice-cold PBS was added and rocked for 10 mins per wash. The wash was repeated 3X. The bound proteins were then eluted with equal volume of sample buffer and resolved on 8% SDS-PAGE. Proteins were transferred and blotted for α_4 , α_9 , and β_1 integrins.

Expression and purification of recombinant native and mutated N-terminal osteopontin fragments

Recombinant osteopontin fragment constructs, pGEX6P2-hnOPNc-RGD, and pGEX6P2-hnOPNc-RAA were a generous gift from Y.Yokosaki, Hiroshima University, Hiroshima, Japan (Yokosaki et al., 1999). Competent DH5 α cells were transformed with pGEX6P2-hnOPNc-RGD or pGEX6P2-hnOPNc-RAA, and grown on LB plate containing ampicillin (100 μ g/ml). Individual colonies were inoculated in 150ml

LB/Amp (100 μ g/ml) liquid media and cultures were grown at 37°C until OD600 reached 0.3-0.5. Then, isopropyl-1-thio--D-galactopyranoside (IPTG) was added to a final concentration of 100 μ M and cultures were grown for 4-6 hrs. Cells were collected and lysed by French Press Cell Disruptor (Thermo Electron Corp., MA). Glutathione S-transferase (GST) fusion proteins were purified from cell lysates with glutathion-agarose resin (Clontech, CA), and then cleaved from GST with PreScission protease (Amersham Biosciences, NJ) according to the manufacturer's protocol. Purity of the product was confirmed by 12% SDS-polyacrylamide gel electrophoresis followed by Coomassie blue staining.

Neutrophil isolation from blood

Neutrophils were isolated from fresh rat blood. Briefly, 3.5 ml of heparinized blood was layered on 3ml of Mono Poly resolving media (Bio-Med, Solon, OH), and centrifuged at 300xg for 30mins at room temperature. The layer below the plasma-media interface was collected. The cells were washed 3X and resuspended in PBS. The purity of the cells was assessed by microscope, and the viability was assessed by trypan blue staining.

Boyden chamber assay

In vitro migration assay was performed using a 6-well Transwell tissue culture plate (Costar, Corning, NY) with polycarbonate filters (0.8 μ m). Freshly isolated rat neutrophils were incubated at 37°C with different blocking antibodies [anti- β_1 , α_4 and M5 (raised against the SLAYGLR sequence of OPN protein)] at a concentration of 100 μ g/ml unless otherwise mentioned. The neutrophils in the control group were incubated

with saline. These cells were then placed in the upper chamber of the well, and the lower chambers had different concentrations of chemoattractants like OPN, cleaved OPN (cOPN), RGD mutated N-terminal of OPN, IL-8 and saline in HBSS (Hyclone, Logan, UT). After incubation at 37°C for 2 hrs, the polycarbonate filters were stained with Diff-Quik stain, and the cell numbers were quantified under a microscope.

2-D gel electrophoresis

Preparation of protein extracts for 2-D gel electrophoresis

Frozen liver tissue samples (0.1mg) were homogenized using 3ml of 2M-thiourea/7M-urea buffer (2M thiourea, 7Murea, 4%CHAPS, 50mM DTT, 0.5% ampholytes (Bio-RAD, Hercules, CA), and 1 tablet of mini protease inhibitor (total volume of 10ml), as previously described before (16,17). Briefly, frozen livers were powdered with liquid nitrogen and homogenized using a Ultra-Turrax 25 homogenizer (IKA, Wilmington, NC). Following homogenization, 300µl of 10X nuclease was added to the homogenate and vortexed occasionally for 10mins, after which they were centrifuged at 13,000xg for 15mins. The resulting supernatant was further used as the homogenate. The protein concentration of the homogenates was measured by Bradford assay with BSA as the standard (18). BioRad readyprep 2-D kit (Bio-RAD, Hercules, CA) was further used to clean up the homogenate according to the manufactures protocol. The protein concentration in the cleaned homogenates was again measured by Bradford assay. All samples were stored at -20°C until further use.

2-D methodology

2-DE was carried out for all male and female treated rats as well as the corresponding control groups. To assure 2-DE reproducibility and to prevent variations occurring due to the technique, all 2-DE gels were carried out under exactly similar conditions with 3 liver samples from each group and 2 experimental replicates. With 3 control and 3 treated animals in each group, a total of 48 gels were run altogether for the entire study (Table 9). 2-D gel electrophoresis was carried out using the Protean IEF cell (Bio-RAD, Hercules, CA) and mini electrophoresis system (Bio-Rad, Hercules, CA). 20 µg of cleaned protein were mixed with rehydration buffer (9.5M urea, 2% CHAPS, 18mM DTT, 0.5% Ampholytes, 1 tablet of mini protease inhibitor in a total 10ml volume and trace amount of Bromophenol blue), and loaded onto first dimension IPG strips (Bio-RAD, Hercules, CA; 7cm, pH 4-7). The IPG strips (Bio-RAD, Hercules, CA) were rehydrated with the samples overnight. The strips were then focused in a three-step procedure for 20,000 Volt-hour (15min at 250V; 2h with voltage ramping linearly to 4000V; finally to 20,000 V-h), and frozen at -80° C until further use.

Table 9
Table showing number of samples and replicate groups used for running 2-D gel electrophoresis in male and females alcoholic steatosis and steatohepatitis model.

Groups	Male			Female		
	Samples	Replicates	Total	Sample	Replicates	Total
Control	3	2	6	3	2	6
EtOH	3	2	6	3	2	6
Control+LPS	3	2	6	3	2	6
EtOH+LPS	3	2	6	3	2	6

Prior to second dimension SDS-PAGE, the frozen strips were equilibrated for 15min in DTT buffer (50mM Tris-Hcl, 6M Urea, 30% Glycerol, 2% SDS, 1%DTT, few grains of bromophenol blue), followed by another 15min incubation in iodoacetamide buffer (50mM Tris-Hcl, 6M Urea, 30% Glycerol, 2% SDS, 2.5% iodoacetamide, few grains of bromophenol blue) in a shaker. For 2-D separation, the IPG strips were positioned on 10% polyacrylamide gels, and the proteins were separated at 125V, room temperature.

In-gel protein visualization by silver staining

After SDS-Page, the gels were washed in ultrapure water and fixed in 30% ethanol and 10% acetic acid solution for 30mins. Prior to staining, the gels were again washed in ethanol and water for 10mins each respectively. Then the gels were sensitized 2 times for 1 mins each and stained in silver snap stain (Pierce, Rockford, IL) for 30mins. The gels were developed in the developer working solution till the spots were visible, after which, the gels were washed in ultrapure water twice for 1min. The reaction was finally stopped using 5% acetic acid for 10mins. To eliminate the concerns associated with silver staining, some of the replicate gels were also stained with SYPRO Ruby, as per the manufacturer's protocol (Bio-Rad, Hercules, CA).

Image analysis

Digitized images of the silver stained gels were analyzed using the PD quest advanced 2-D analysis software (Bio-Rad, Hercules, CA). The image analysis software was used for spot detection, quantification and analysis according to the manufacturer's instructions. Briefly, the basic analysis scheme consisted of five steps: detection of spots,

identification of landmark proteins, aligning and matching of spots in gels, quantification of matches spots and manual inspection of the spots to verify the accuracy of matching. Any errors in the spot matching procedure were manually corrected prior to the final data analysis. The spot volume was used as the analysis parameter for quantifying protein expression.

Spot excision and in-gel digestion

After identification of spots of interest, 80 μ g of protein samples were run on 17cm IPG strips, and 10% SDS-PAGE, to scale-up and enhance accurate identification as described previously in the methodology section. The gels were then stained with Commassie blue (Bio-RAD, Hercules, CA), as per the manufacturers protocol and excised. Protein spots were excised from Commassie blue stained 2nd dimension gels, which were run at the same time as the silver stained gels, using different set of apparatus. After running the 7 and 17cms gels, PD quest software was employed to match and align the proteins in both the gels. This software was also employed to pick the spots that are altered in both males and females. The excised gel plugs were approximately 2 mm in diameter and ranged from 0.75 mm to 1.0 mm in thickness. Digestion was performed similar to standard protocols (17). Briefly, the method consisted of a series of washing and dehydrating steps using 25-mM ABC (ammonium bicarbonate) and ACN (acetonitrile), respectively. The next step was reduction via DTT (Di Thiothreitol) at 60°C for 30 min followed by alkylation with IAA (iodoacetamide) for 45 min at room temperature. The gel spots then underwent another series of washing/dehydrating steps prior to digestion with trypsin at 37°C for 4 hrs.

Preparation for MALDI-MS

The MALDI matrix consists of 5 mg/ml CHCA (α -cynao-4- hydroxy cinnamic acid, a matrix solution) prepared in 50:50 ACN:ddH₂O containing 10-mM AP and 0.1 % TFA (trifluoroacetic acid). The ProMS (a sample preparation equipment that does both desalting and concentration of peptides for MS, Genomic Solutions, Ann Arbor, MI) required 10 mL solutions of both 70% ACN and 0.1% FA (formic acid), for cleaning up the samples with ziptips. A clean MALDI target was placed on the target holder in a certain position. In our case, we employed Applied Biosystems (Foster City, CA) 192 well MALDI targets with the A1 positioned in the front left hand corner. The robot was then setup to process the user-defined samples that correspond to the samples ran on the ProGest (Genomic Solutions, Ann Arbor, MI). The ProMS used a procedure similar to those used for manual ziptipping. The ProMS method (for automated spotting) used two 10 μ L sample loadings followed by washing steps and elution with the MALDI matrix described above. The location of the MALDI spots on the target was chosen prior to starting the program. Upon completion of the program the MALDI target was ready for MS analysis.

Protein identification by MALDI-MS and MALDI-MS/MS

All MALDI-MS experiments were performed using a 4700 Proteomics Analyzer (Applied Biosystems, Foster City, CA). The MS data for the MALDI plates were acquired using the reflectron detector in positive mode (700-4500 Da, 1900 Da focus mass) using 800 laser shots (40 shots per sub-spectrum) with internal calibration. Collision induced dissociation tandem MS spectra were acquired using air at the medium

pressure setting as the collision gas with 1 kV of collision energy. All MS and MS/MS data were searched against the Swiss-Prot protein sequence database using the GPS Explorer (Applied Biosystems, Foster City, CA) software.

Statistics

Group comparisons were performed using independent t-test. A one-way analysis of variance was used to determine statistical significance that might exist between more than two distributions or sample groups. Statistical analyses were made using SPSS 10.0 software (SPSS Inc., Chicago, IL). Statistical significance was set at $p \leq 0.05$.

CHAPTER III

RESULTS*

Rat alcoholic steatohepatitis model

Male and female rats fed EtOH for 6 weeks had significant fat accumulation in the liver. EtOH administered for 6 weeks followed by LPS injection resulted in fat accumulation along with multi-focal neutrophilic infiltration and oncotic necrosis (ASH) both in the males and the females. The pathology noted in the ASH model was mostly similar to that seen in human cases of ASH, with the exception of the Mallory bodies.

The body weight gain of rats both in the control and the EtOH-fed group were not different indicating no nutritional differences between the rats in the ASH and the control groups. No significant differences in the body weight between the male and the

Table 10

Comparison of the body weight of control and EtOH -fed male and female rats. * weights are indicated in grams.

Groups	Male*	Female*
Control	302±7	262± 4
EtOH	294±15	274± 18

* Reprinted with permission from “Higher neutrophil infiltration mediated by osteopontin as a likely contributing factor to the increased susceptibility of females to alcoholic liver disease” by Banerjee et al., 2006, *Journal of Pathology*, 208: 473-485, © 2006 by Wiley Interscience.

female animals in the ASH group were also observed (Table 10). There was also no difference in the average blood alcohol content in the male ($83.65 \pm 16.75\text{mg/dl}$) and female ($81.73 \pm 11.29\text{mg/dl}$) EtOH-fed rats

Liver injury as assessed by serum transaminase levels and hepatic pathology

Liver injury was assessed by the serum transaminase (ALT and AST) levels. Both in the male and the females, no or little increase in transaminase levels was observed following EtOH-alone treatment. However, a significant increase in plasma transaminase activity was noted in the females in the EtOH-treated rats following LPS challenge (Fig 8A,B). The female rats had >25-fold higher plasma transaminase activity than males indicating extensive hepatocellular injury. The H&E stained liver sections confirmed the findings of the plasma transaminase activity, with minimal or no injury in the EtOH-alone treated group both in the male and females (Fig 9), and extensive multi-focal coagulative necrosis with neutrophilic infiltration in the ASH group in females (Fig 9H). No distinct lobular pattern of injury was observed in both the sexes. The increase in plasma transaminase activity in control rats treated with LPS was minimal and histological sections corroborated the transaminase findings. Scoring of H&E-stained liver sections from EtOH-alone group suggested extensive steatosis (Fig 9C,D) in both male and female rats. However, steatosis in females was about 1.5-fold greater as compared to the males (Table 11).

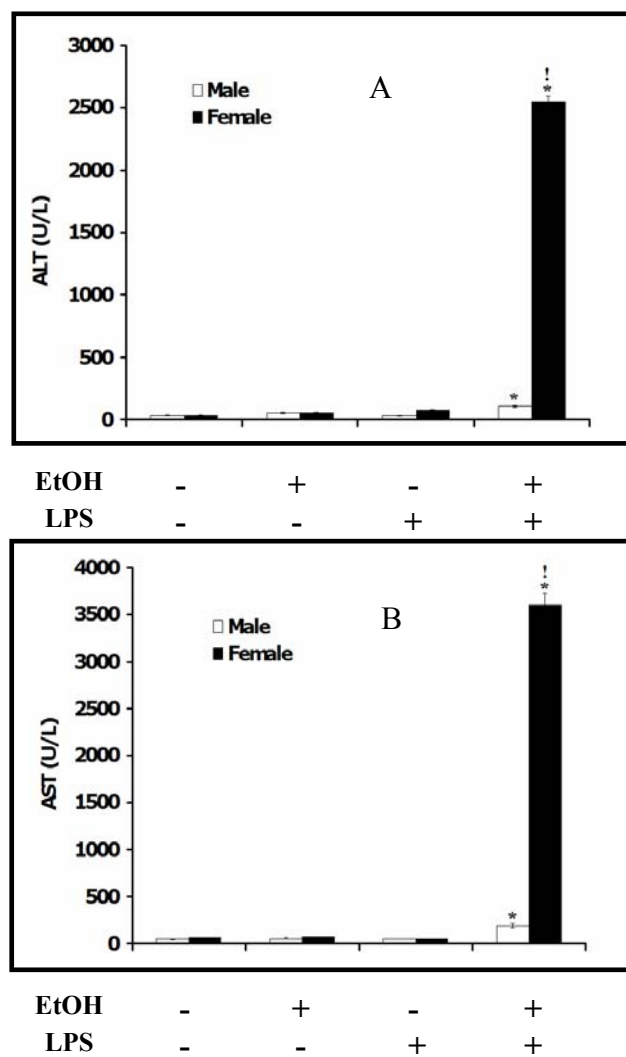


Fig. 8. ALT (A) and AST(B) activities in plasma of male and female rats fed either control or EtOH-containing Lieber DeCarli diet followed by a single dose of LPS injection * Values significantly different from the controls. ! Values significantly different from the male counterparts. Data are expressed as mean \pm SE, $p \leq 0.05$.

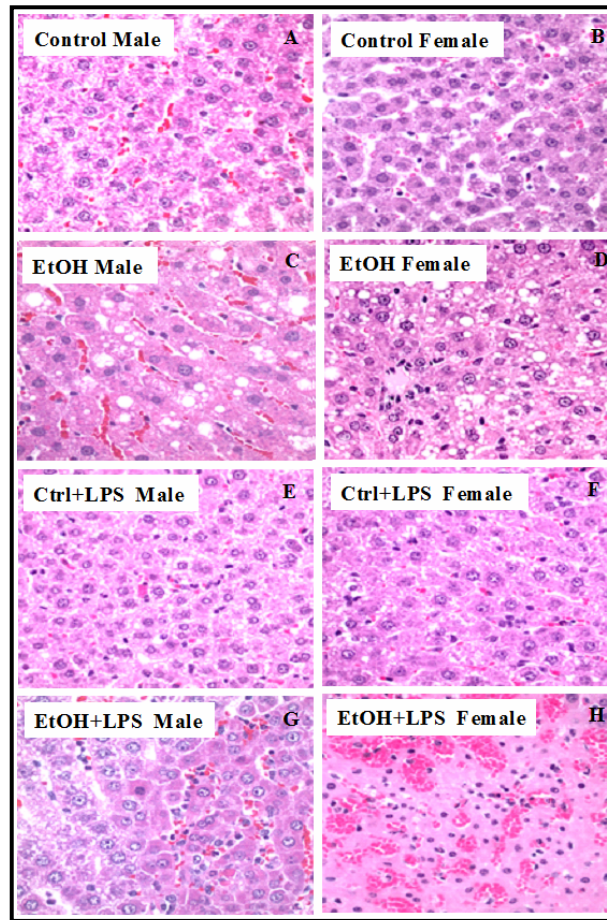


Fig. 9. Representative photomicrographs of H&E sections of male and female rats fed either control or an EtOH-containing Lieber De-Carli liquid diet for 6 weeks. The male and female rats in the ASH groups were also fed either control or an EtOH-containing Lieber DeCarli liquid diet for 6 weeks, followed by a single dose of LPS, and sacrificed 12h post-LPS injection.

Hepatic neutrophil infiltration

Neutrophilic infiltration in the male and female rats in the ASH model was confirmed by immunohistochemical chloroacetate esterase staining. LPS alone treated rats experienced mild neutrophilic infiltration in both males and females. Significantly higher neutrophilic inflammation (≥ 2 -fold) (Fig 10A, B) was observed in the females in ASH group compared to their male counterparts 12 hrs post LPS injection. Neutrophilic

infiltration and necrotic foci was noted as early as 2 hrs (Fig 10A,B) following LPS challenge in the ethanol treated female rats, but no necrotic foci was noted in the ethanol-treated male rat at this time point. The necrotic foci and neutrophilic infiltration was noted in both male and female ethanol treated rats at 12 hrs following LPS challenge. However, the neutrophilic infiltration and necrotic foci in females was 2-fold greater than their male counterparts (Table 11).

Table 11

Steatosis and neutrophilic inflammation in male and female rats in the alcoholic steatohepatitis model. *Values significantly different from the controls, $p < 0.05$. ! Values significantly different from the male counterparts, $p < 0.05$. Hepatic steatosis: <25%, 1+; <50%, 2+; <75%, 3+; >75%, 4+. Inflammation score: the number of neutrophils per five high power fields (40X) was counted. The neutrophilic foci (defined as an aggregate of ≥ 4 neutrophils) were quantitated per five-40X field (Ctrl.; Control, L; Lipopolysaccharide, E; Ethanol).

	Male (mean \pm SE, n=4)				Female (mean \pm SE, n=4)			
	Ctrl.	C+L	EtOH	E+L	Ctrl.	C+L	EtOH	E+L
Steatosis	1 \pm 0.19	1 \pm 0.3	3.5 \pm 0.83	3.5 \pm 0.79	1 \pm 0.2	1 \pm 0.19	4.9 \pm 0.7*	4.9 \pm 0.84*
Inflammation	1 \pm 0.16	1.5 \pm 0.49	0.5 \pm 0.01	3 \pm 0.32	1 \pm 0.2	2 \pm 0.35	1 \pm 0.1	6 \pm 0.59!

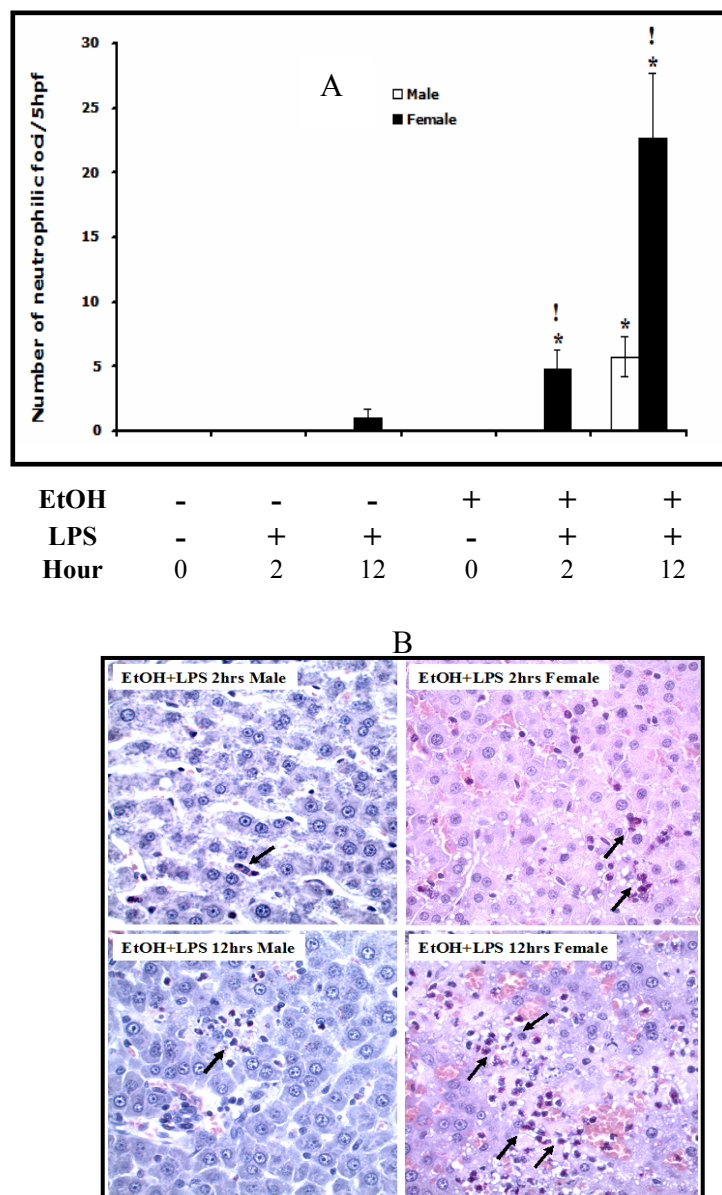


Fig. 10. Neutrophil infiltration in the liver in alcoholic steatohepatitis. (A) Kinetics of neutrophil infiltration in the liver of male and female rats fed either control or an EtOH-containing Lieber DeCarli diet and sacrificed at 2 and 12 h time points following LPS (L) injection, as described before. * Values significantly different from the male counterparts. Data are expressed as mean \pm SE, $p \leq 0.05$. (B) Representative photomicrographs of chloroacetate esterase-stained liver sections of male and female rats fed an EtOH-containing Lieber DeCarli diet for 6 weeks, followed by a single injection of LPS, and sacrificed at 2 and 12h post-LPS injection. Arrows indicate neutrophil infiltration.

Endotoxin levels

Endotoxin levels were detected in the plasma of control, control+LPS, EtOH and EtOH+LPS treated rats using standard limulus amebocyte lysate endpoint assay. EtOH treatment alone did not increase circulating levels of endotoxin, both in the male and female rats. However, increased endotoxin levels were noted in control and EtOH-fed rats after LPS challenge. There was no significant difference in the levels of plasma endotoxin between control+LPS and EtOH+LPS treated rats (Fig 11). No significant difference in plasma endotoxin level was observed in the male and female rats post LPS challenge in the ASH group.

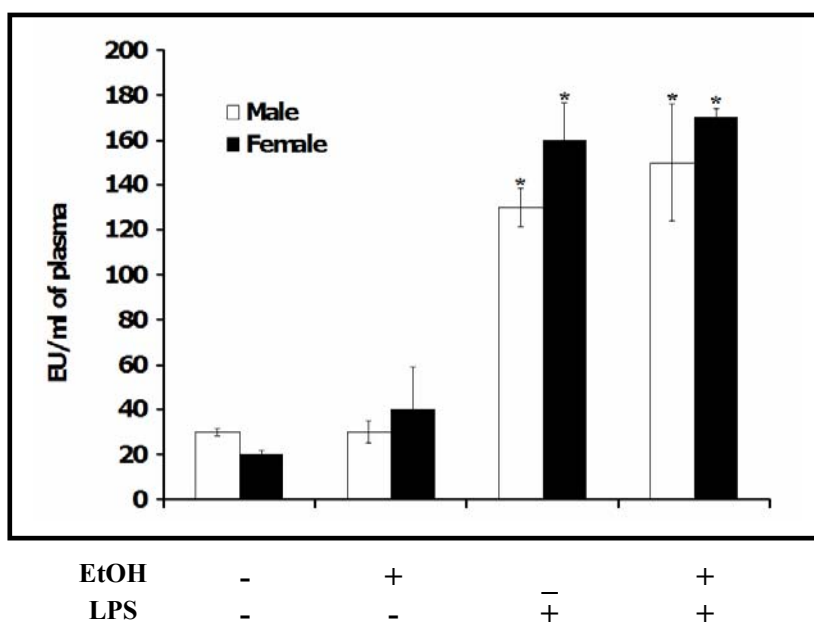


Fig. 11. Endotoxin level in plasma of male and female rats fed either control or EtOH-containing Lieber DeCarli diet followed by a single dose of LPS injection. * Values are significantly different from the male counterparts. Data are expressed as mean \pm SE, $p \leq 0.05$.

GRO/CINC-1 & IL-6 levels in plasma

To understand the mechanistic basis of higher hepatic neutrophil infiltration in females, GRO-CINC-1 and IL-6 levels were detected in the plasma of both male and female rats in the ASH model, using a standard endpoint assay. Ethanol treatment alone did not increase circulating level of GRO-CINC-1 and IL-6. However, significant increase in both GRO-CINC-1 and IL-6 level were noted in both male and female rats treated with EtOH+LPS (Fig 12A,B). An increase in GRO-CINC-1 and IL-6 level was also noted following LPS treatment alone. No significant difference in both GRO-CINC-1 and IL-6 levels were observed in the males and the females post LPS challenge in the ASH group.

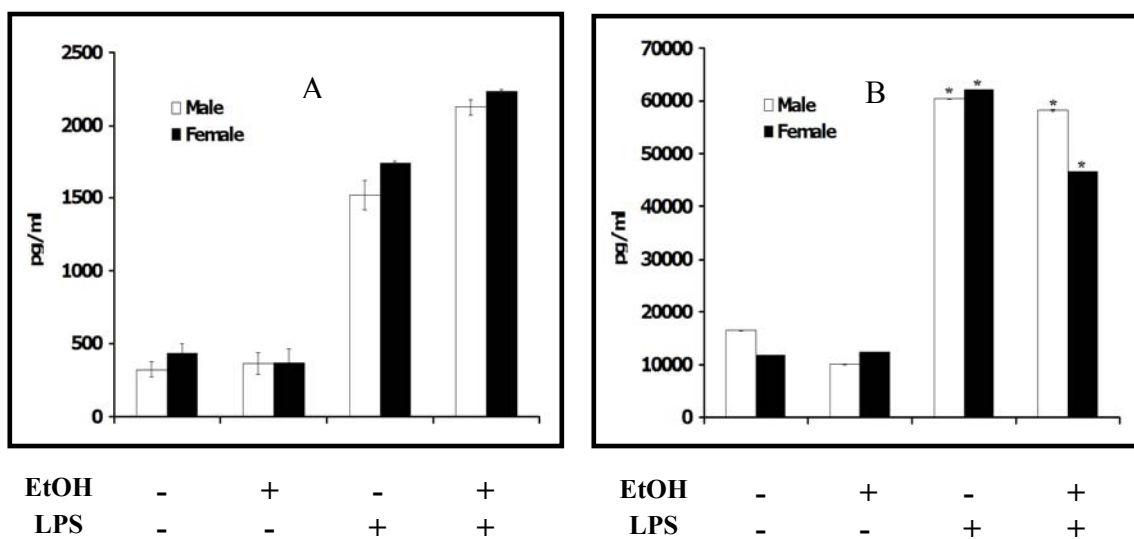


Fig. 12. GRO/CINC-1 (A) and IL-6 (B) levels in plasma of male and female rats fed either control or EtOH-containing Lieber DeCarli diet followed by a single dose of LPS injection. * Values are significantly different from the control. ! Values are significantly different from the male counterparts. Data are expressed as mean \pm SE, $p \leq 0.05$.

CYP2E1 expression and activity

Significant induction in the expression of CYP2E1 apoprotein was observed in EtOH treated male and female rats, as compared to the controls (Fig13A), indicating that ingestion of EtOH leads to higher expression of CYP2E1 apoprotein. However, no difference was observed in the induction of CYP2E1 between the ethanol treated male

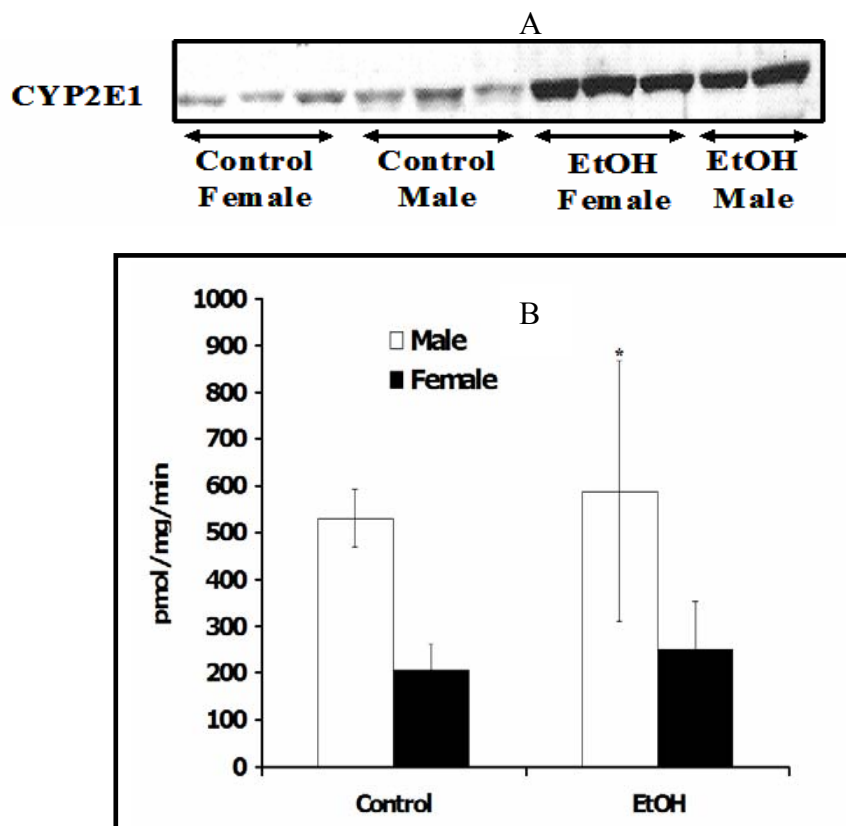


Fig. 13. Hepatic microsomal CYP2E1 protein and activity in rats fed either control or EtOH-containing Lieber DeCarli diet for a period of six weeks. CYP2E1 protein expression was detected by Western blot analysis (A) and CYP2E1 activity (B) was quantified by p-nitrophenol hydroxylation activity. *Values are significantly different from female control. Data are expressed as mean \pm SE, $p \leq 0.05$.

and the female rats. Measurement of hepatic CYP2E1 microsomal activity, by p-nitrophenol hydroxylation assay indicated that males both in the control and ethanol treated group, have higher activity as compared to their female counterparts (Fig13B).

OPN protein expression following EtOH alone treatment

EtOH ingestion resulted in induction of OPN both in the male and female rats, although statistically not significant (Fig 14A,B). However, OPN was significantly higher the female rats compared to controls (Fig 14B).

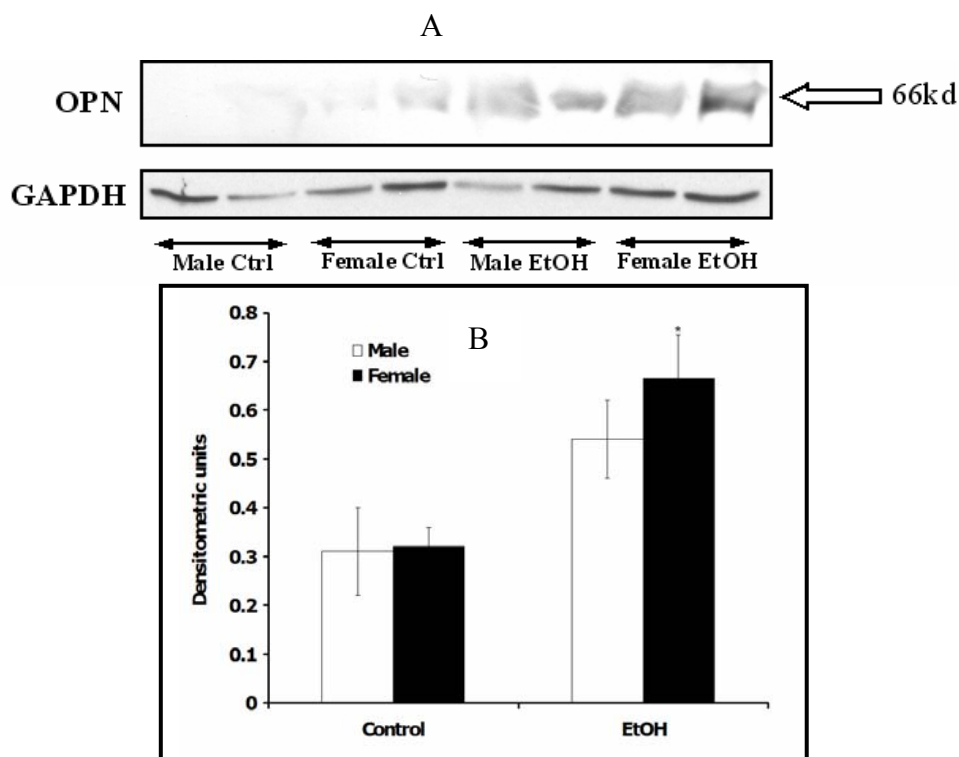


Fig. 14. Osteopontin protein expression in alcoholic steatosis. OPN protein were detected by Western blot (A) and quantified by densitometric analysis (B). The values are normalized with GAPDH, employed as an internal control for Western blot to ensure equal loading of protein. * Values are significantly different from the controls. Data are expressed as mean \pm SE, $p \leq 0.05$.

OPN protein expression following EtOH+LPS treatment

.EtOH+LPS (ASH group) treatment caused a statistically significant induction (~2-fold) of cleaved OPN in female rats compared to males (Fig 15A,B).

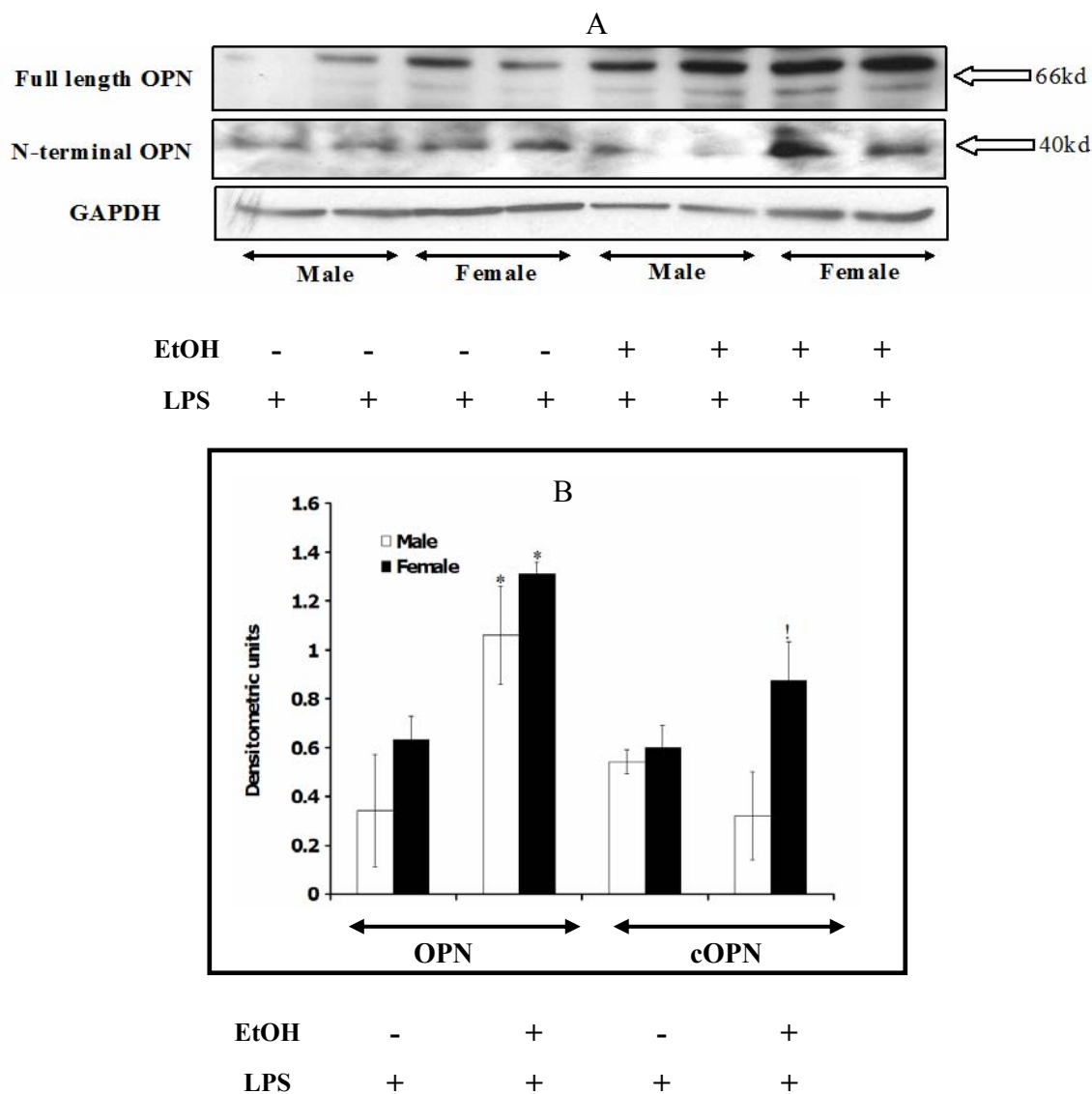


Fig. 15. Osteopontin protein expression in alcoholic steatohepatitis. (A) Representative Western blotting showing OPN expression in male and female rats in control+LPS and EtOH+LPS treated group. OPN and cOPN were detected by Western blot and quantified by densitometric analysis (B). The values were normalized with GAPDH, employed as an internal control for Western blot to ensure equal loading of protein. ! Values are significantly different from the male rats in the EtOH group. Data are expressed as mean \pm SE, $p \leq 0.05$.

The uncleaved OPN levels were significantly higher both in the males and the female rats, although statistically not significant. Induction of hepatic OPN levels was confirmed by immunohistochemistry (Fig 16). The OPN expression was predominantly localized to the biliary epithelial cells and some inflammatory cells in the hepatic parenchyma.

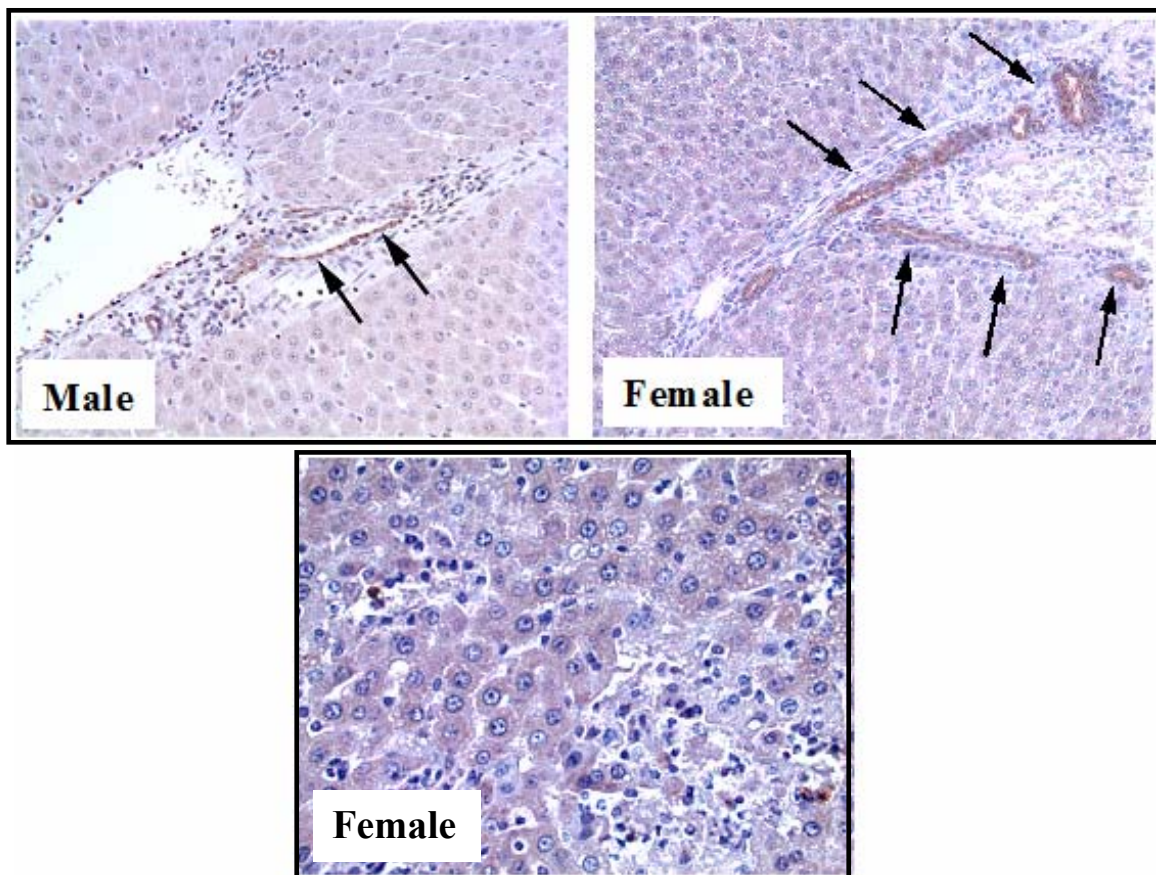


Fig. 16. Representative photomicrograph of liver sections stained for OPN in male and female rats fed EtOH-containing Lieber DeCarli diet for a period of six weeks. The dark brown stain indicates OPN staining.

OPN mRNA expression in ASH

Real time RT-PCR results showed that EtOH+LPS treated male and female rats had significantly higher expression of OPN mRNA as compared to the controls+LPS treated groups. However, the females in the EtOH+LPS treated group had about ~ 40-fold higher expression of OPN mRNA as compared to their male counterparts (Fig 17).

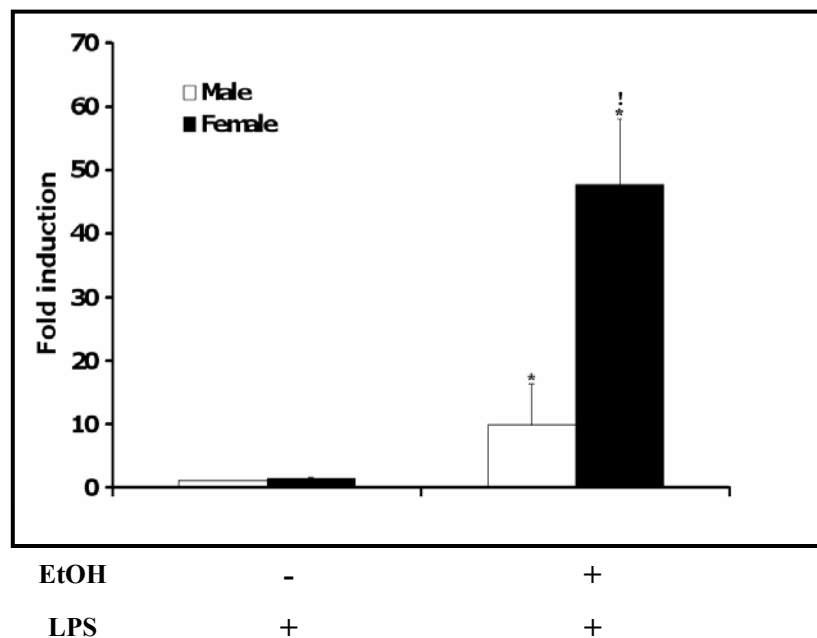


Fig. 17. Real time PCR analysis of OPN mRNA in liver of rats fed either control or EtOH-containing Lieber DeCarli diet for a period of six weeks, followed by a single injection of LPS. The values have been normalized with β -actin, the house keeping gene. * Values significantly different from the controls. ! Values significantly different from the males. Data are expressed as mean \pm SE, $p \leq 0.05$.

Localization of OPN mRNA by in-situ hybridization

In-situ hybridization was carried out to determine the precise hepatic source of the OPN mRNA expression during ASH. OPN mRNA was predominantly localized in the biliary epithelium. No or minimal signal of OPN mRNA was detected in the control and control+LPS treated groups both in the males and the females. However, the animals in the ASH group had significant induction of OPN expression as compared to the controls. OPN mRNA localization was significantly higher in the females in the ASH group as compared to their male counterparts (Fig 18B). The higher expression of OPN mRNA in the females in ASH correlated with the Real time RT-PCR data. Application of a RNA sense probe for OPN showed no signal (Fig 18A), thus confirming the selectivity of the anti-sense OPN probe.

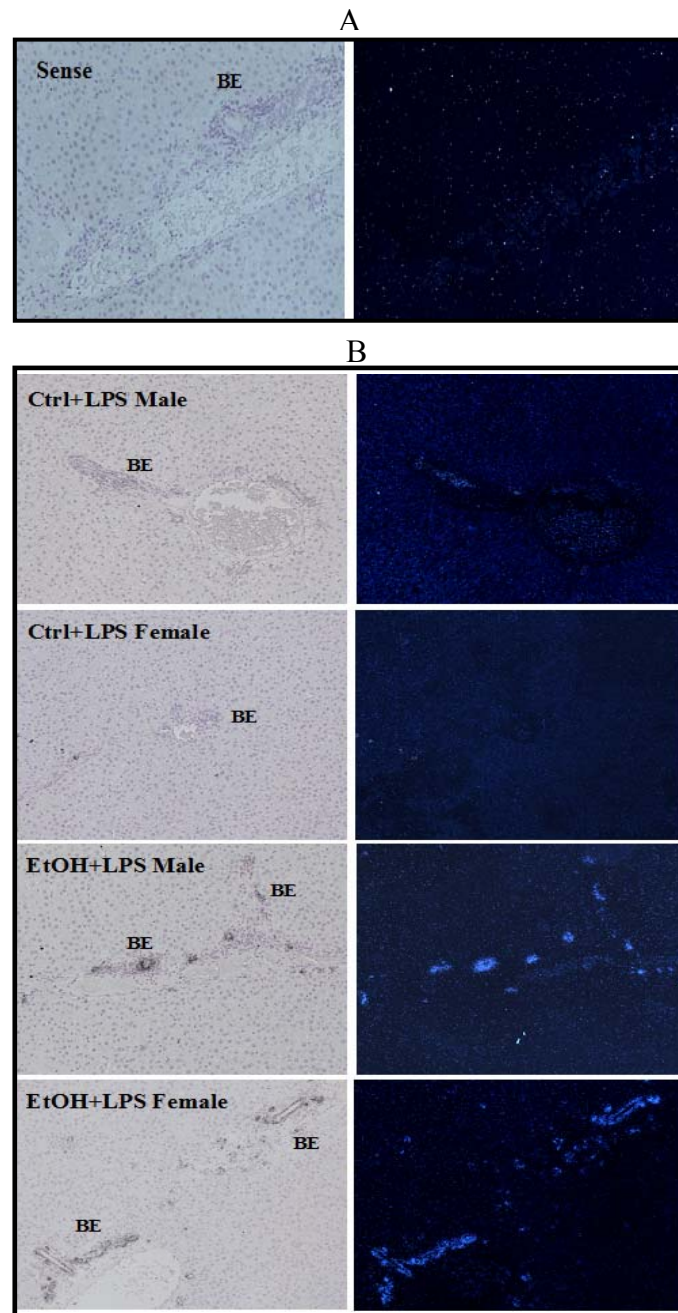


Fig. 18. In-situ hybridization analysis of OPN mRNA in the liver of male and female rats. Corresponding bright and dark field images in different groups are shown. (A) A section hybridized with radiolabelled cRNA probe served as the negative control. (B) Control+LPS and EtOH+LPS male and female sections. BE: Biliary epithelium.

Gender difference in OPN-mediated neutrophils chemotactic responses in a rat peritonitis model

A rat zymosan-induced peritonitis model (Yao et al., 2003) was modified to assess the relationship between neutrophils infiltration and OPN expression in an ASH model. Zymosan injection intraperitoneally is known to significantly enhance peritoneal neutrophil accumulation resulting in peritonitis which was confirmed by our studies (Fig. 19A). OPN-treated male and female rats showed significant increase of total WBC (>2-fold) and neutrophils (>50-fold) in the peritoneal fluid, and was comparable to that of the zymosan treated animals. Higher neutrophil infiltration was also noted in the cOPN treated animals (Fig 19B). However, when the OPN and cOPN chemotactic response was compared between males and females, there was no gender differences in the total WBC and neutrophil numbers noted in this model.

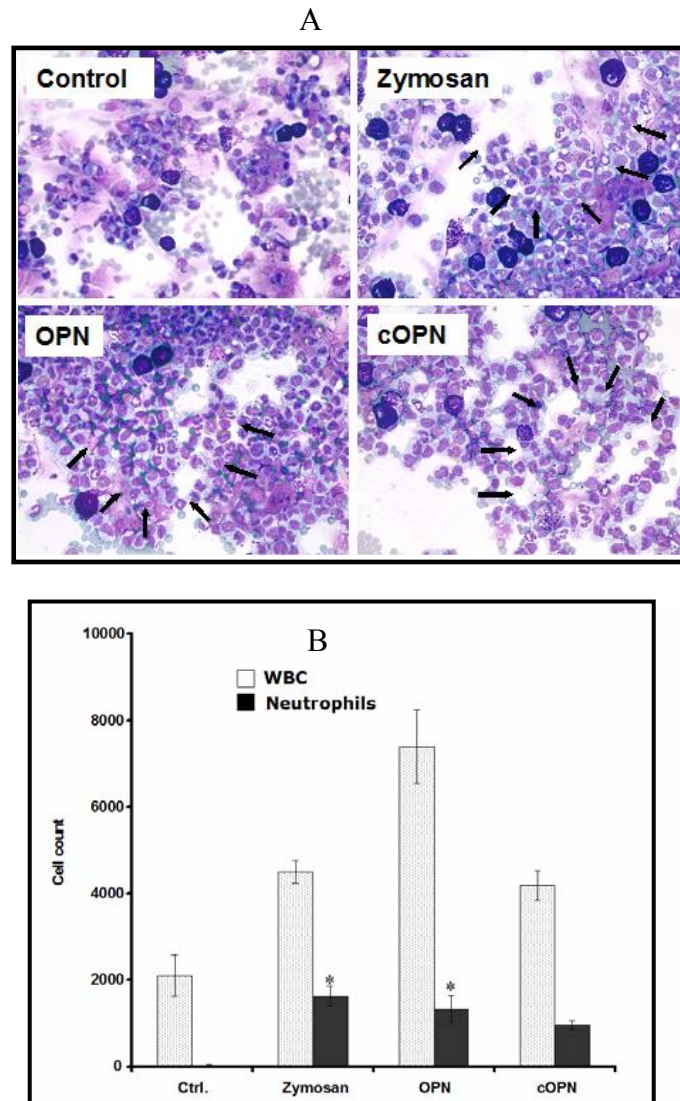


Fig. 19. Peritonitis experiment in a rat model. Representative photomicrograph of Diff-Quik R stained (A) peritoneal fluid, showing WBC and neutrophils in control, zymosan , OPN and cOPN treated animals. SD rats were sacrificed 4 hrs post injection and peritoneal fluid was collected and (B) quantified as mentioned in the materials and methods section Arrows indicate neutrophils in the peritoneal fluid.

OPN neutralizing antibody experiment

nOPN antibody intervention experiments were carried out in LPS-hepatitis rat model to confirm further the contributing role of OPN in higher neutrophils infiltration in females during ASH. Both male and female LPS-treated group had significant hepatic

neutrophilic infiltration compared to the control (Fig 20). nOPN administration prior to LPS injection resulted in an approximately 50% reduction in hepatic neutrophil infiltration compared with the LPS-alone group, in both males and females. nOPN-alone injection did not result in increased neutrophils in the liver parenchyma. Higher hepatic neutrophil infiltration correlate significantly with hepatic necrosis, and administration of nOPN prior to LPS injection reduced multi-focal hepatic necrosis remarkably in both male and female rats.

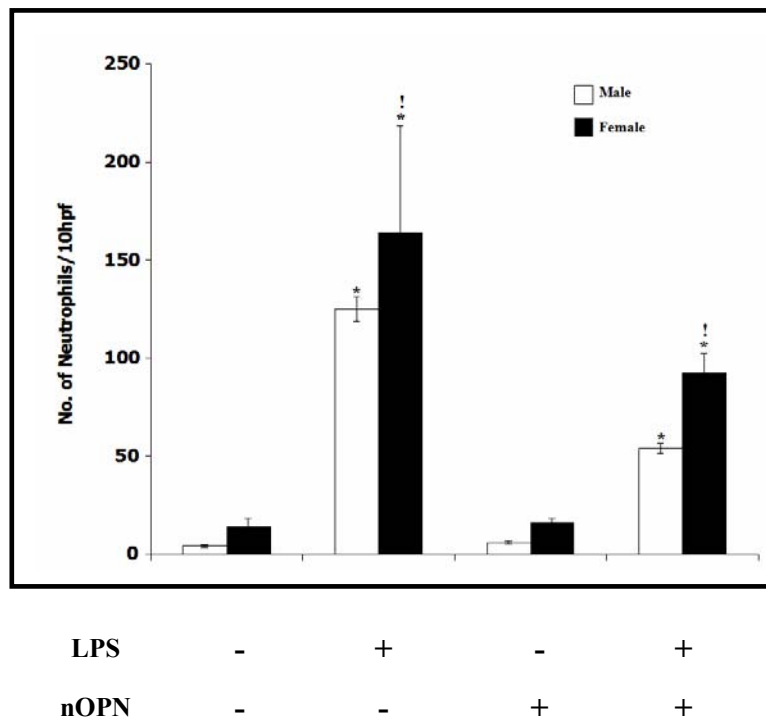


Fig. 20. Enumeration of hepatic neutrophils following nOPN administration in the LPS hepatitis model. The number of neutrophils per 10 high power fields (hpf) was measured in chloroacetate esterase-stained liver sections of male and female rats treated with either PBS, LPS+PBS, nOPN or nOPN+LPS. * Values significantly different from the controls. ! Values are significantly different from the nOPN+LPS-treated group. Data are expressed as mean \pm SE, $p \leq 0.05$.

Analysis of neutrophil activation (expression of β_2 integrin) by OPN in vitro

Activation of neutrophils by OPN was analyzed based on the upregulation of CD11b by flow cytometry. Neutrophils incubated with OPN and cOPN in vitro showed a significant increase in CD11b integrins compared to the controls, indicating that activation of neutrophils by OPN take place via CD11b or Mac1 (Fig 21).

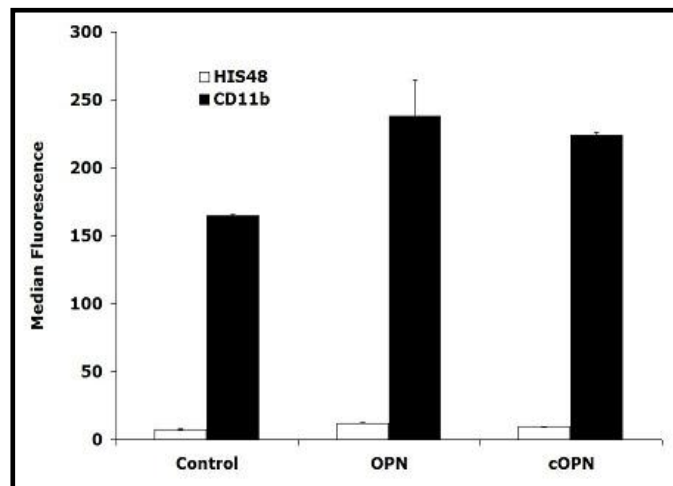


Fig. 21. Flow cytometric analysis of CD11b expression. Neutrophils were incubated in vitro with OPN and cOPN, and then labeled with HIS 48 and CD 11b antibodies. * Values significantly different from the controls. Data are expressed as mean \pm SE, $p \leq 0.05$

Role of osteopontin in neutrophil mediated-integrin signaling

Effect of EtOH+LPS feeding on α_4 , α_9 , and β_1 integrin protein expression

Previously we have shown that EtOH+LPS feeding increases hepatic neutrophil infiltration and liver injury in females. Also, both intact and thrombin cleaved OPN induction appear to correlate with hepatic neutrophil infiltration and liver injury. Interestingly, cleavage of OPN exposes the SLAYGLR sequence, which promotes the adherence and migration of cells exposing $\alpha_4\beta_1$, and $\alpha_9\beta_1$ integrin (Green et al., 2001). In this study, EtOH+LPS treatment caused significant induction of α_4 and β_1 integrins in the females as compared to their male counterparts (Fig 22A, B). Although the expression of α_9 integrin appeared to be higher in females in this group, it was not statistically significant compared to the males (Fig 22A, B). The females in the EtOH+LPS group had significant induction of α_4 , α_9 and β_1 integrin as compared to their controls.

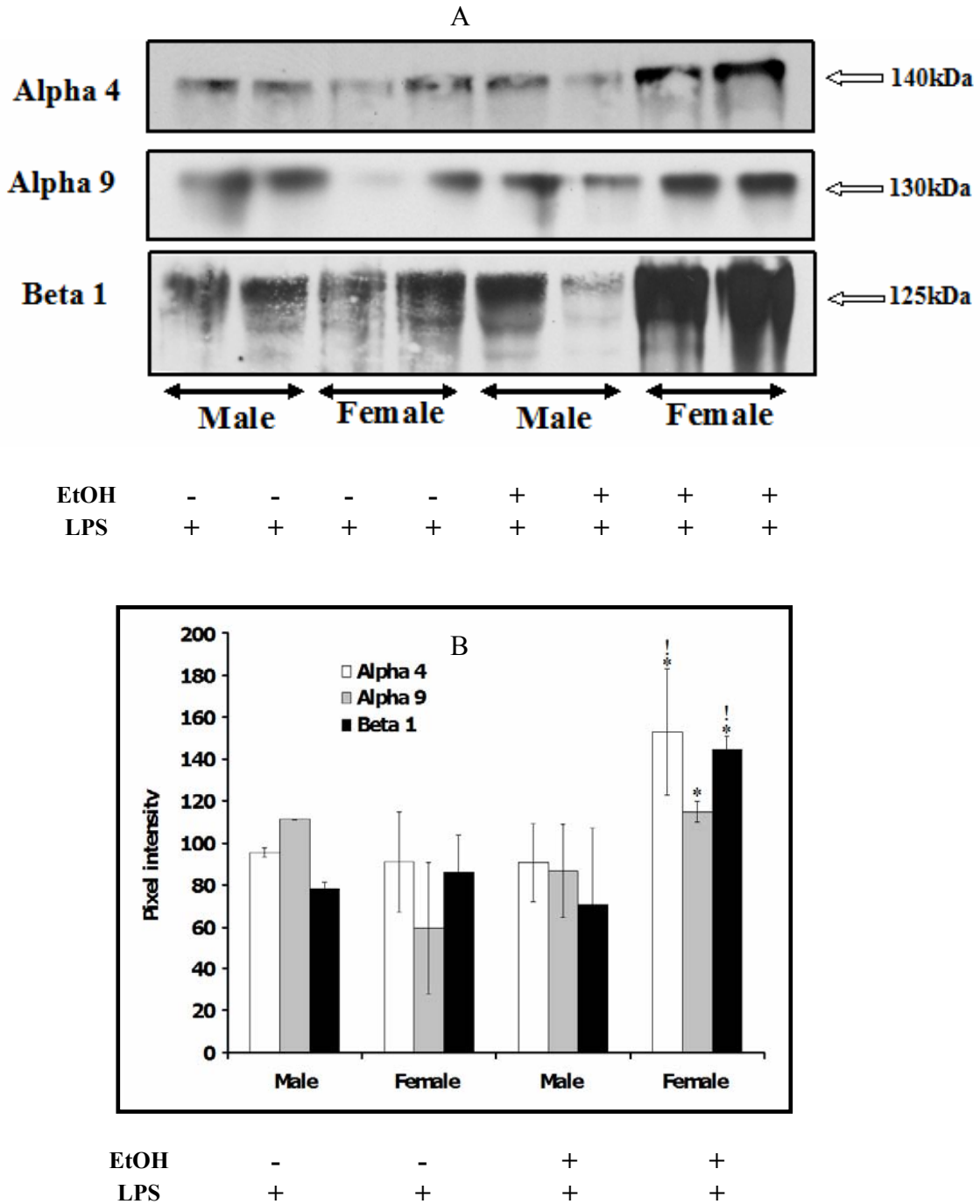


Fig. 22. Representative Western blots showing α_4 , α_9 and β_1 integrin protein expression in rats fed either control or EtOH-containing Lieber-DeCarli liquid diet for six weeks followed by a single dose of LPS. α_4 , α_9 and β_1 was detected by Western blot (A) and quantified by densitometric analysis (B). * Values significantly different from the controls. ! Values are significantly different from the male rats in the EtOH+LPS group. Data are expressed as mean \pm SE, $p \leq 0.05$.

Effect of EtOH+LPS feeding on α_4 , α_9 , and β_1 integrin mRNA expression

Real-time RT-PCR showed a significant increase in α_4 and α_9 mRNA in the females in EtOH+LPS treated group as compared to the males (Fig 23A,B).

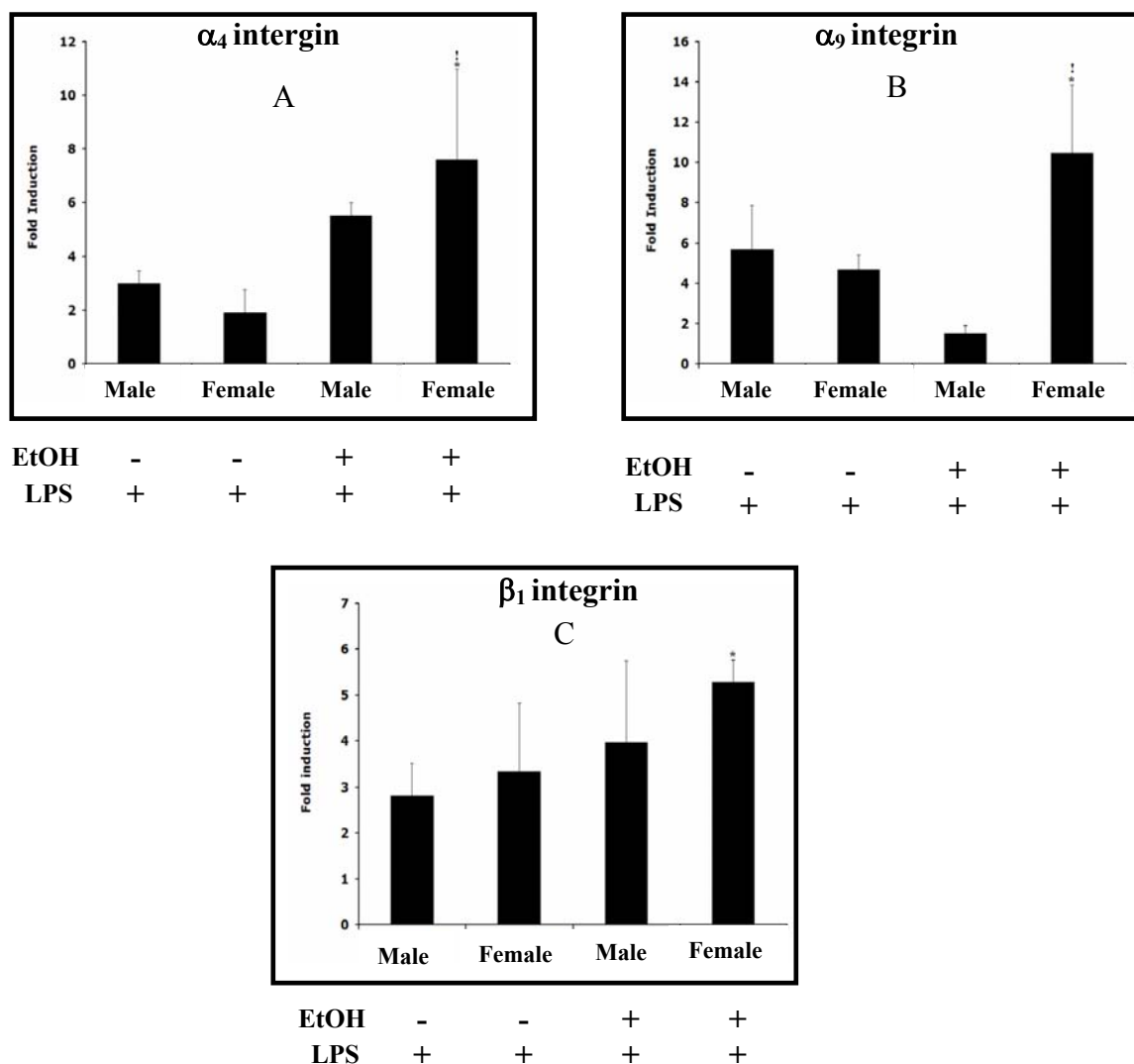


Fig. 23. Real time PCR analysis of α_4 (A), α_9 (B), β_1 (C) mRNA in the liver of rats fed either control or EtOH containing Lieber-DeCarli diet for a period of six weeks, followed by a single dose of LPS. The values have been normalized with β actin, the housekeeping gene. * Values significantly different from the controls. ! Values are significantly different from the male rats in the EtOH+LPS group. Data are expressed as mean \pm SE, $p \leq 0.05$.

Although females in the ASH group had increase in the mRNA expression of β_1 integrin as compared to the males, this was not significantly different (Fig 23C). When the females in the ASH group were compared to its control, there was significantly higher mRNA expression of α_4 and α_9 integrins (Fig 23A,B).

Immunoprecipitation to assess binding of OPN to integrins

Since OPN promoted the adherence of cells expressing $\alpha_4\beta_1$ and $\alpha_9\beta_1$ integrins, we wanted to test if OPN is binding to these integrins. Total liver homogenates immunoprecipitated with OPN antibody were found to coimmunoprecipitate α_4 , α_9 and β_1 integrins both in the male and females, suggesting that OPN binds to these integrins in our ASH model (Fig 24). IgG was used as a negative control for these experiments.

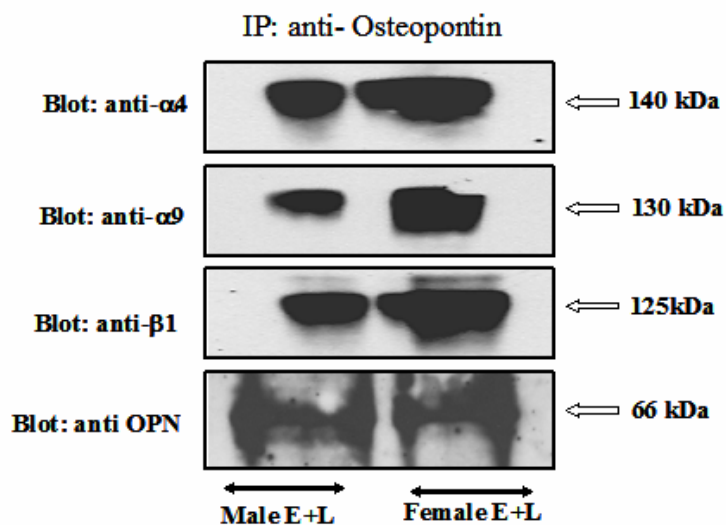


Fig. 24. Immunoprecipitation assay to detect the binding of OPN to $\alpha_4\beta_1$ and $\alpha_9\beta_1$ integrin in EtOH+LPS treated male and female rat. The cell lysates were immunoprecipitated with rabbit OPN antibody, and separated by SDS-PAGE and detected with anti α_4 , α_9 and β_1 antibodies as described in the materials and the methods section.

Effect of neutralizing OPN antibody on α_4 , α_9 , and β_1 integrin protein expression

In order to assess the specificity of OPN interaction with these integrins, α_4 , α_9 and β_1 integrin expression was evaluated in a nOPN antibody intervention experiment, in a rat model of LPS mediated hepatitis.

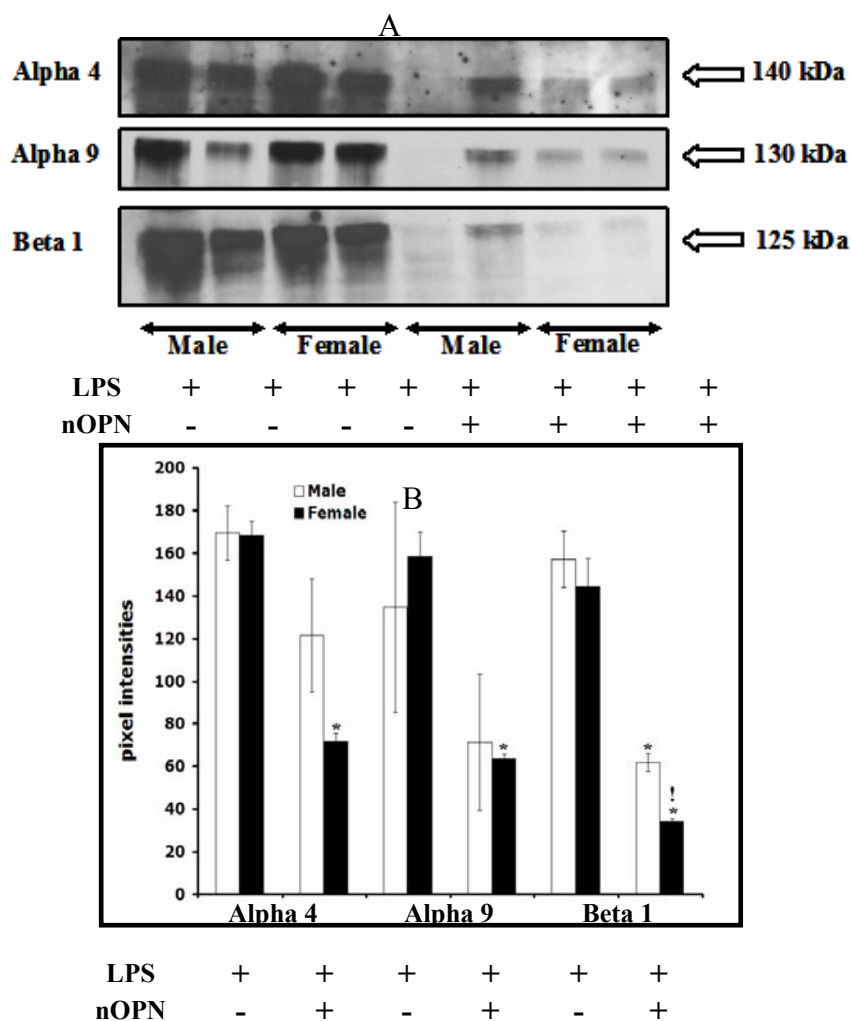


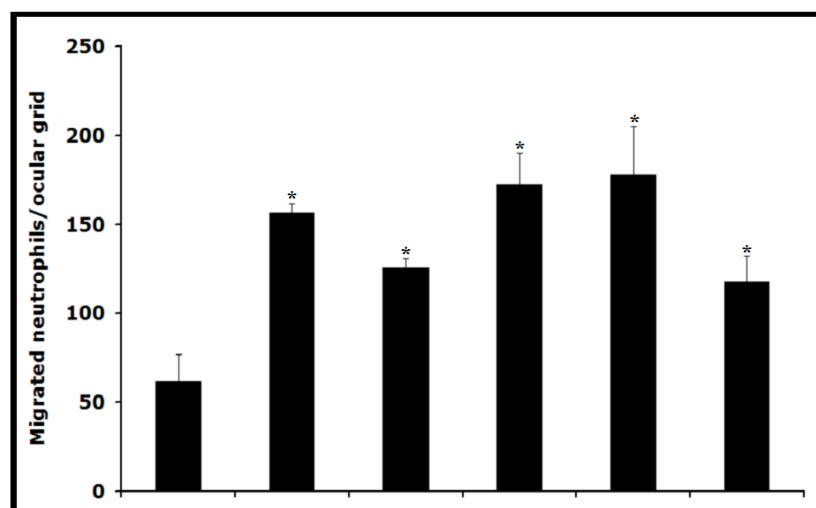
Fig. 25. Representative Western blotting showing α_4 , α_9 and β_1 integrin protein expression in rats injected with either LPS or nOPN+LPS. α_4 , α_9 and β_1 integrins was detected by Western blot (A) and quantified by densitometric analysis (B). * Values significantly different from the controls. ! Values are significantly different from the male rats in the EtOH+LPS treated group. Data are expressed as mean \pm SE, $p \leq 0.05$.

LPS mediated hepatitis model was employed since LPS alone induces higher expression of these integrins. Compared to the LPS treated animals, the nOPN antibody treated male and female rats showed down regulation of protein expression of α_4 , α_9 , and β_1 integrins (Fig 25A,B).

Role of OPN and α_4 , α_9 and β_1 integrins on neutrophil migration

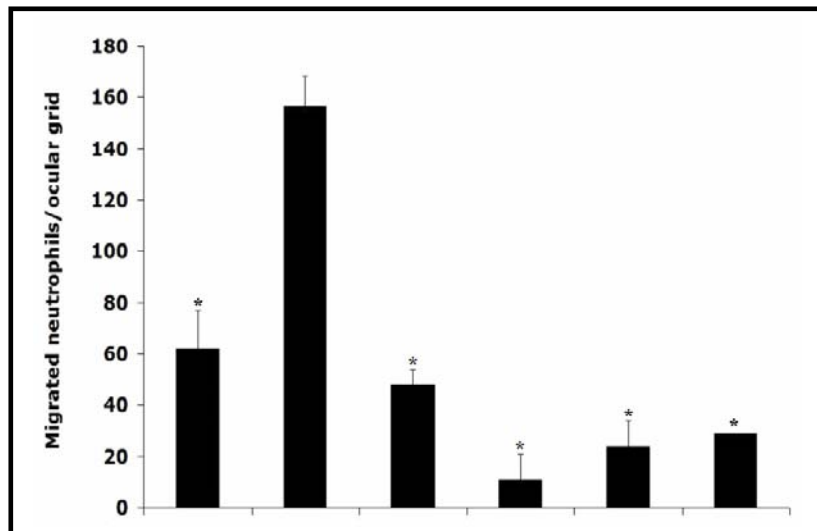
To determine whether OPN functions in the migration of neutrophils, studies of chemotaxis were performed in modified Boyden chambers. Addition of IL-8 (a well-known chemoattractant for neutrophils), to the lower side of the chamber resulted in chemotaxis of freshly isolated neutrophils. Addition of recombinant full length OPN was found to attract about 3-fold higher neutrophils at both the (50ng/ml and 500ng/ml) doses as compared to the controls. Compared to full-length OPN, cOPN was found to attract more neutrophils (Fig 26). Both the N-terminal fragment and the mutated N-terminal fragment (mutated RGD sequence) appeared to be similar in their ability to attract neutrophils (4-fold compared to controls) suggesting that the RGD sequence of OPN was playing a minimal role in attracting neutrophils in this model. To further assess if cOPN is mediating its neutrophil chemotaxis effects through α_4 , α_9 and β_1 integrins, studies were performed using antibodies with specificity towards different integrins and SLAYGLR sequence of OPN. Antibodies directed against α_4 integrins inhibited cOPN-mediated neutrophil migration by more than 4-fold, whereas those directed against β_1 integrins were found to be more potent and inhibited neutrophil migration by more than 8-fold. More interestingly, the antibody M5 directed against SLAYGLR peptide (Yamamoto et al., 2003), also inhibited (>5-fold) the migration of neutrophils (Fig 27).

The M5 antibody is reported to inhibit the interaction between the OPN cryptic epitope with its receptors $\alpha_4\beta_1$ and $\alpha_9\beta_1$ integrins (Diao et al., 2004).



OPN (ng/ml)	0	50	500	0	0	0
N-terminal, cOPN (ng/ml)	0	0	0	50	0	0
N-terminal, cOPN (mutated RGD ng/ml)	0	0	0	0	50	0
IL-8 (ng/ml)	0	0	0	0	0	50
IgG (ng/ml)	50	0	0	0	0	0

Fig. 26. Boyden chamber experiment to test migration of neutrophils toward OPN and c-OPN. Neutrophils isolated from blood was incubated with different concentration of OPN, cOPN (N-terminal) and cOPN with mutated RGD sequence as mentioned in the materials and methods section. Migrated cells were stained with Diff-Quik stain, and quantitated. * Values significantly different from the controls. Migration assays were also performed in the presence of various antibodies to assess the role of α_4 , β_1 and SLAYGLR sequence in migration of neutrophils towards OPN. Migrated cells were stained with Diff-Quik stain and quantitated. * Values are significantly different from the OPN group.



OPN (ng/ml)	0	50	50	50	50	50
anti-Alpha 4 ($\mu\text{g/ml}$)	0	0	100	0	0	0
anti-Beta 1 ($\mu\text{g/ml}$)	0	0	0	100	0	0
M5 ($\mu\text{g/ml}$)	0	0	0	0	10	100
IgG ($\mu\text{g/ml}$)	0	100	0	0	0	0

Fig. 27. Boyden chamber experiment to assess the role of α_4 , β_1 and SLAYGLR sequence in migration of neutrophils towards OPN. Migrated cells were stained with Diff-Quik stain and quantitated. * Values are significantly different from the OPN group.

Influence of estrogen on osteopontin and hepatic neutrophil infiltration in females

Role of alcohol in influencing estrous cycle

Consistent with Long and Evans (1922), estrous cycle in normal rats in this study were found to be 4 days long for about 88% of the animals studied. The remaining animals were either 5 day cyclers or they cycled irregularly. Only animals cycling for 4 days were fed EtOH in Lieber DeCarli diet for six weeks. After the initiation of EtOH-feeding, the animals were found to have prolonged diestrus cycle marked by the predominance of leukocytes and nucleated epithelial cells in the vaginal smear, indicating that EtOH was interfering with the estrous cycle in these rats (Fig 28 A, B).

Role of estrogen in alcohol-mediated liver pathology

Both the intact and the ovariectomized females had little or no increase in plasma transaminase (ALT) activity following EtOH alone treatment. A significant increase in plasma transaminase activity was noted in both the intact and ovariectomized group following EtOH+LPS treatment as compared to the respective controls (Fig 29A).

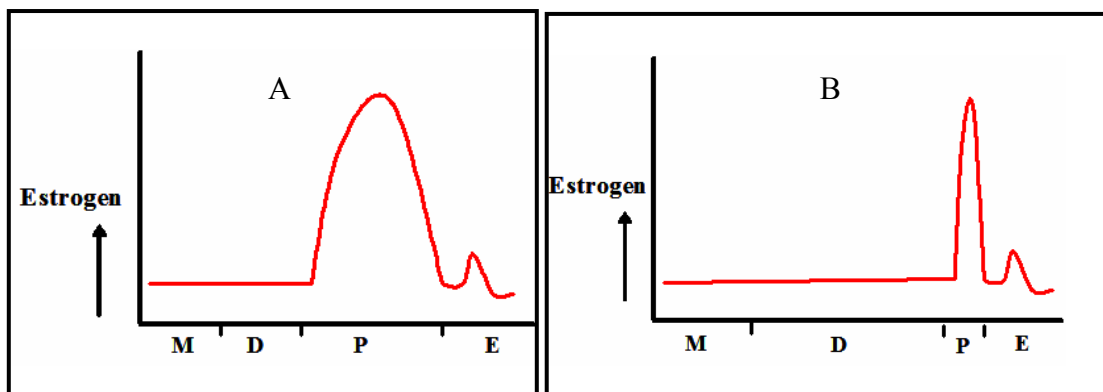


Fig. 28. Schematic representation of the different stages of the estrous cycle of the representative rat before (A) and after (B) ethanol treatment. M: Metestrus; D: Diestrus; P: Proestrus; E: Estrus.

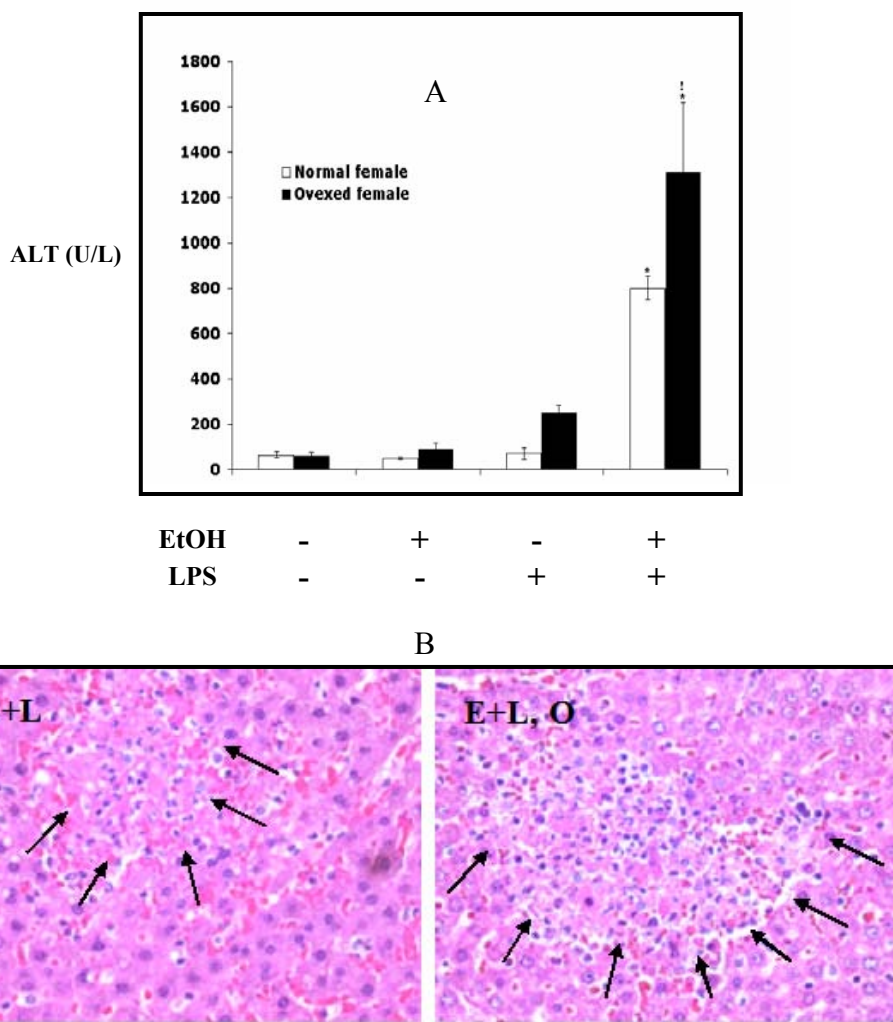


Fig. 29. Liver injury in normal and ovariectomized rats. ALT (A) activities in plasma of normal and ovariectomized female rats fed either control or EtOH-containing Lieber DeCarli diet followed by a single dose of LPS injection and sacrificed 12 hours thereafter, as described in the materials and methods section. * Values significantly different from the controls. ! Values are significantly different from the male counterparts. Data are expressed as mean \pm SE, $p \leq 0.05$. (B) Representative photomicrographs of H&E stained liver sections of normal and ovariectomized female rats fed EtOH-containing Lieber-DeCarli diet for 6 weeks, followed by a single dose of LPS and sacrificed 12hrs post LPS injection. Arrows indicate neutrophil infiltration. (E: Ethanol, L: Lipopolysaccharide; O: Ovariectomy).

When the liver injury was compared, the ovariectomized females in EtOH+LPS treated group had about 1.5 fold higher plasma transaminase activity as compared to the

intact female in the same group indicating higher hepatocellular injury. H&E stained liver sections confirmed the findings of the plasma transaminase activity showing increased multifocal necrosis and neutrophilic infiltration in the ovariectomized EtOH+LPS treated animals as compared to the normal EtOH+LPS treated animals (Fig 29 B).

To assess the effect of estradiol on hepatic injury, plasma transaminase activity was also evaluated in ovariectomized+ E2 implanted rats fed EtOH+LPS. Compared to the ovariectomized group, all the animals in the estrogen implanted group had significant decrease in plasma transaminase activity. However, a somewhat biphasic response to ASH was observed in the ovariectomized+E2 implanted rats. Low doses of E2 (0.18g, 0.36mg) resulted in significant down-regulation of plasma transaminase activity, however with the highest E2 employed dose (1.7mg), the degree of protection appear to decrease based on elevation of plasma transaminase activity (Fig 30 A). Animals treated with 0.36mg dose of E2 seemed to have the least liver injury in these groups. The plasma transaminase activity was further confirmed with H&E stained liver sections, where minimum or no neutrophilic infiltration and multi-focal coagulative necrosis was observed in animals treated with 0.36mg estrogen (Fig 30 B). In animals treated with 0.72mg and 1.7mg E2, an increase in neutrophilic infiltration and multi-focal necrosis was observed.

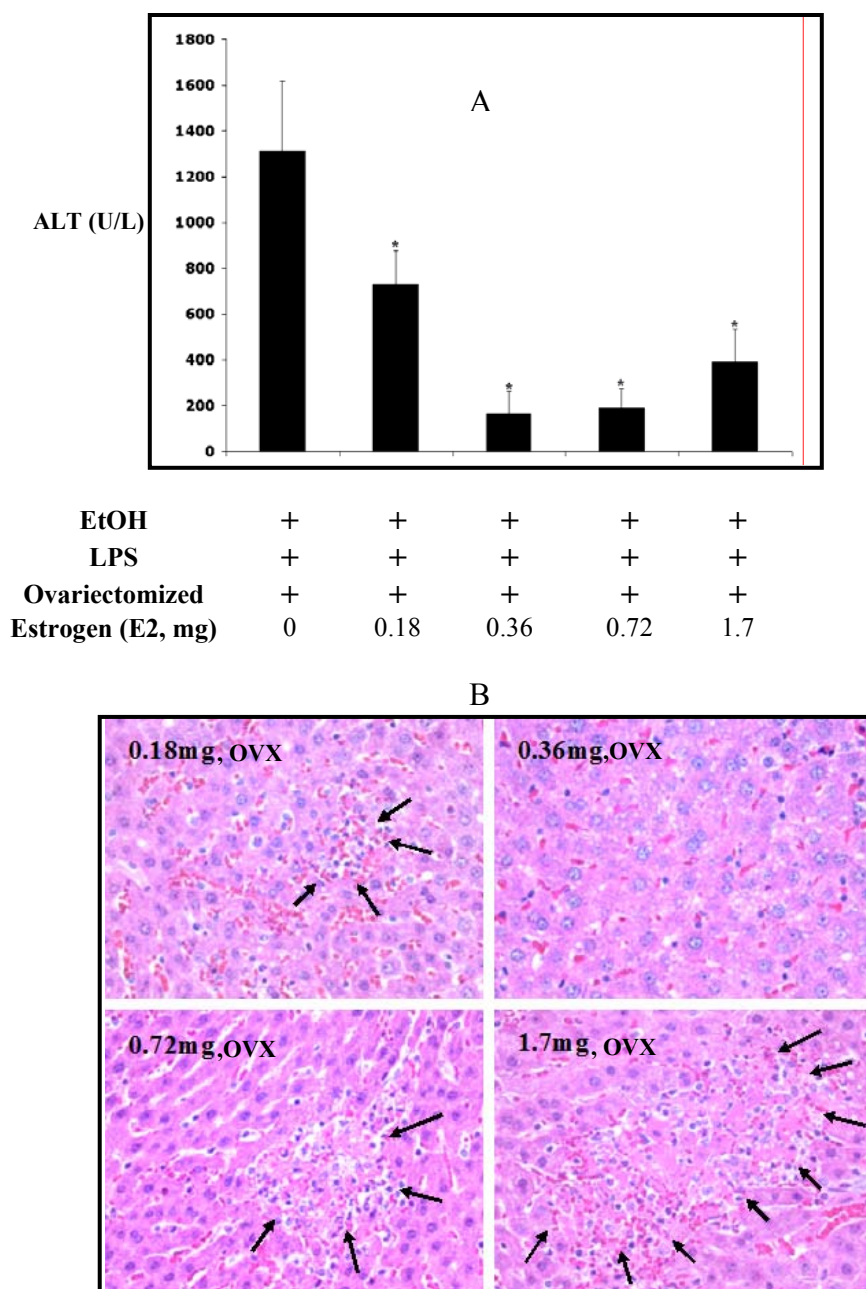


Fig. 30.Effect of estrogen on liver injury. ALT (A) activities in plasma of ovariectomized and ovariectomized + estrogen implanted female rats fed either control or EtOH-containing Lieber DeCarli diet followed by a single dose of LPS injection and sacrificed 12 hours thereafter, as described in the materials and methods section. * Values are significantly different from the controls. Data are expressed as mean \pm SE, $p \leq 0.05$. (B) Representative photomicrographs of H&E stained liver sections of ovariectomized+estrogen implanted female rats fed EtOH-containing Lieber-DeCarli diet for 6 weeks, followed by a single dose of LPS and sacrificed 12hrs post LPS injection.

Relation between hepatobiliary osteopontin expression and estrogen in ASH

A decrease (~2 fold) in the level of OPN protein was observed in the ovariectomized animals treated with EtOH+LPS+E2 (0.18mg, 0.36mg, 0.72mg) as compared to the EtOH+LPS alone treated group. However, the animals treated with 1.7mg dose of estrogen experienced >2.5-fold higher expression of OPN protein as compared to the EtOH+LPS alone treated group (Fig 31A,B). Similar pattern of induction of hepatic OPN protein was also confirmed by immunohistochemistry (Fig 32), where animals treated with 0.18mg and 0.36mg dose of E2 had little expression of OPN, with maximal expression at the highest dose of E2 employed in this study.

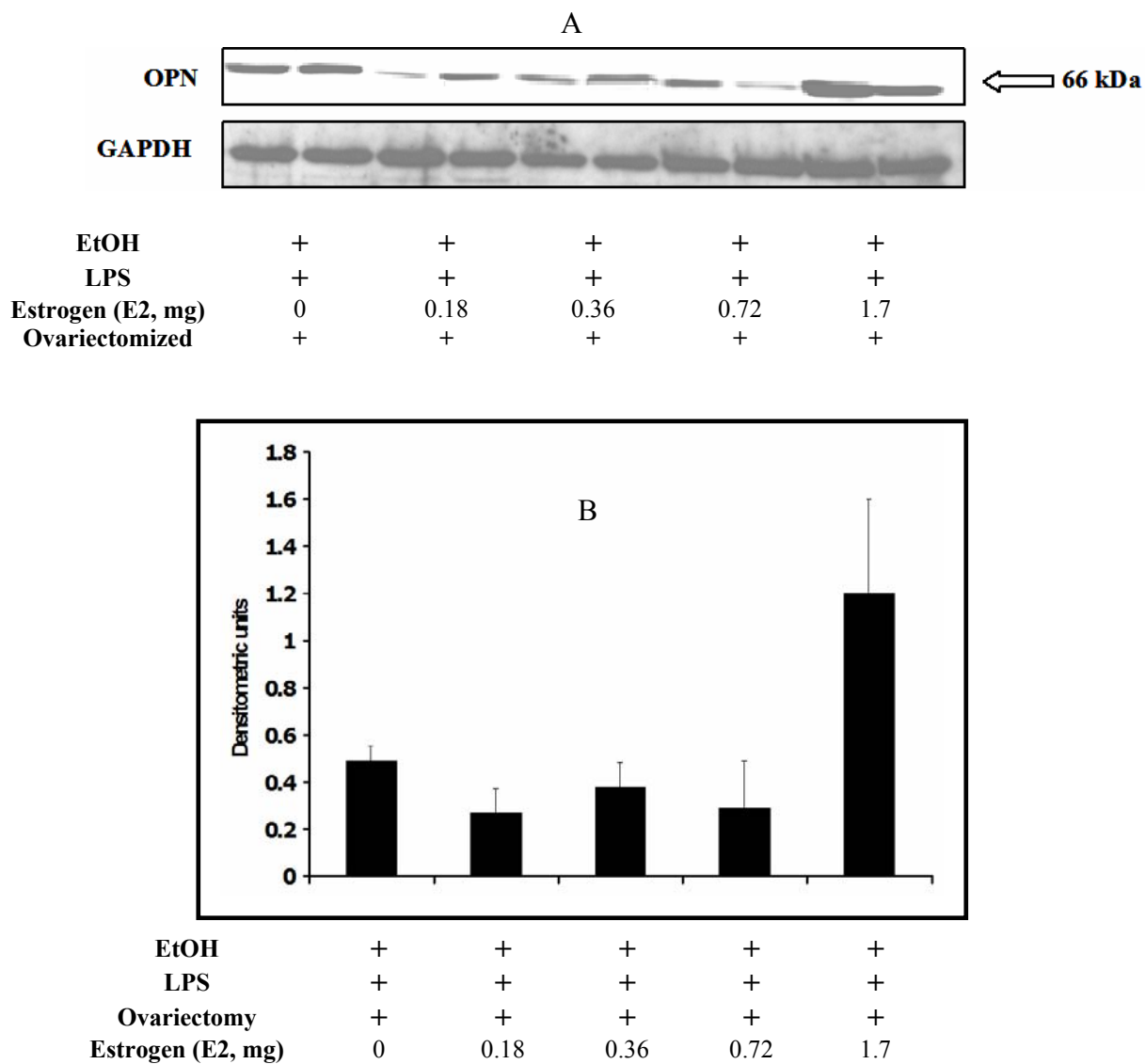


Fig. 31. OPN protein expression in ovarioctomized rats. Representative Western blotting (A) showing OPN expression in ovarioctomized female rats fed EtOH-containing Lieber-DeCarli diet for 6 weeks as mentioned in the materials and methods section. OPN was detected by Western blot and quantified by densitometric analysis (B). The values were normalized with GAPDH, employed as an internal control for Western blot to ensure equal loading of protein. * Values are significantly different from the controls. Data are expressed as mean \pm SE, $p \leq 0.05$. (C)

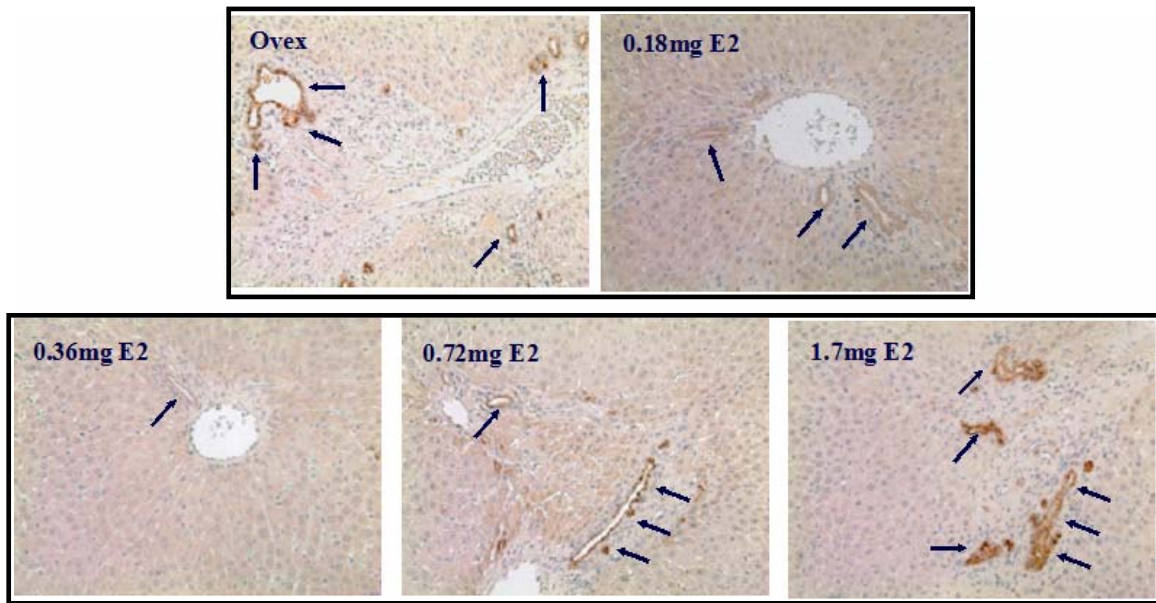
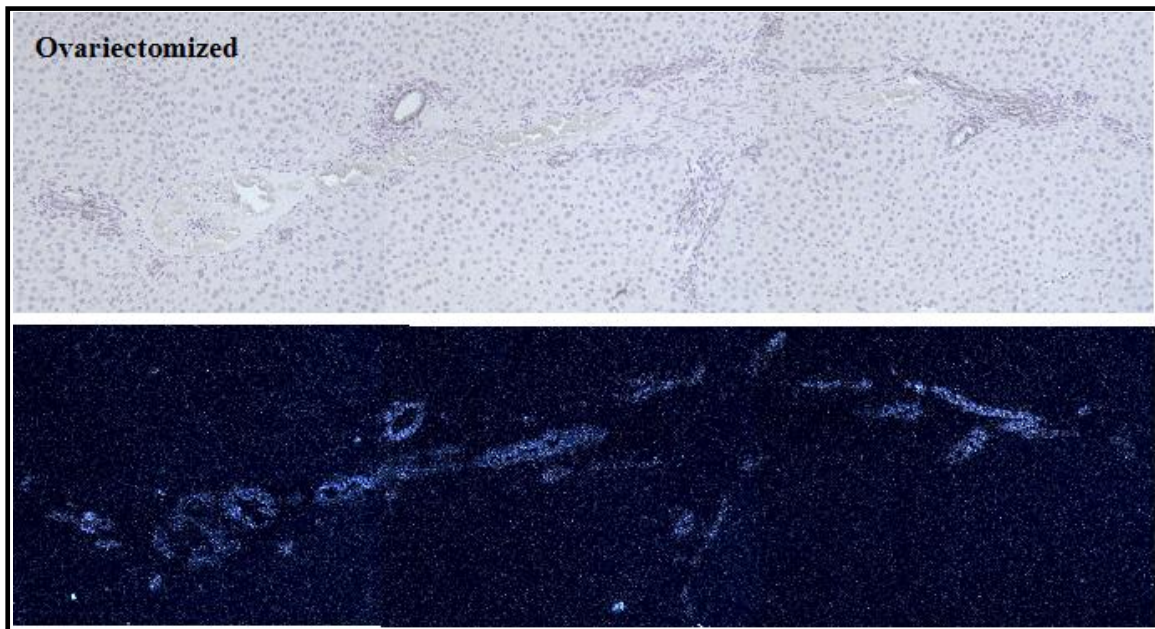


Fig. 32. Representative photomicrograph of liver sections stained for OPN in ovariectomized female rats fed EtOH-containing Lieber-DeCarli diet. The dark brown stain indicates OPN staining. Arrows indicate biliary epithelial cells stained positive for OPN.

Localization and expression of OPN mRNA by in-situ hybridization

In-situ hybridization was carried out to determine the hepatic source of OPN expression in ovariectomized EtOH+LPS treated animals. Consistent with the protein expression data, EtOH+LPS treated animals had higher OPN mRNA signal as compared to the EtOH+LPS+E2 (0.18mg, 0.36mg) treated ovariectomized groups (Fig 33A). However, a biphasic response of OPN was observed in this model. As compared to the low doses of E2 (0.18g, 0.36mg), significantly higher OPN mRNA signal was observed in the animals treated with the increasing doses (0.72mg and 1.7mg) of estrogen (Fig 33 B). Least OPN mRNA signal was observed in the animals treated with 0.36mg dose of E2. The localization of OPN was mostly within biliary epithelium and hepatocytes.

A



B

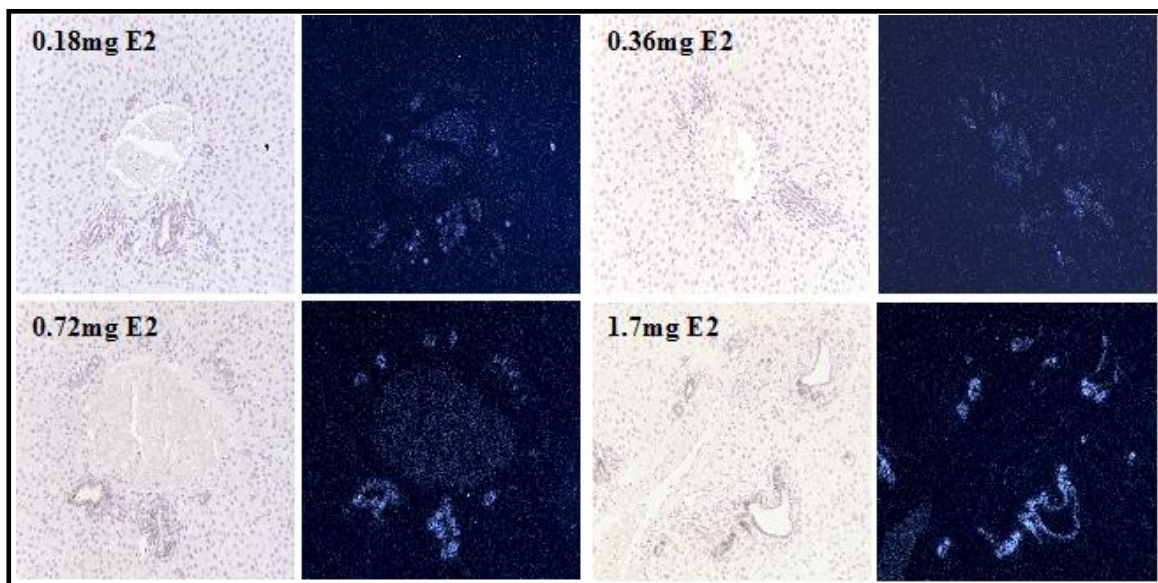


Fig. 33. In-situ hybridization analysis of OPN mRNA in the liver of female ovariectomized rats fed EtOH-Containing Lieber DeCarli diet followed by a single dose of LPS injection. Corresponding bright and dark field images in different groups are shown. (A) Liver section of ovariectomized female rat (B) liver sections of ovariectomized female rats with different doses of estrogen implants. (E2: estradiol)

Proteomics approach to study differential protein expression between male and females in alcoholic steatohepatitis

Identification of OPN protein by 2-D gel proteomics

2-D gels were performed to identify OPN protein in this model. Fig 34 shows representative 2-D gels and Western blots of OPN protein identified in this model. 2 different protein spots were identified by OPN antibody at about 60-68 kDa region. In addition to this, another spot was also identified at about 25-40 kDa region., corresponding to the cleaved OPN.

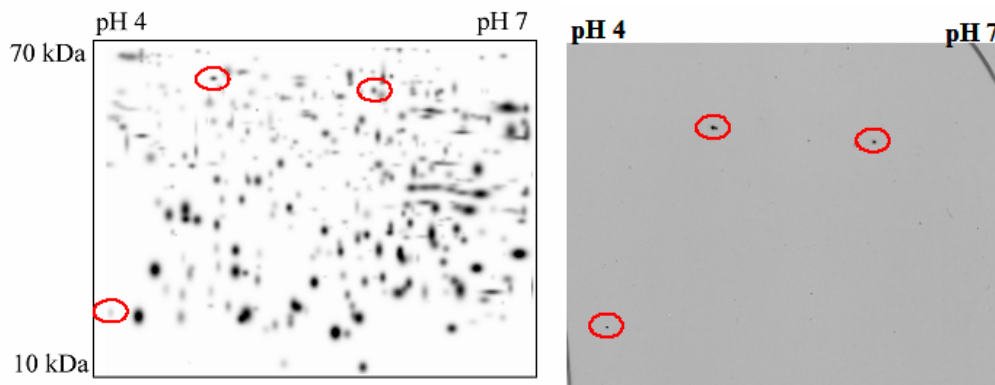


Fig. 34. 2-D gel analysis of osteopontin protein from liver of female rats. Following 2-D electrophoresis and transfer to nitrocellulose membrane, the proteins were detected using an anti-osteopontin antibody. The left panel shows the total protein by silver staining, while the right panel shows the osteopontin and its cleaved fragment on the replicate sample of the same 2-D gel.

Differential protein expression, identification and optimization

2D gels were performed from the respective control and ASH groups both in the male and female rats. Fig 35 shows representative 2-D gels with proteins from male and

female rats in the control and ASH group. On these gels, approximately 250-300 spots were detected by the software between 10-70kDa. Of these, the spots that were statistically different in expression when compared between males and females in control+LPS and ASH group, were identified based on the established criteria outlined in experimental procedures.

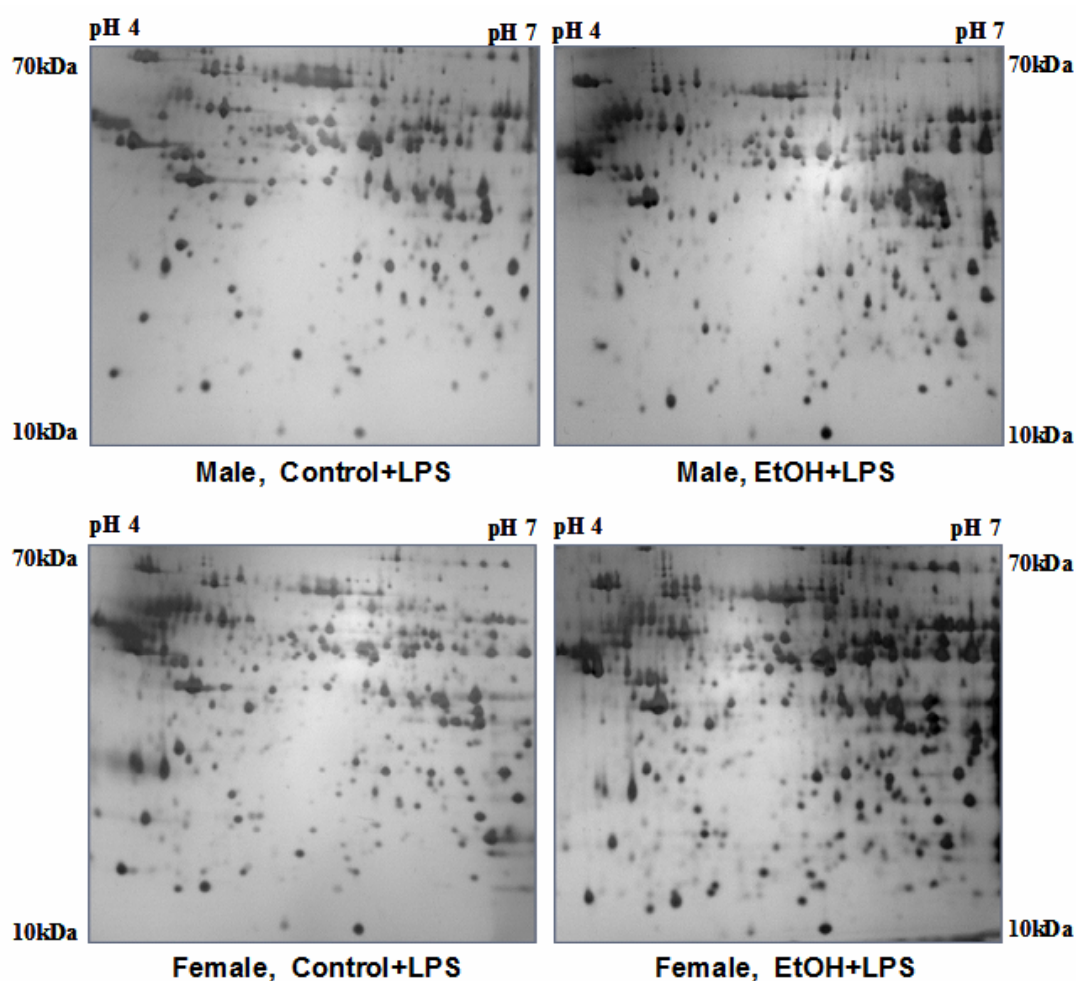


Fig. 35. Representative cropped 2D gel image of liver protein in male (A) and female (B) rat in alcoholic steatohepatitis group. The first-dimensional separation was performed using 7cm immobilized pH 4-7 gradient strips, followed by SDS-PAGE with 10% polyacrylamide gels in second dimension. The staining of the proteins were carried out using silver stain.

Differentially expressed protein identification in males in the ASH group

To identify the proteins deregulated in males in the ASH group, 2D gels of rat liver both in the control+LPS and EtOH+LPS treated male were analyzed. Analysis of the resulting images showed 28 protein spots to be statistically different between the two groups. Of these, 9 protein spots were found to be up-regulated and 19 protein spots down regulated. By mass spectrometry, 9 of the up regulated and 10 of the down regulated protein spots were identified both from the control and the experimental group. The spots identified are listed in Table 12.

Differentially expressed proteins in females in the ASH group

To identify the proteins deregulated in females in the ASH group, 2D gels of rat liver both in the control+LPS and EtOH+LPS treated female were analyzed. Analysis of the resulting images showed 30 protein spots to be statistically different between the two groups. Of these, 18 spots were found to be up regulated and 12 spots down regulated. Mass Spectrometry analysis identified 13 up regulated and 8 of the down-regulated spots. The spots identified are listed in Table 12.

Table 12
Differentially altered proteins between males and females in a rat alcoholic steatohepatitis model.

SSP	Swiss-Prot AN*	Protein	MS/MS seq	Protein score	Female (E+L/C+L)	Male (E+L/C+L)	Ratio
Metabolism related proteins							
1308	P19112	Fructose-1,6 bisphosphate	DALQPGR, FVLEEGR	853	2.08	3.7	0.55
3202	P46953	3-hydroxyanthranilate 3,4-dioxygenase	VPHPQR, SVVVEENR	763	0.5	1.72	0.29
5401	P11960	2-oxoisoverate dehydrogenase alpha subunit	ILYESQR, IGHHSTSDSSAYR	65	18.78	2.71	6.93
5805	P31210	3-oxo-5-beta-steroid 4-dehydrogenase	GLVVIPK, TAIDEGYR	189	0.19	0.04	4.4
6305	P15650	Acyl CoA dehydrogenase, long chain specific	LETPSAK, KLTDIGIR	623	0.21	4.36	0.05
7206	P15651	Acyl CoA dehydrogenase	AAMLKDNK, HAFGAPLTK	262	5.76	1.44	4
7207	P23457	3-alpha hydroxysteroid dehydrogenase	GVVPLIR, HAFGAPLTK	467	1.12	0.39	2.88
9105	P10860	Glutamate dehydrogenase 1	ELEDFK, GASIVEDK	532	0.27	1.08	0.25
Oxidative stress related proteins							
3002	XP_235823	Ferritin heavy chain	SKPPEKK, KNLQLLK	669	2.9	-	2.9
3401	Rf/NP_071565.1	HSP 60	GIIDPTK, KGVITVK	139	2.51	0.62	4.01
4003	Gb/AAA40996.1	Cu-Zn Superoxide dismutase	GGNEESTK, TMVVHEK	591	2.32	1.23	1.88
4806	P11598	ER 60	GSNYWR, IVAYTEK	1470	3.48	0.89	3.91
5008	Q35244	Peroxiredoxin 6	GMPVTAR, ELPSGKK	1070	0.41	0.1	3.91
7610	P04762	Catalase	VANYQR, GIPDGHR	931	2.47	0.32	7.5
Other proteins							
2002	P31044	Phosphotidykethanolamine binding protein (PEBP)	FANFIEK, LEEETRK	388	2.36	-	2.36
3104	P67779	Prohibitin	VFESIGK, ARFVVEK	1070	0.31	0.32	0.98
4101	Q63797	Protease activator complex subunit 1	IVVLLQR, VHPEAQAK	302	0.47	0.3	1.53
1403	Q63279	Keratin type 1 cytoskeletal 19	TIEDLR, IVLQIDNAR	79	37.53	22.88	1.64
3403	P04639	Apolipoprotein A-1 precursor (Apo-A1)	ENLAQR, VNADALR	264	2	-	2
3506	P21807	Peripherin	FANFIEK, KLHEEELR	65	3.7	0.98	3.82
7102	P04764	Alpha enolase	EIFDSR, YNQLR	929	0.45	0.36	1.23
8001	Rf/XP_235823.2	Translokoin	SKPPEKK, KNLQLLK	21	2.77	1.03	2.68

* Rat liver proteins differentially regulated in alcoholic steatohepatitis analyzed by MALDI-MS. Accession numbers were extracted from the Swiss-Prot database.

Comparison of the differentially expressed proteins between males and females in the ASH group

In order to identify the differentially expressed proteins and explain the basis for higher susceptibility of females to ASH, 2D gels of rat liver both in the male and female EtOH+LPS treated groups were analyzed. Analysis of the resulting images showed 40 proteins to be statistically different between the two groups (Fig 36). Of these, 31 spots were upregulated and 9 spots were downregulated in females as compared to the males in ASH group. By mass spectrometry, 17 of the upregulated and 5 of the downregulated spots were identified. In addition, Apolipoprotein 1, identified, was significantly deregulated only in the females, but not in the males of the ASH group. The spots identified are listed in Table 12. In addition to the several metabolism-related proteins, oxidative stress related proteins like HSP 60, ER60, Ferritin, Catalase, Peroxiredoxin 6, Cu-Zn dismutase were found to be upregulated in the females in the ASH group as compared their male counterparts.

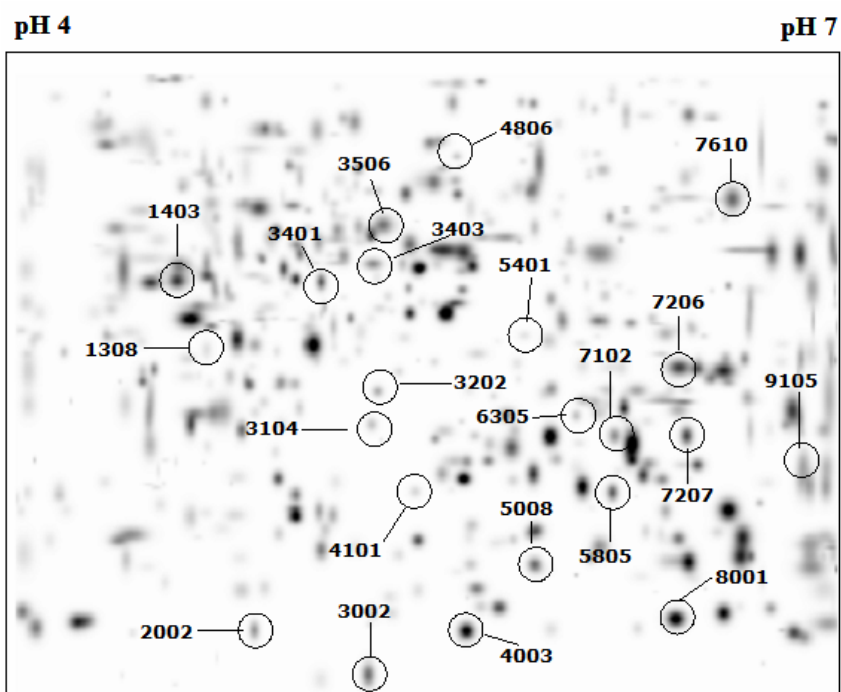


Fig. 36. 2D master gel indicating proteins identified as potential inflammatory markers in alcoholic steatohepatitis. Analysis revealed several proteins to be highly altered in females in alcoholic steatohepatitis as compared to their male counterparts. A total of 22 proteins were identified using the MALDI-TOF.

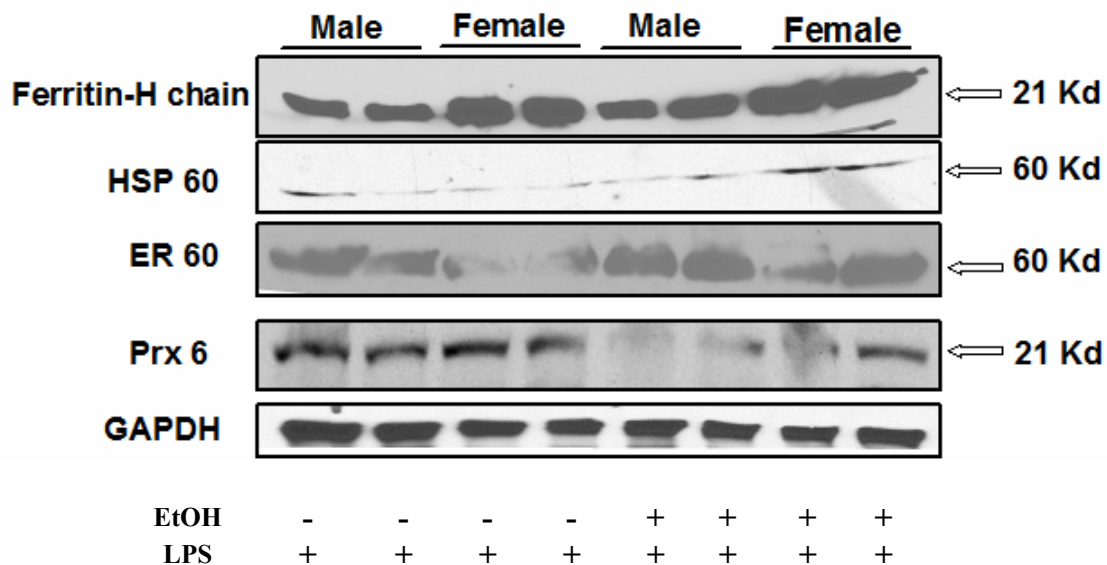


Fig. 37. Representative Western blot showing Ferritin H chain, HSP60, ER60 and PrX6 protein expression in male and female rats fed either control or EtOH-containing Lieber DeCarli diet followed by a single dose of LPS injection. (GAPDH was employed as an internal control, to ensure equal loading of protein.)

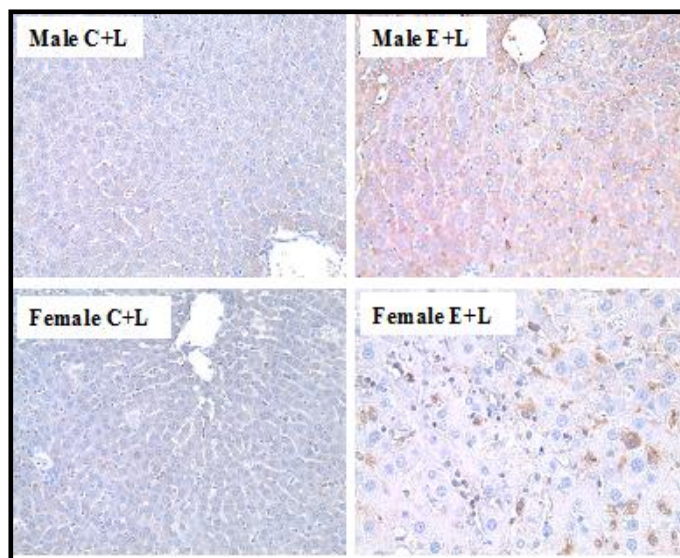


Fig. 38. Representative photomicrographs of Ferritin stained sections of male and female rats fed either control or EtOH-containing Lieber-DeCarli diet for 6 weeks. The brown stains indicate ferritin H chain staining.

Detection of selected oxidative stress proteins by immunoblotting

Since oxidative stress is implicated to play a major role in the pathogenesis of higher liver injury during ALD, changes in the expression of selected oxidative stress-related proteins were further characterized by Western blot. As indicated by Western blots, Ferritin H chain protein was upregulated in the females in the ASH group, as compared to the controls and their male counterparts (Fig 37). Ferritin H chain was localized in the hepatocytes as well as in some inflammatory cells in the females in the ASH group (Fig 38). Chaperone proteins like HSP 60 and ER60 was also found to be significantly deregulated in the females in the ASH group. Females had > 2-fold higher expression of HSP60 as compared to the controls and their male counterparts (Fig 34). Although the chaperone protein ER60 was not significantly different between the males and females in ASH group, there was significant up regulation of this protein in females when compared to the controls (Fig 34). In addition to this, Peroxiredoxin 6 the antioxidant enzyme, was found to be significantly downregulated in the EtOH+LPS group, as compared to the control+LPS group both in the males as well as the females (Fig 34).

Development of the mouse alcoholic steatohepatitis model

Mouse ASH model was developed to test the effects of OPN in the OPN^{-/-} mice. Pilot studies with the mice study indicated that LPS is not necessary to produce the neutrophilic pathology that we observed in rats.

Male and female mice fed EtOH for 6 weeks experienced significant fat accumulation and multi-focal neutrophilic infiltration. The pathology noted in the mice ASH model, was mostly similar to that seen in our rat model of ASH.

The body weight gain of the control and the EtOH-fed group were not different indicating no nutritional differences between the mice in the ASH and the control groups. However, the females in the ASH group had lower body weight as compared to the males, but they were not significantly different.

Liver injury as assessed by serum transaminase activity and hepatic pathology

Liver injury was assessed by ALT levels. Both males and females in the ASH group experienced significant increase in ALT levels as compared to the controls. However, the female mice in ASH had significantly higher (~ 2-fold) ALT values than males, indicating higher liver injury (Fig 39A). The findings of the plasma transaminase activity was further confirmed by the H&E stained liver sections. Both the male and the females in the ASH group experienced extensive steatosis, neutrophilic infiltration as compared to the controls (Fig 39B).

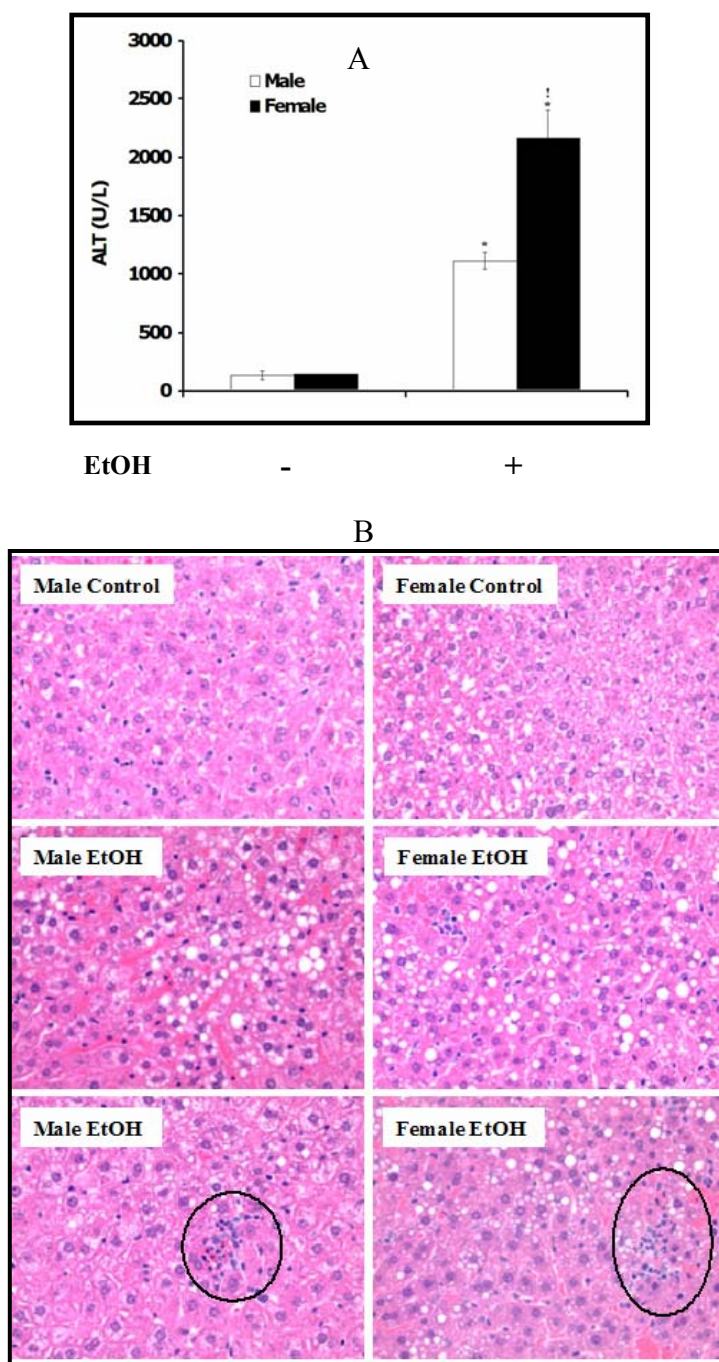


Fig. 39. Liver injury in mice alcoholic steatohepatitis model. (A) ALT activities in plasma of male and female mice fed either control or EtOH-containing Lieber DeCarli diet for six weeks as described in the materials and methods section. *Values significantly different from the controls. ! Values are significantly different from the male counterparts. Data are expressed as mean \pm SE, $p \leq 0.05$. (B) Representative photomicrographs of H&E stained sections of male and female mice fed either control or EtOH-containing Lieber-DeCarli diet for 6 weeks. The marked area indicates neutrophilic foci formation indicating inflammation.

Scoring of the H&E stained liver sections suggested extensive steatosis in both the males and females in the ASH group. However, steatosis in females was about 1.3-fold greater than that of the males (Fig 40A). In addition, the females in ASH experienced both micro and macrovesicular steatosis, whereas, in case of males, diffuse infiltration of microvesicular fat droplets were observed throughout the parenchyma. In addition, random sinusoidal congestion was also observed in this model. Steatosis noted in this model, was periportal in nature, with the sparing of the centrilobular region.

Hepatic neutrophil infiltration in mice ASH model

Both the males and the females in the ASH group experienced significantly higher neutrophilic infiltration as compared to their respective controls (Fig 40B). However, the females in the ASH group had about 1.6-fold higher neutrophilic infiltration as compared to the males. In addition to the neutrophilic foci, females in the ASH group had neutrophils scattered all over the hepatic parenchyma, which was not noted in males (Fig 39).

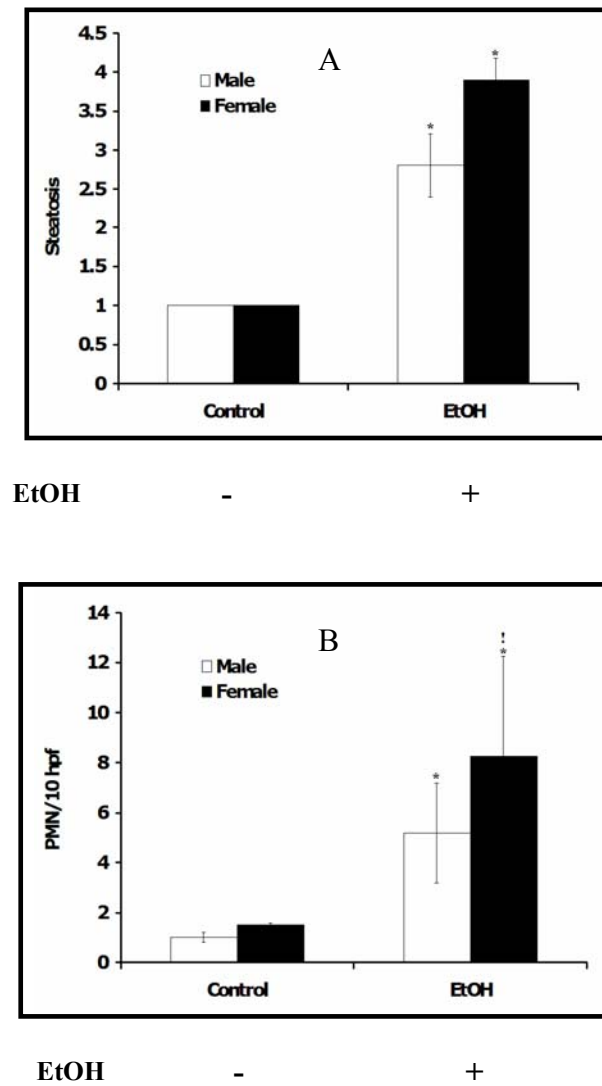


Fig. 40. Quantitation of (A) steatosis and (B) neutrophils as an index of inflammation in the livers of mice fed either control or EtOH-containing Lieber-DeCarli diet for 6 weeks.* Values significantly different from the controls. ! Values are significantly different from the male counterparts. Data are expressed as mean \pm SE, $p \leq 0.05$.

OPN protein expression in ASH group

A significant induction in the level of OPN protein was observed in the male and female mice in ASH group as compared to the controls (Fig 41 A,B). The females in the ASH group had higher expression of OPN protein as compared to the males, although

statistically not significant. Induction of OPN protein levels were confirmed by immunohistochemistry (Fig 42). OPN expression was predominantly localized in the hepatocytes. However, in the case of females in ASH, neutrophilic infiltrates were also found to be positive for OPN protein (Fig 42). In addition, neutrophils isolated from the animals in ASH group were found to produce OPN protein (Fig 43), contributing to the increased OPN.

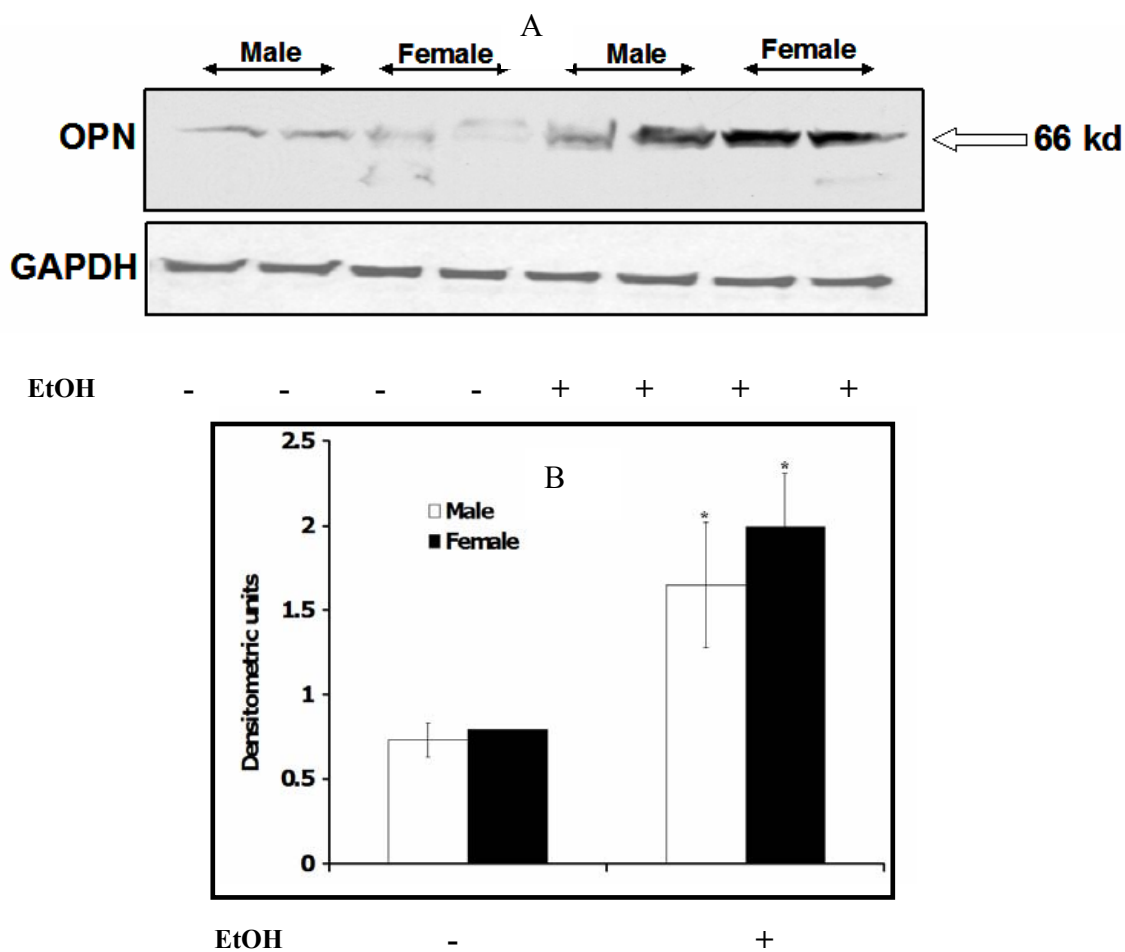


Fig. 41. Osteopontin protein expression in mice alcoholic steatohepatitis model. Representative Western blotting (A) showing OPN expression in male and female mice fed either control or EtOH-containing Lieber-DeCarli diet for 6 weeks. OPN was detected by Western blot and quantified by densitometric analysis (B). The values were normalized with GAPDH, employed as an internal control for Western blot to ensure equal loading of protein. * Values are significantly different from the controls. Data are expressed as mean \pm SE, $p \leq 0.05$.

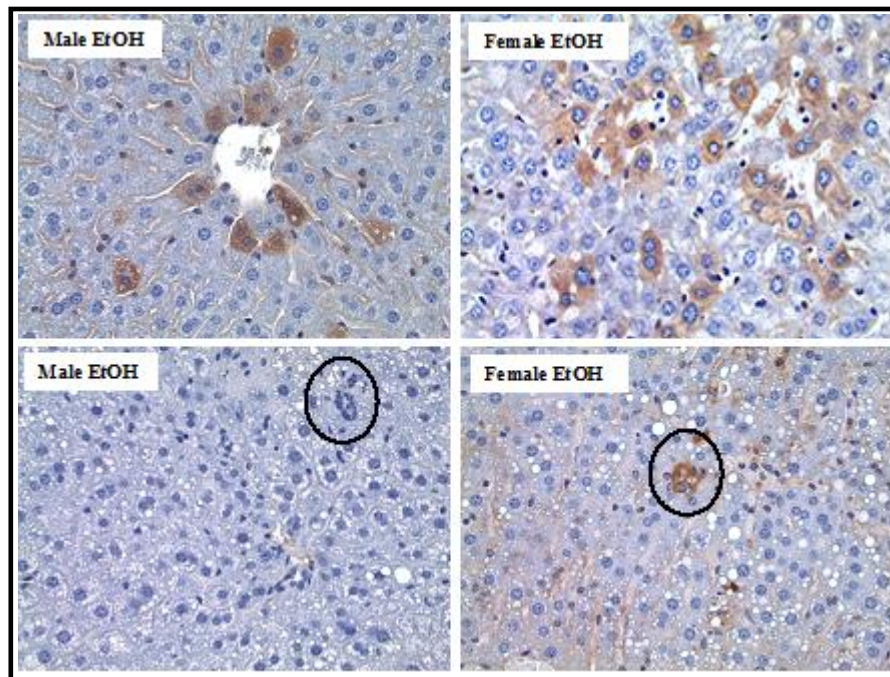


Fig. 42. Representative photomicrograph of liver sections stained for OPN in male and female mice fed alcoholic steatohepatitis model. The dark brown stain indicates OPN staining.

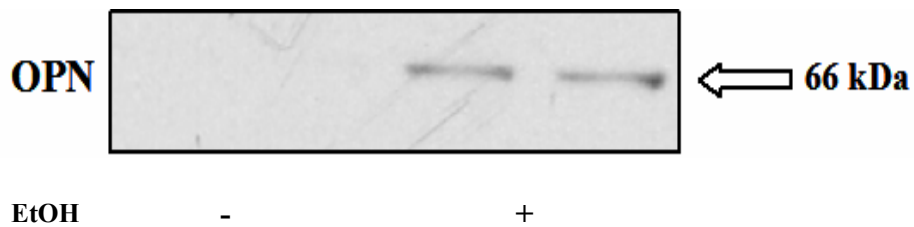


Fig. 43. Representative Western blotting showing OPN isolated from neutrophils in mice fed EtOH-containing Lieber-DeCarli diet for 6 weeks

OPN mRNA expression in ASH group

Real-time PCR results showed that EtOH treated animals had significantly higher expression of OPN mRNA as compared to their respective controls (Fig 44). However, EtOH treated females showed >1.6-fold higher expression of OPN mRNA as compared to their male counterparts.

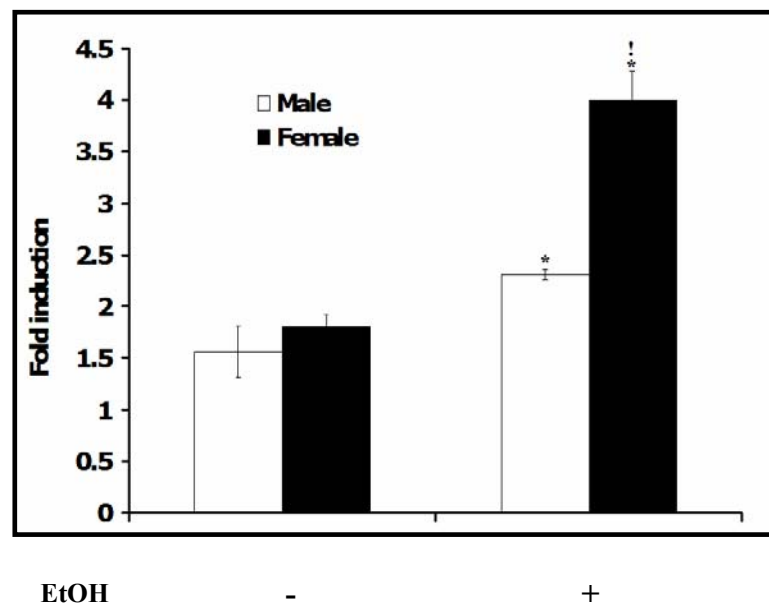


Fig. 44. Osteopontin mRNA expression in mice alcoholic steatohepatitis model. Real time PCR analysis of OPN mRNA in liver of mice fed either control or EtOH-containing Lieber-DeCarli diet for a period of 6 weeks as described in the materials and the methods section. The values have been normalized with β -actin- the house keeping gene. *Values significantly different from the controls. ! Values are significantly different from the male counterparts. Data are expressed as mean \pm SE, $p \leq 0.05$.

CHAPTER IV

DISCUSSION, SUMMARY AND CONCLUSIONS*

Females are susceptible to ALD

Alcoholic liver disease is responsible for approximately 150,000 deaths per year in US alone (Tsukamoto, 2007), and its medical and social costs are estimated to exceed \$116 billion annually. Epidemiological studies suggest higher female susceptibility to ALD. Although there are a variety of different medical interventions practiced to treat ALD patients, none of them have been successful. Therefore it is of immense importance to understand the molecular basis behind ASH so that the progression to fibrosis and cirrhosis can be prevented. This is especially important in female alcoholics where the progression and severity of ALD is much higher than males.

The simplified experimental rat models of AS and ASH are based on the previous investigations (Enomoto et al., 1999; de la Hall et al., 2001; Murohisa et al., 2002; Tamai et al., 2002) utilizing the interaction of chronic EtOH consumption combined with a single LPS exposure. In our model, we were able to demonstrate the complete spectrum of pathology associated with ASH including steatosis, neutrophilic inflammation, hepatocyte oncotoc necrosis and apoptosis. This simple model of alcoholic steatosis and steatohepatitis is highly reproducible and perfectly mimic the human ALD,

* Reprinted with permission from “Higher neutrophil infiltration mediated by osteopontin as a likely contributing factor to the increased susceptibility of females to alcoholic liver disease” by Banerjee et al., 2006, *Journal of Pathology*, 208: 473-485, © 2006 by Wiley Interscience.

and allows for detailed mechanistic investigations into higher neutrophilic infiltration and higher liver injury in female alcoholics.

Several theories proposed to explain the higher susceptibility of females to alcoholic liver disease include differences in metabolism, pharmacokinetics (Lieber 2000; Baraona et al., 2001), endotoxemia (Kono et al., 2000) and cytokines and chemokines (Roll et al., 1986; Gallucci et al., 2004).

Of the three main enzymatic pathways involved in hepatic EtOH metabolism (alcohol dehydrogenase, CYP2E1 and peroxisomal catalase), CYP2E1-mediated metabolism plays a major pathogenic role during sustained exposure to EtOH (Roberts et al., 1995; McGehee et al., 1997; Lieber, 2000; Oneta et al., 2002). The significant induction of hepatic CYP2E1 in the EtOH treated rats in our ASH model, corroborates with the previous studies (Lieber, 2000). However, the level of CYP2E1 induction was similar between male and female rats ruling out CYP2E1 as a major player in the differential liver injury, noted in males and females. In addition, there was no significant difference noted in the body weight and blood alcohol levels of the male and female rats administered EtOH, suggesting that pharmacokinetics is a less-likely factor in the gender difference observed in our model of ASH.

Endotoxemia is another major mechanism implicated to cause higher liver injury in the females (Rivera et al., 1998; Kono et al., 2000). A study by Kono et al., (2000) have shown that higher female susceptibility is due to increased level of endotoxin in females which was attributed to possible enhanced estrogen mediated endotoxin absorption from the gut during EtOH exposure. However, in our model, there was no

significant difference noted between the genders in the ASH group. Based on this it can be interpreted that endotoxin is not a major candidate for higher liver injury in female rats, noted in our ASH model. Clearly, we were able to reproduce a rodent model of ALD for mechanistic investigation.

Osteopontin as a mediator of hepatic neutrophil infiltration

In pursuit of the reason for higher liver injury in females, histopathologic evaluation of liver sections in the ASH model revealed an excellent correlation between earlier and higher neutrophilic infiltration and observed higher liver injury in females. Based on these findings, the mechanistic basis for higher hepatic neutrophil infiltration in females was further investigated in this study. A recent study from our laboratory showed the involvement of osteopontin (OPN) in hepatic neutrophil infiltration (Apte et al., 2005). OPN – a novel extracellular matrix protein is known to play a role in several inflammatory diseases like glomerular nephritis (O'Reagan and Burman, 2000), non-alcoholic steatohepatitis (Sahai et al., 2004), ischemic injury and CCl₄ mediated liver injury (Kawashima et al., 1999). OPN is also a known chemoattractant for macrophages both in vivo and in vitro (Denhardt et al., 2001a,b). OPN has a RGD sequence and a thrombin cleavage site which play a role in inflammatory diseases (Denhardt et al., 2001a,b). Cleaved OPN (cOPN) with its exposed SLAYGLR (or SVVYGLR) sequence is known to have higher chemotactic potential than the native form of OPN (Giachelli et al., 1998; Apte et al., 2005), and is known to attract more lymphocytes and neutrophils (Giachelli et al., 1998; Yokosaki et al., 1999; Denhardt et al., 2001a,b). Based on these we evaluated the OPN and cOPN between males and females in the ASH model.

Excellent correlation between increase in OPN (both uncleaved and cleaved OPN) and higher neutrophilic infiltration in the females was noted in the ASH model, suggesting the role of OPN in the higher neutrophil infiltration in the liver.

To further test the role of OPN in attracting higher neutrophils in females, a cause and effect study was designed in a rodent peritonitis model (Yao et al., 2003; Apte et al., 2005). This model was employed to test if (1) OPN attracts neutrophils and if it does, (2) whether female rats have higher chemotactic response to OPN than males. Based on the results, OPN demonstrated a significant neutrophil chemotactic response in this model. However, there was no gender difference noted in OPN-mediated neutrophil chemotaxis. This discrepancy can be attributed to the differences in the mechanism of neutrophil transmigration between hepatic vasculature and the peritoneum, although not tested in the current study. In the mouse peritoneum, Leukotriene B4 receptor has been shown to modulate neutrophil migration, but not in the liver and the lung (Scott et al., 2004). Studies by Dangerfield et al., (2005) have shown that neutrophil migration into the peritoneum is induced by IL-1 β and not TNF- α . In addition, the amount and type of serum and hepatic proinflammatory cytokines and chemokines may be different in the peritonitis versus the ASH model. For example, in ALD, TNF- α has been indicated as an important cytokine playing a crucial role in inflammation (Kono et al., 2000).

In addition, a neutralizing OPN antibody experiment was carried out in a LPS mediated hepatitis model to further confirm the role of OPN in neutrophil infiltration. Studies by Rose et al., (2006, 2007), have shown that LPS or endotoxin causes neutrophil infiltration into the liver in a rat model of hepatitis. Based on this, in the

present study, nOPN antibody treated animals had significant lower neutrophilic infiltration in the liver indicating that OPN was acting as a chemokine for neutrophils.

Other mechanisms involved in higher hepatic neutrophil infiltration include proinflammatory cytokines (Gallucci et al., 2004) and chemokines (Roll et al., 1986). Inflammatory cytokines are known to promote neutrophil activation, accumulation and chemotaxis in a wide range of inflammatory diseases (Rajaratnam et al., 1994). The proinflammatory cytokine IL-6 and the chemokine IL-8 have been known to play a significant role in neutrophil chemotaxis during ALD (Jayatilleke and Shaw, 1997; Gallucci et al., 2004). However, in the present study, gender difference was not noted in either IL-6 or IL-8 suggesting that they are less likely contributing to the higher neutrophilic infiltration in the female rats. Together these data suggest that higher OPN expression is the reason for higher neutrophilic transmigration into the hepatic parenchyma leading to higher liver injury in females in the ASH model.

Involvement of β_1 and β_2 integrins in OPN-mediated neutrophil chemotaxis

Since OPN attracts higher neutrophils, our next question was to address the mechanistic basis of OPN-mediated hepatic neutrophil infiltration. Of the several steps in hepatic neutrophil migration, neutrophil activation is the first important step (Jaeschke, 1997), and shedding of CD62L (L-selectin) and up-regulation of β_2 integrins is usually an indicator of neutrophil activation (Jaeschke et al., 1998). However, in the sinusoids of the liver, L-selectin is not known to play a role in neutrophil activation (Lawson et al., 2000). Instead of the adhesion molecule like L-selectin, determining factors like cell swelling of sinusoidal lining cell, active vasoconstriction and reduced

membrane flexibility of the neutrophils, traps neutrophils in the sinusoids. Based on this, neutrophil activation was assessed by flow cytometry by incubating neutrophils with varying concentration of OPN and cOPN *in vitro*, and the results indicated that OPN was activating neutrophils via Mac-1 or β_2 integrins.

In addition to activation, hepatic neutrophil infiltration typically involves neutrophil transmigration. However the mechanism by which subsequent neutrophils extravasation such as detachment from sites of initial adhesion and ensuing migration across the extracellular matrix takes place are not well understood. The current study suggests that in the rodent model system of ALD employed, $\alpha_4\beta_1$ and $\alpha_9\beta_1$ integrins are likely playing important roles. Both of these integrins could be contributing to migration across endothelial cells where they are encountered with OPN. The M5 antibody that recognizes SLAYGLR sequence and inhibits binding to $\alpha_4\beta_1$ and $\alpha_9\beta_1$ integrins, inhibited neutrophil transmigration. Our findings are in concordance with a recent study showing cOPN to have more affinity towards $\alpha_4\beta_1$ and $\alpha_9\beta_1$ integrins on neutrophils (Diao et al., 2004). The essential roles of $\alpha_4\beta_1$ integrin has also been implicated in the multi-step adhesion and migration of neutrophils in the vascular endothelial cells and in patients with sepsis syndrome (Ibbotson et al., 2001; Ulyanova et al., 2007). Also, an increase in $\alpha_4\beta_1$ on neutrophils following transmigration has also been reported in cardiac myocytes (Reinhardt et al., 1997). Furthermore, studies by Ulyanova and co workers (2007), have shown that recruitment of neutrophils in the inflamed peritoneum, requires the presence of both α_4 and β_2 integrins. It can be argued that in addition to β_1 integrins, β_2 integrins and its associated adhesion molecules are also involved in higher

hepatic neutrophil transmigration. In addition to the role of β_2 integrins, based on our data we also believe that OPN mediated neutrophil infiltration is mediated by $\alpha_4\beta_1$ and $\alpha_9\beta_1$ integrins. Unlike the β_2 integrins, the $\alpha_4\beta_1$ and $\alpha_9\beta_1$ integrins are expressed at low levels, although their expression is increased during persistence inflammation (Bayless et al., 1998). It is possible that a combination of β_2 integrins and non- β_2 integrins, notably $\alpha_4\beta_1$ and $\alpha_9\beta_1$ function together for neutrophil chemotaxis. This is in agreement with a study by Henderson and co workers (2001), which showed that α_4 -integrin and LFA-1 have overlapping roles in post capillary venules for neutrophil transmigration. In addition to this, recently we have observed that neutrophils isolated from mice model of ALD also to be a source of OPN. In this context, it is important to recognize that in addition to extracellular OPN mediating its neutrophil-migration effect through $\alpha_4\beta_1$ and $\alpha_9\beta_1$ integrins, the role of intracellular OPN within neutrophils cannot be ignored. Infact, study by Sodek and coworkers (Sodek et al., 2000) suggests that there is an intracellular OPN that is thought to regulate the formation of cell processes and cell motility.

In summary, higher liver injury and hepatic neutrophilic infiltration in females in ASH was due to higher expression of OPN and cOPN. OPN was found to act as a chemokine in attracting neutrophils into the liver making females more susceptible to alcohol mediated liver injury. In addition, OPN has also been identified as a biologically relevant ligand for $\alpha_4\beta_1$ and $\alpha_9\beta_1$ integrins in the ALD model and the increased expression of these two integrins may be possibly responsible for OPN-mediated hepatic neutrophil transmigration (Fig 45). Based on our studies, biliary epithelium and

hepatocytes are the major source of extracellular OPN which upon thrombin cleavage results in the generation of cOPN exposing the SLAYGLR epitope of OPN to interact with $\alpha_4\beta_1$ and $\alpha_9\beta_1$ integrin on neutrophils.

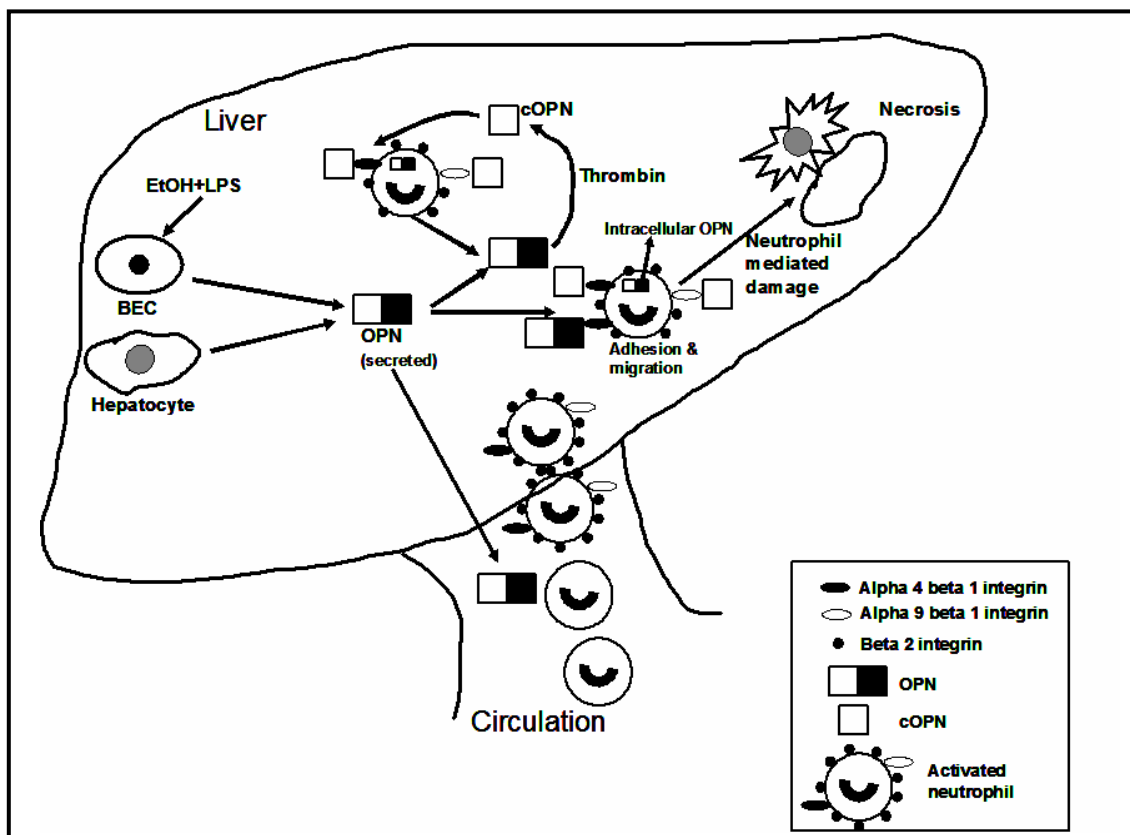


Fig. 45. Scheme to explain the mechanism of involvement of OPN in higher liver injury in females in alcoholic liver disease. In ALD, OPN secreted from the biliary epithelial cells and hepatocytes undergoes thrombin cleavage exposing the cryptic SLAYGLR sequence, where they bind to $\alpha_4\beta_1$ and $\alpha_9\beta_1$ integrins on neutrophils. Binding between SLAYGLR and these integrins lead to neutrophil adhesion and migration contributing to neutrophil mediated liver damage. In addition to secreted OPN, neutrophils may also be contributing to the production of OPN whose intracellular function is not clearly established.

The OPN-SLAYGLR interaction with $\alpha_4\beta_1$ and $\alpha_9\beta_1$ results in adhesion and migration of neutrophils within the liver leading to hepatic damage (Fig 45). In addition, neutrophils also have the ability to produce OPN and the intracellular form of OPN which can potentially bind to these integrins on neutrophils resulting in neutrophil migration.

Potential therapeutic strategies to inhibit OPN in alcoholic liver disease

Based on the proposed role of OPN in higher neutrophil-mediated liver injury in females, different therapeutic interventions (Fig 46) for decreasing OPN expression at the level of mRNA, protein and receptor signaling in the liver is a potential option to treat patients with alcoholic liver disease, so that the progression to fibrosis and cirrhosis can be prevented. In addition, other inflammatory liver diseases with similar pathological progression as ALD can also be potentially treated.

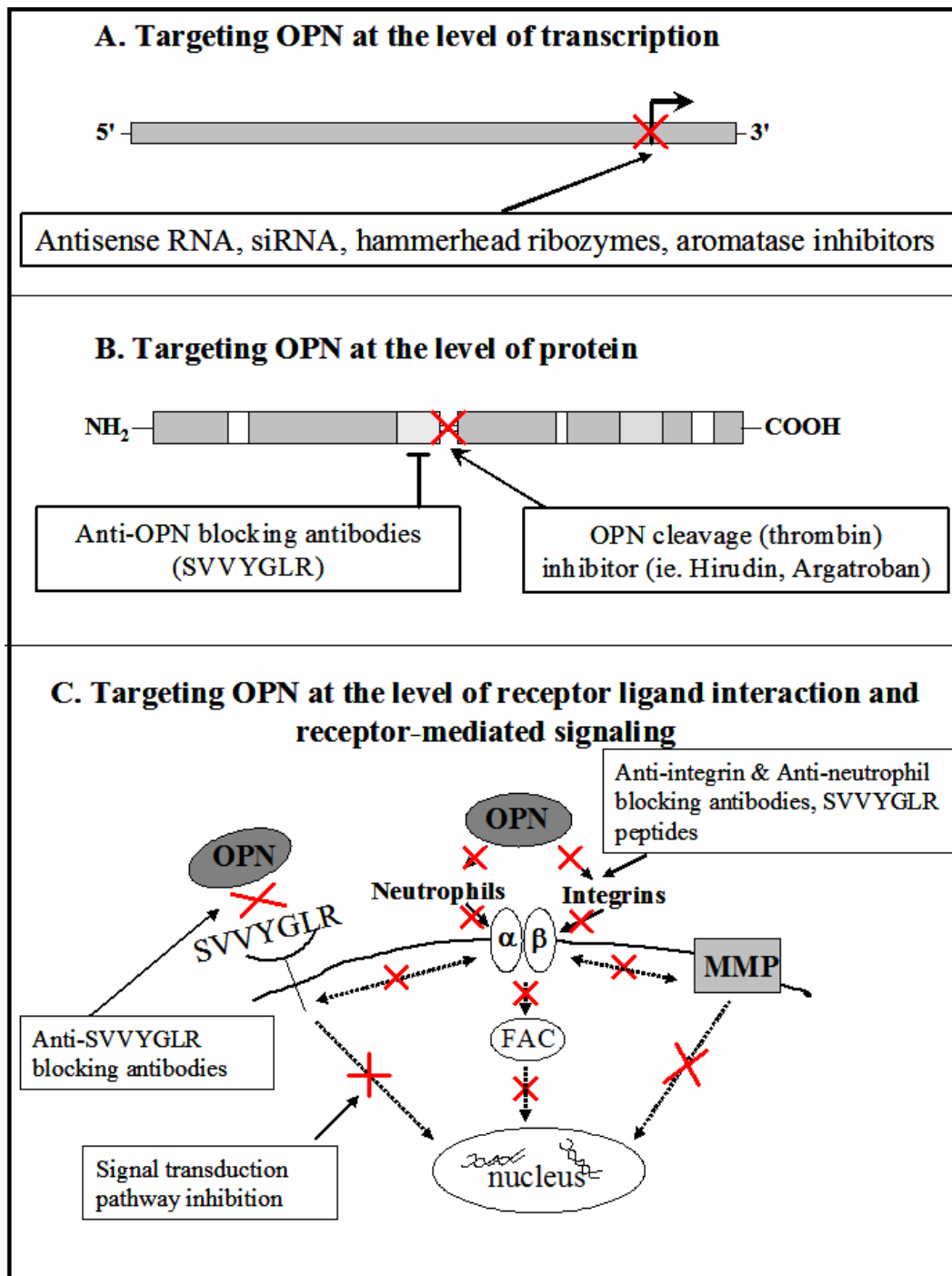


Fig. 46. Potential therapeutic strategies to target OPN and inhibit its inflammatory activities in alcoholic liver disease. There are numerous levels/targets at which potential therapeutics strategies can be directed against OPN, including (A) at the transcriptional level, (B) at the level of the protein, or (C) at the level of receptor-ligand interactions and receptor-mediated signaling. (Adapted from Tuck et al., 2007)

Application of proteomics to detect unique proteins in female susceptibility to ALD

Due of the distinct advantages of proteomics to detect global expression of proteins, the detected histopathologic difference noted between genders in ASH was compared with the differential protein expression. Following protein identification based on the spots and MALDI/MS data, these differentially expressed proteins were categorized according to their biological functions. It was found that proteins related to metabolism of amino acids, carbohydrates, fatty acids, lipids and oxidative stress response were mainly altered in their expression. Accordingly, the proteins were categorized as those belonging to (a) metabolism (b) oxidative stress and (c) miscellaneous proteins relevant to the pathogenesis of ALD are discussed below.

(a) Metabolism related proteins

Administration of EtOH+LPS induced changes in the expression of proteins regulating fatty acid synthesis in both males and females (Lieber, 2000; Nanji et al., 2002; Crabb et al., 2004). However, alterations in the level of these proteins are well correlated with the findings of steatosis that results from the perturbation of the β -oxidation pathway (Reddy and Hasimoto, 2001). Proteins like 2-oxoisoverate dehydrogenase and Acyl CoA dehydrogenase are known to contribute to the β -oxidation pathway of the lipids (Lieber, 2005). Dysregulation of these proteins in the present study suggests higher triglyceride accumulation leading to higher steatosis or fatty liver, and is consistent with higher steatosis noted in the female livers in our model. Several studies have investigated the mechanism underlying steatosis following alcohol ingestion. Studies by Crabb et al., (2004) have suggested the role of PPAR- α in fat accumulation

in the liver and reported that ethanol feeding decreases the level of retinoid X receptor alpha (RXR α) as well as the ability of PPAR α /RXR in liver nuclear extracts to bind to its consensus sequence, resulting in decreased levels of mRNAs for several PPAR α regulated genes like Acyl CoA dehydrogenase long chain (Crabb et al., 2004). Lower levels of Acyl CoA dehydrogenase long chain in females in the current study as compared to the males indicates higher fat accumulation and consequent higher oxidative injury in females.

(b) Oxidative stress related proteins

Oxidative stress is known to play an important role in the pathogenesis of ALD (Di Luzio, 1966; Shaw et al., 1981). Infact, there are studies that report oxidative stress to be the reason for higher liver injury in female alcoholics (Kono et al., 2000; Colantoni et al., 2000). Oxidative stress is induced either by the increased production of toxic radicals or by decreased endogenous antioxidants (Colantoni et al., 2000). In our study, various oxidative stress related proteins like ER 60, Ferritin Heavy chain, HSP 60, Catalase and Cu-Zn dismutase were found to upregulated in females in ASH as compared to their male counterparts. It was also evident in this study that the antioxidant enzyme PRX6, was less downregulated in females as compared to the males in ASH. A few of these proteins were analyzed and will be discussed.

Peroxiredoxin 6: Peroxiredoxins belong to a superfamily of nonheme and nonselenium peroxidases containing two conserved cysteines participating in intramolecular disulphide/sulphydryl redox cycling with thioredoxin resulting in the reduction of hydrogen peroxide (Manevich et al., 2004). However, 1-cys peroxiredoxin or

Peroxiredoxin VI (Prx VI) has a single conserved cysteine and does not use thioredoxin as reductant. Although Prx VI has been reported to be protective against cellular membrane damage acting as an anti-oxidant, recent studies by Kim et al., (2006), have reported markedly increased levels of oxidized PrxVI in alcohol exposed mouse livers and ethanol-sensitive hepatoma cells as compared to the corresponding controls. Furthermore, these studies demonstrate increased oxidation or modification of proteins leading to enzymatic inactivation thus likely predisposing the tissue for irreversible damage in the presence of additional stress (Kim et al., 2006). Although we have not measured the inactive oxidative form of PrxVI, it can be postulated that higher liver injury in females ASH group in our studies, could be attributed due to the presence of higher Peroxiredoxin VI as compared to their male counterparts. The higher PrX VI in females ASH in our model, likely points to the presence of the higher inactivated protein in this group. Future studies aimed at determining Prx VI inactivation will likely confirm this hypothesis.

HSP60: Oxidative stress results in the synthesis of a group of highly conserved protein called heat shock proteins (HSPs). The 60kDa HSP is one of the molecular chaperone proteins localized in the mitochondria that participates in the folding of newly synthesized proteins, unfolding and aggregation (Habich et al., 2002). In addition, they also play a role during transportation and degradation of proteins (Becker and Craig, 1994; Ellis and vander Vies, 2001; Fink, 2001). Needless to say, HSP60 is also expressed in response to oxidative stress. Increased expression of HSP60 has also been reported in various inflammatory diseases like rheumatoid arthritis, insulinitis and

atherosclerosis (Holoshitz et al., 1986; Brudzynski et al., 1992; Xu et al., 1993). While the precise mechanism for higher expression of HSP60 in females is not tested, the upregulation of HSP60 in this study points to the adaptive mechanism due to higher liver injury in females. This is consistent with the previous report that increase in oxidative stress resulted in higher synthesis of HSP's (Tacchini et al., 1995).

Ferritin heavy chain: Ferritin is a ubiquitous and highly conserved cytosolic iron-binding protein. The cytosolic form consists of 2 subunits, termed heavy (H) and light (L) chain (Harrison and Arosio, 1996). Although Ferritin-L is predominantly present in the liver, it is readily modified in many inflammatory and infectious conditions and in response to environmental stress (Torti and Torti, 2002). In the literature, Ferritin-H has been reported to be regulated by various cytokines. The proinflammatory cytokines TNF- α and Interleukin (IL)-1 α , have been known to induce Ferritin-H suggesting that inflammatory pathways and stress can impact ferritin regulation (Torti et al., 1988; Wei et al., 1990). Since females have been reported to have higher expression of TNF- α during ALD, higher expression of Ferritin-H in females in ASH correlates with higher inflammation and more severe ALD noted compared to the males. This is also supported by the fact that the females in the control+LPS group had significant higher expression of Ferritin-H as compared to the males. The mechanism by which Ferritin-H leads to higher liver injury in females is unknown and worthy of additional investigation.

ER60: The ER60 is an endoplasmic reticulum-resident multifunctional protein with both cysteine protease activity and disulphide bond folding activity (Piec et al., 2005). To confer protection against stress, cells use quality control mechanisms to detect, refold

and eventually eliminate abnormal proteins. It has been suggested that ER60 may be a component of the proteolytic machinery for the degradation of misfolded proteins (Otsu et al., 1995). Although there is no significant difference between males and females in the ASH group, additional temporal studies are required to confirm this finding. Based on the significant induction of this protein in female ASH group as compared to controls, additional time points may be needed to achieve significance. So higher expression of ER60 in females in the ASH group in our model, as compared to the controls suggests that in females, degradative pathways are significantly impaired and this may contribute to significant stress and higher liver injury in the females noted in ASH group.

(c) Others

In addition to the metabolism and oxidative stress related proteins, few other proteins like Cytokeratin (CK) 19 and translokine were found to be significantly upregulated in the females in ASH. Cytokeratins are normal constituents of epithelial cell cytoskeleton (Omary et al., 2002) and serum CK levels are often used as biomarkers for epithelial malignancies (Barak et al., 2004). In addition to this, serum CK levels have also been found to increase in other non-malignant diseases like alcoholic liver disease (Gonzalez-Quintela et al., 2006), especially in ASH. Normally, adult hepatocytes express only CK-8 and CK-18 (VanEyken, 2000; Omary et al., 2002). However in ASH, Mallory bodies formed by the rearrangement of CK-8 and CK-18 also contain newly synthesized CK-19 as inclusions (Pei et al., 2004). Upregulation of CK-19 in our female ASH model not only points to the severity of ASH in this group, but also indicates the potential of using CK-19 as a biomarker for ASH.

In summary, the current proteomics study has identified a potential set of proteins that correlates with the liver pathology and highlights certain mechanisms associated with the mechanism of higher liver injury noted in our female rat ASH model. The proteomics study in this project identified additional protein that can be potentially investigated to identify differential female susceptibility to ALD.

REFERENCES

- Adachi, Y., Bradford, B.U., Gao, W., Bojes, H.K., Thurman, R.G., 1994. Inactivation of kupffer cells prevents early alcohol-induced liver injury. *Hepatology* 20, 453-460.
- Afford, S.C., Fisher, N.C., Neil, D.A., Fear, J., Brun, P., Hubscher, S.C., Adams, D.H., 1998. Distinct patterns of chemokine expression are associated with leukocyte recruitment in alcoholic hepatitis and alcoholic cirrhosis. *J. Pathol.* 186, 82-89.
- Al-Shami, R., Sorensen, E.S., Ek-Rylander, B., Andersson, G., Carson, D.D., Farach-Carson, M.C., 2005. Phosphorylated osteopontin promotes migration of human choriocarcinoma cells via a p70 S6 kinase-dependent pathway. *J. Cell Biochem.* 94, 1218-1233.
- Anand, B.S., 1999. Cirrhosis of liver. *West. J. Med.* 171, 110-115.
- Angulo, P., 2002. Nonalcoholic fatty liver disease. *N. Engl. J. Med.* 346, 1221-1231.
- Apte, U.M., Banerjee, A., McRee, R., Wellberg, E., Ramaiah, S.K., 2005. Role of osteopontin in hepatic neutrophil infiltration during alcoholic steatohepatitis. *Toxicol. Appl. Pharmacol.* 207, 25-38.
- Apte, U.M., Limaye, P.B., Desai, D., Bucci, T.J., Warbritton, A., Mehendale, H.M., 2003. Mechanisms of increased liver tissue repair and survival in diet-restricted rats treated with equitoxic doses of thioacetamide. *Toxicol. Sci.* 72, 272-278.

- Apte, U.M., McRee, R., Ramaiah. S.K., 2004. Hepatocyte proliferation is the possible mechanism for the transient decrease in liver injury during steatosis stage of alcoholic liver disease. *Toxicol. Pathol.* 32, 567–576.
- Arteel, G.A., 2003. Oxidants and antioxidants in alcohol-induced liver disease, *Gastroenterology* 24, 778–790.
- Ashkar S., Weber, G.F., Panoutsakopoulou, V., Sanchiro, M.E., Jansson, M., Rittling, S.R., Denhardt, D.T., Glimcher, M.J., Cantor, H., 2000. Eta-1 (Osteopontin): an early component of type-1 (cell-mediated) immunity. *Science* 287, 860-864.
- Ashley, M.J., Olin, J.S., leRiche, W.H., Kornaczewski, A., Schmidt, W., Rankin, J.G., 1977. Morbidity in alcoholics. Evidence for accelerated development of physical disease in women. *Arch. Intern. Med.* 137, 883-887.
- Badger, T. M., Ronis, M.J., Ingelman-Sundberg, M., Hakkak, R., 1993. Pulsatile blood alcohol and CYP2E1 induction during chronic alcohol infusions in rats. *Alcohol* 10, 453-457.
- Bajt, M.L., Farhood, A., Jaeschke, H., 2001. Effects of CXC chemokines on neutrophil activation and sequestration in hepatic vasculature. *Am. J. Physiol. Gastrointest. Liver Physiol.* 281, G1188-G1195.
- Banerjee, A., Apte, U.M., Smith, R., Ramaiah, S.K., 2006. Higher neutrophil infiltration mediated by osteopontin as a likely contributing factor to the increased susceptibility of females to alcoholic liver disease. *J. Pathol.* 208, 473-485.
- Barak, V., Goike, H., Panaretakis, K.W., Einarsson, R., 2004. Clinical utility of cytokeratins as tumor markers. *Clin. Biochem.* 37, 529-540.

- Baraona, E., Abittan, C.S., Dohmen, K., Moretti, M., Pozzato, G., Chayes, Z.W., Schaefer, C., Lieber, C.S., 2001. Gender difference in pharmacokinetics of alcohol. *Alcohol Clin. Exp. Res.* 25, 502-507.
- Bardag-Gorce, F., Yuan, Q.X., Li, J., French, B.A., Fang, C., Ingelman-Sundberg, M., French, S.W., 2000. The effect of ethanol-induced cytochrome p4502E1 on the inhibition of proteasome activity by alcohol. *Biochem. Biophys. Res. Commun.* 279, 23-29.
- Bathgate, A.J., Simpson, K.J., 2002. Alcoholic fatty liver. In: Sherman, D.I.N., Preedy, V., Watson, R.R. (Eds.), *EtOH and the Liver: Mechanisms and Management*. Taylor and Francis, London, pp.3-20.
- Bautista, A.P., 2000. Impact of alcohol on the ability of Kupffer cells to produce chemokines and its role in alcoholic liver disease. *J. Gastroenterol. Hepatol.* 15, 349-356.
- Bautista, A.P., 2002. Neutrophilic infiltration in alcoholic hepatitis. *Alcohol* 27, 17-21.
- Bautista, A.P., Meszaros, K., Bojta, J., Spitzer, J.J., 1990. Superoxide anion generation in the liver during the early stage of endotoxemia in rats. *J. Leukoc. Biol.* 48, 123-128.
- Bautista, A.P., Spitzer, J.J., 1992. Acute ethanol intoxication stimulates superoxide anion production by in-situ perfused rat liver. *Hepatology* 15, 892-898.
- Baykov, I., Jarvelainen, H., Lindros, K., 2003. l-Cartinine alleviates alcohol-induced liver damage in rats: role of tumor necrosis factor-alpha. *Alcohol* 38, 400-406.

- Bayless, K.J., Meininger, G.A., Scholtz, J.M., Davis, G.E., 1998. Osteopontin is a ligand for the $\alpha 4 \beta 1$ integrin. *J. Cell. Sci.* 111, 1165-1174.
- Becker, J. E., Craig, A., 1994. Heat-shock proteins as molecular chaperones. *Eur. J. Biochem.* 219, 11-23.
- Bidder, M., Shao, J.S., Charlton-Kachigian, N., Loewy, A.P., Semenkovich, C.F., Towler, D.A., 2002. Osteopontin transcription in aortic vascular smooth muscle cells is controlled by glucose-regulated upstream stimulatory factor and activator protein-1 activities. *J. Biol. Chem.* 277, 44485-44496.
- Bilzer, M., Lauterburg, B.H., 1991. Effects of hypochlorous acid and chloramines on vascular resistance, cell integrity and biliary glutathione disulfide in the perfused rat liver: modulation by glutathione. *J. Hepatol.* 13, 84-89.
- Bonnelye, E., Vanacker, J.M., Dittmar, T., Begue, A., Desbiens, X., Denhardt, D.T., Aubin, J.E., Laudet, V., Fournier, B., 1997. The ERR-1 orphan receptor is a transcriptional activator expressed during bone development. *Mol. Endocrinol.* 11, 905-916.
- Boskey, A.L., Maresa, M., Ullrich, W., Doty, S.B., Butler, W.T., Ponce, C.W., 1993. Osteopontin-hydroxyapatite interactions in vitro: inhibition of hydroxyapatite formation and growth in a gelatin-gel. *Bone Miner.* 22, 147-159.
- Brudzynski, K., Martinez, V., Gupta, R.S., 1992. Immunocytochemical localization of heat-shock protein 60-related protein in β -cell secretory granules and its altered distribution in non-obese diabetic mice. *Diabetologia* 35, 316-324.

- Chan, J.R., Hyduk, S.J., Cybulsky, M.I., 2001. Chemoattractants induce a rapid and transient upregulation of monocyte alpha4 integrin affinity for vascular cell adhesion molecule 1 which mediated arrest: an early step in the process of emigration. *J. Exp. Med.* 193, 1149-1158.
- Chatterjee, M., 2001. Vitamin D and genomic stability. *Mutat. Res.* 475, 69-87.
- Christensen, B., Kazanecki, C.C., Peterson, T.E., Rittling, S.R., Denhardt, D.T., Sorensen, E.S., 2007. Cell type-specific post-translational modifications of mouse osteopontin are associated with different adhesive properties. *J. Biol. Chem.* 282, 19463-19472.
- Christensen, B., Nielsen, M.S., Haselmann, K.F., Peterson, T.E., Sorensen, E.S., 2005. Post-traslationally modified residues of native human osteopontin are located in clusters: identification of 36 phosphorylation and five O-glycosylation sites and their biological implications. *Biochem. J.* 390, 285-292.
- Chrostek, L., Jelski, W., Szmitkowski, M., Puchalski, Z., 2003. Gender-related differences in hepatic activity of alcohol dehydrogenase isoenzymes and aldehyde dehydrogenase in humans. *J. Clin. Lab. Anal.* 17, 93-96.
- Colantoni, A., Idilman, R., De Maria, N., La Paglia, N., Belmonte, J., Wezeman, F., Emanuele, N., Van Thiel, D.H., Kovacs E.J., Emanuele, M.A., 2003. Hepatic apoptosis and proliferartion in male and female rats fed alcohol: role of cytokines. *Alcohol Clin. Exp. Res.* 27, 1184-1189.
- Colantoni, A., La Paglia, N., De Maria, N., Emanuele, M.A., Emanuele, N.V., Idilman, R., Harig, J., VanThiel, D.H., 2000. Influence of sex hormonal status on alcohol-

- induced oxidative injury on male and female rat. *Alcohol Clin. Exp. Res.* 24, 1467-1473.
- Colell, A., Ruiz, C.G., Miranda, M., Ardite, E., Mari, M., Morales, A., Corrales, F., Kaplowitz, N., Fernandez-Checa, J.C., 1998. Selective glutathine depletion sensitizes hepatocytes to tumor necrosis factor. *Gastroenterology* 115, 1541-1551.
- Costet, P., Legendre, C., More, J., Edgar, A., Galtier, P., Pineau, T., 1998. Peroxisome proliferator-activated receptor alpha-isoform deficiency leads to progressive dyslipidemia with sexually dimorphic obesity and steatosis. *J. Biol. Chem.* 273, 29577-29585.
- Crabb, D.W., Galli, A., Fischer, M., You, M., 2004. Molecular mechanisms of alcoholic fatty liver: role of peroxisome proliferator-activated receptor alpha. *Alcohol* 34, 35-38.
- Craig, A.M., Denhardt, D.T., 1991. The murine gene encoding secreted phosphoprotein 1 (osteopontin): promoter structure, activity, and induction in vivo by estrogen and progesterone. *Gene* 100, 163-171.
- Dangerfield, J.P., Wang, S., Nourshargh, S., 2005. Blockade of α_6 integrin inhibits IL-1 β - but not TNF- α - induced neutrophil transmigration in vivo. *J. Leuko. Biol.* 77, 159-165.
- Das, R., Mahabeleshwar, G.H., Kundu, G.C., 2004. Osteopontin induces AP-1 mediated secretion of urokinase-type plasminogen activator through c-Src-dependent epidermal growth factor receptor transactivation in breast cancer cells. *J. Biol. Chem.* 279, 11051-11064.

- Day, C.P., James, O.F., 1998. Hepatic steatosis: innocent bystander or guilty party? *Hepatology* 27, 1463-1466.
- Deaciuc, I.V., D'Souza, N.B., Burikhanov, R., Lee, E.Y., Tarba, C.N., McClain, C.J., de Villiers, W.J., 2002. Epidermal growth factor protects the liver against alcohol-induced injury and sensitization to bacterial lipopolysaccharide. *Alcohol Clin. Exp. Res.* 26, 864-874.
- de la Hall, P., Lieber, C.S., DeCarli, L.M., French, S.W., Lindros, K.O., Jarvelainen, H., Bode, J.C., Parlesak, A., Bode, J.C., 2001. Models of alcoholic liver disease in rodents: a critical evaluation. *Alcohol Clin. Exp. Res.* 25, 254S-261S.
- Denhardt, D.T., Noda, M., 1998. Osteopontin expression and function: role in bone remodeling. *J. Cell Biochem. Suppl.* 30, 92-102.
- Denhardt, D.T., Giachelli, C., Rittling, S.R., 2001a. Role of osteopontin in cellular signaling and toxicant injury. *Annu. Rev. Pharmacol. Toxicol.* 41, 723-749.
- Denhardt, D.T., Noda, M., O'Regan, A.W., Pavlin, D., 2001b. Osteopontin as a means to cope with environmental insults: regulation of inflammation, tissue remodeling and cell survival. *J. Clin. Invest.* 107, 1055-1061.
- Di Luzio, N. R., 1966. A mechanism of the acute ethanol-induced fatty liver and the modification of liver injury by antioxidants. *Lab. Invest.* 15, 50-63.
- Diao, H., Kon, S., Iwabuchi, K., Kimura, C., Morimoto, J., Ito, D., Segawa, T., Maeda, M., Hamuro, J., Nakayama, T., Taniguchi, M., Yagita, H., Kaer, L.V., Onoe, K., Denhardt, D., Rittling, S., Uede, T., 2004. Osteopontin as a mediator of NKT cell function in T-cell mediated liver disease. *Immunity* 21, 539-550.

- Diehl, A.M., 2002. Liver disease in alcohol abusers: clinical perspective. *Alcohol* 27, 7-11.
- Ding, Z.M., Babensee, J.E., Simon, S.I., Perrard, J.L., Bullard, D.C., Dai, x.Y., Bromley, S.K., Dustin, M.L., Entman, M.L., Smith, C.W., Ballantyne, C.M., 1999. Relative contribution of LFA-1 and Mac-1 to neutrophils adhesion and migration. *J. Immunol.* 163, 5029-5038.
- Edenberg, H.J., Brown, C.J., Zhang, L., 1994. Alcohol dehydrogenases: molecular biology and gene regulation. *Alcohol Alcohol Suppl.* 2, 121-125.
- Eferl, R., Wagner, E.F., 2003. AP-1: a double-edged sword in tumorigenesis. *Nat. Rev. Cancer.* 3, 859-868.
- Ek-Rylander, B., Flores, M., Wendel, M., Heinegard, D., Andersson, G., 1994. Dephosphorylation of osteopontin and bone sialoprotein by osteoclastic tartrate-resistant acid phosphatase. Modelation of osteoclast adhesion in vitro. *J. Biol. Chem.* 269, 14853-14856.
- Ellis, R. J., vander Vies, S. M., 2001. Molecular chaperones. *Ann. Rev. Biochem.* 60, 321.
- El-Tanani, M., Fernig, D.G., Barraclough, R., Green, C., Rudland, P., 2001. Differential modulation of transcriptional activity of estrogen receptors by direct protein-protein interactions with the T cell factor family of transcriptional factors. *J. Biol. Chem.* 276, 41675-41682.

- El-Tanani, M., Platt-Higgins, A., Rudland, P.S., Campbell, F.C., 2004. Ets gene PEA3 cooperates with β -catenin-Lef-1 and c-Jun in regulation of osteopontin transcription. *J. Biol. Chem.* 279, G671-G677.
- Enomoto, N., Yamashina, S., Kono, H., Schemmer, P., Rivera, C.A., Enomoto, A., Nishiura, T., Nishimura, T., Brenner, D.A., Thurman, R.G., 1999. Development of a new, simple rat model of early alcohol-induced liver injury based on sensitization of Kupffer cells. *Hepatology* 29, 1680-1689.
- Entman, M.L., Youker, K., Shoji, T., Kukielka, G., Shappell, S.B., Taylor, A.A., Smith, C.W., 1992. Neutrophil induced oxidative injury of cardiac myocytes. A compartmented system requiring CD11b/CD18-ICAM-1 adherence. *J. Clin. Invest.* 90, 1335-1345.
- Essani, N.A., Fisher, M.A., Farhood, A., Manning, A.M., Smith, C.W., Jaeschke, H., 1995. Cytokine-induced upregulation of hepatic intercellular adhesion molecule-1 messenger RNA expression and its role in the pathophysiology of murine endotoxin shock and acute liver failure. *Hepatology* 21, 1632-1639.
- Essani, N.A., Fisher, M.A., Simons, C.A., Hoover, J.L., Farhood, A., Jaeschke, H., 1998. Increased P-selectin gene expression in the liver vasculature and its role in the pathophysiology of neutrophils-induced liver injury in murine endotoxin shock. *J. Leukoc. Biol.* 63, 288-296.
- Everett, L., Galli, A., Crabb, D., 2000. The role of hepatic peroxisome proliferator-activated receptors (PPARs) in health and disease. *Liver* 20, 191-199.
- Fink, A., 2001. Chaperone-mediated protein folding. *Physiol. Rev.* 79, 425.

- Fischer, M., You, M., Matsumoto, M., Crabb, D.W., 2003. Peroxisome proliferator-activated receptor alpha (PPARalpha) agonist treatment reverses PPARalpha dysfunction and abnormalities in hepatic lipid metabolism in ethanol-fed mice. *J. Biol. Chem.* 278, 27997–28004.
- Fisher, L.W., Torchia, D.A., Fohr, B., Young, M.F., Fedarko, N.S., 2001. Flexible structures of SIBLING proteins, bone sialoprotein and osteopontin. *Biochem. Biophys. Res. Commun.* 280, 460-465.
- French, S.W., 2002. Alcoholic hepatitis: inflammatory cell-mediated hepatocellular injury. *Alcohol* 27, 43-46.
- French, S.W., Miyamoto, K., Ohta, Y., Geoffrion, Y., 1988. Pathogenesis of experimental alcoholic liver disease in the rat. *Methods Achiev. Exp. Pathol.* 13, 181-207.
- Frezza, M., di Padova, C., Pozzato, G., Terpin, M., Barahona, E., Lieber, C.S., 1990. High blood alcohol levels in women. The role of decreased gastric alcohol dehydrogenase activity and first pass metabolism. *N. Engl. J. Med.* 322, 95-99.
- Fujii, H., Seki, S., Kobayashi, S., Kitada, T., Kawakita, N., Adachi, K., Tsutsui, H., Nakanishi, K., Fujiwara, H., Ikarashi, Y., Taniguchi, M., Kronenberg, M., Ikemoto, M., Nakajima, Y., Arakawa, T., Kaneda, K., 2005. A murine model of NKT cell-mediated liver injury induced by alpha-galactosylceramide/d-galactosamine. *Virchows. Arch.* 446, 663-673.
- Galambos, J.T., 1972. Natural history of alcoholic hepatitis. Histological changes. *Gastroenterology* 63, 1026–1035.

- Galli, A., Pinaire, J., Fischer, M., R. Dorris, R., Crabb, D.W., 2001. The transcriptional and DNA binding activity of peroxisome proliferator-activated receptor alpha is inhibited by ethanol metabolism. A novel mechanism for the development of ethanol-induced fatty liver. *J. Biol. Chem.* 276, 68–75.
- Gallucci, R.M., Sloan, D.K., O'Dell, S.J., Reinke, L.A., 2004. Differential expression of liver interleukin-6 receptor- α in female versus male ethanol-consuming rats. *Alcohol Clin. Exp. Res.* 28, 365-373.
- Gao, C., Guo, H., Mi, z., Wai, P.Y., Kuo, P.C., 2005. Transcriptional regulatory function of heterogeneous nuclear ribonucleoprotein-U and A/B in endotoxin-mediated macrophage expression of osteopontin. *J. Immunol.* 175, 523-530.
- Gegner, J.A., Ulevitch, R.J., Tobias, P.S., 1995. Lipopolysaccharide (LPS) signal transduction and clearance. Dual roles for LPS binding protein and membrane CD14. *J. Biol. Chem.* 270, 5320-5325.
- Giachelli, C.M., Lombardi, D., Johnson, R.J., Murry, C.E., Almeida, M., 1998. Evidence for a role of osteopontin in macrophage infiltration in response to pathological stimuli in vivo. *Am. J. Pathol.* 152, 353-358.
- Giachelli, C.M., Steitz, S., 2000. Osteopontin: a versatile regulator of inflammation and biomineralization. *Matrix Bio.* 19, 615-622.
- Goldman, J.M., Murr, A.S., Cooper, R.L., 2007. The rodent estrous cycle; characterization of vaginal cytology and its utility in toxicological studies. *Birth Defects. Res. B. Dev. Reprod. Toxicol.* 80, 84-97.

- Gonzalez, A.L., El-Bjeirami, W., West, J.L., McIntire, L.V., Smith, C.W., 2007. Transendothelial migration enhances integrin-dependent human neutrophils chemokinesis. *J. Leukoc. Biol.* 81, 686-695.
- Gonzalez-Quintela, A., Garcia, J., Campos, J., Perez, L.F., Alende, M.R., Otero, E., Abdulkader, I., Tome, S., 2006. Serum cytokeratins in alcoholic liver disease: contrasting levels of cytokeratin-18 and cytokeratin-19. *Alcohol* 38, 45-49.
- Green, P.M., Ludbrook, S.B., Miller, D.D., Hogan, C.M.T., Barry, S.T., 2001. Structural elements of the osteopontin SVVYGLR motif important for the interaction with alpha 4 integrins. *FEBS. Lett.* 503, 75-79.
- Gujral, J.S., Hinson, J.A., Farhood, A., Jaeschke, H., 2004. NADPH oxidase-derived oxidant stress is critical for neutrophils cytotoxicity during endotoxemia. *Am. J. Physiol. Gastrointest. Liver Physiol.* 287, G243-252.
- Guo, H., Cai, C.Q., Schroeder, R.A., Kuo, P.C., 2001. Osteopontin is a negative feedback regulator of nitric oxide synthesis in murine macrophages. *J. Immunol.* 166, 1079-1086.
- Habich, C., Baumgart, K., Kolb, H., Burkart, V., 2002. The receptor for heat shock protein 60 on macrophages in saturable, specific and distinct form receptors for other heat shock proteins. *J. Immunol.* 168, 569-76.
- Harrison, P.M., Arosio, P., 1996. The ferritins: molecular properties, iron storage function and cellular regulation. *Biochem. Biophys. Acta.* 1275, 161-203.
- Henderson, R.B., Lim, L.H., Tessier, P.A., Gavins, F.N., Mathies, M., Perretti, M., Hogg, N., 2001. The use of lymphocyte function-associated antigen (LFA)-1

deficient mice to determine the role of LFA-1, Mac-1 and alpha 4 integrin in the inflammatory response of neutrophils. *J. Exp. Med.* 194, 219-226.

Higashikawa, F., Eboshida, A., Yokosaki, Y., 2007. Enhanced biological activity of polymeric osteopontin. *FEBS. Lett.* 581, 2697-2701.

Ho, J.S., Buchweitz, J.P., Roth, R.A., Ganey, P.E., 1996. Identification of factors from rat neutrophils responsible for cytotoxicity to isolated hepatocytes. *J. Leukoc. Biol.* 59, 716-724.

Hoek, J.B., Pastorino, J.G., 2002. Ethanol, oxidative stress and cytokine-induced liver cell injury. *Alcohol* 27, 63-68.

Holoshitz, J., Klajman, A., Drucker, I., Lapidot, Z., Yaretzky, A., Frenkel, A., van Eden, W., Cohen, I.R., 1986. T lymphocytes of rheumatoid arthritis patients show augmented reactivity to a fraction of mycobacteria cross-reactive with cartilage. *Lancet.* 2, 305-309.

Horie, Y., Kato, S., Ohki, E., Tamai, H., Yamagishi, Y., Ishii, H., 2000. Hepatic microvascular dysfunction in endotoxemic rats after acute ethanol administration. *Alcoholism Clin. Exper. Res.* 24, 691-698.

Hoyer, J.R., Asplin, J.R., Otvos, L., 2001. Phosphorylated osteopontin peptides suppress crystallization by inhibiting the growth of calcium oxalate crystals. *Kidney, Int.* 60, 77-82.

Ibbotson, G.C., Doig, C., Kaur, J., Gill, V., Ostrovsky, L., Fairhead, T., Kubes, P., 2001. Functional Alpha 4 integrin: a newly identified pathway of neutrophil recruitment in critically ill septic patients. *Nat. Med.* 7, 465-470.

- Iimuro, Y., Frankenberg, M.V., Arteel, G.E., Bradford, B.U., Wall, C.A., Thurman, R.G., 1997. Female rats exhibit greater susceptibility to early alcohol-induced liver injury than males. *Am. J. Physiol. Gastrointest. Liver Physiol.* 272, G1186-G1194.
- Iimuro, Y., Ikejima, K., Rose, M.L., Bradford, B.U., Thurman, R.G., 1996. Nimodipine, a dihydropyridine-type calcium channel blocker, prevents alcoholic hepatitis caused by chronic intragastric ethanol exposure in the rat. *Hepatology* 24, 391-397.
- Ip, E., Farrell, G.C., Robertson, G., Hall, P., Kirsch, R., Leclercq, I., 2003. Central role of PPARalpha-dependent hepatic lipid turnover in dietary steatohepatitis in mice. *Hepatology* 38, 123-132.
- Jaeschke, H., 1997. Cellular adhesion molecules: regulation and functional significance in the pathogenesis of liver diseases. *Am. J. Physiol.* 273, G602-G611.
- Jaeschke, H., 2002. Neutrophil-mediated tissue injury in alcoholic hepatitis. *Alcohol* 27, 23-27.
- Jaeschke H., 2003. Molecular mechanisms of hepatic ischemia- reperfusion injury and preconditioning. *Am. J. Physiol. Gastrointest. Liver Physiol.* 284, G15-G26.
- Jaeschke, H., Farhood, A., Bautista, A.P., Spolarics, Z., Spitzer, J.J., 1993. Complement factor activates Kupffer cells and neutrophils during reperfusion after hepatic ischemia. *Am. J. Physiol.* 264, G801-G809.
- Jaeschke, H., Farhood, A., Smith, C.W., 1990. Neutrophils contribute to ischemia/reperfusion injury in rat liver in vivo. *FASEB J.* 4, 3355-3359.

- Jaeschke, H., Farhood, A., Smith, C.W., 1991. Neutrophil-induced liver cell injury in endotoxin shock is a CD11b/CD18-dependent mechanism. *Am. J. Physiol.* 253, H699–H703.
- Jaeschke, H., Fisher, M.A., Lawson, J.A., Simmons, C.A., Farhood, A., Jones, D.A., 1998. Activation of caspase 3(CPP32)-like proteases is essential for TNF-alpha-induced hepatic parenchyma cell apoptosis and neutrophils-mediated necrosis in a murine endotoxin shock model. *J. Immunol.* 160, 3480-3486.
- Jaeschke, H., Hasegawa, T., 2006. Role of neutrophils in acute inflammatory liver injury. *Liver Int.* 26, 912-919.
- Jayathilleke, A., Shaw, S., 1997. Stimulation of Monocyte Interleulin-8 by lipid peroxidation products: A mechanism for alcohol-induced liver injury. *Alcohol* 16, 119-123.
- Jezerski, M.K., Sohrabji, F., 2000. Region- and peptide-specific regulation of the neurotrophins by estrogen. *Brain. Res. Mol. Brain. Res.* 85, 77-84.
- Johnson, G.A., Spencer, T.E., Burghardt, R.C. Bazer, F.W., 1999. Ovine osteopontin: I. Cloning and expression of mRNA in the uterus during the peri-implantation period. *Biol. Reprod.* 61, 884–891.
- Johnson, J.L., Wallace, B.H., Mareen, C.D., Garves, D.B., Ferrer, T.J., Robertson, R.D., Cone, J.D., 2001. Intraperitoneal blood exacerbates the remote inflammatory responses to murine peritonitis. *J. Trauma.* 51, 253-260.

- Jones, B.M., Jones, M.K., 1976. Male and female intoxication levels for three alcohol doses or do women really get higher than men. *Alcohol Technical Report* 5, 544-583.
- Jono, S., Peinado, C., Giachelli, C.M., 2000. Phosphorylation of osteopontin is required for inhibition of vascular smooth muscle cell calcification. *J. Biol. Chem.* 275, 20197-20203.
- Julkunen, R.J., Tannenbaum, L., Barona, E., Lieber, C.S., 1985. First pass metabolism of ethanol: an important determinant of blood levels after alcohol consumption. *Alcohol* 2, 437-441.
- Kamimura, S., Gaal, K., Britton, R.S., Bacon, B.R., Triadafilopoulos, G., Tsukamoto, H., 1992. Increased 4-hydroxynonenal levels in experimental alcoholic liver disease: association of lipid peroxidation with liver fibrogenesis. *Hepatology* 16, 448-453.
- Karaa, A., Kamoun, W.S., Clemens, M.G., 2005. Chronic ethanol sensitizes the liver to endotoxin via effects on endothelial nitric oxide synthase regulation. *Shock* 24, 447-454.
- Kawashima, R., Mochida, S., Matsui, A., YouLuTuz, Y., Ishikawa, K., Toshima, K., Yamanobe, F., Inao, M., Ikeda, H., Ohno, A., Nagoshi, S., Uede, T., Fujiwara, K., 1999. Expression of osteopontin in Kupffer cells and hepatic macrophages and stellate cells in rat liver after carbon tetrachloride intoxication: A possible factor for macrophage migration into hepatic necrotic areas. *Biochem. Biophys. Res. Commun.* 256, 527-531.

- Keykhosravani, M., Doherty-Kirby, A., Zhang, C., Brewer, D., Goldberg, H.A., Hunter, G.K., Lajoie, G., 2005. Comprehensive identification of post-translational modification of rat bone osteopontin by mass soectrometry. *Biochemistry* 44, 6990-7003.
- Khare, S., Fichth, T.A., santos, R.L., Romano, J., Ficht, A.R., Zhang, S., grant, I.R., Libal, M., Hunter, D., Adams, L.G., 2004. Rapid and sensitive detection of *Mycobacterium avium* subsp. Paratuberculosis in bovine milk and feces by a combination of immunomagnetic bead separation-conventional PCR and real-time PCR. *J.Clin. Microbiol.* 42, 1075-1081.
- Kim, B.J., Hood, B.L., Aragon, R.A., Hardwick, J.P., Conrads, T.P., Veenstra, T.D., Song, B.J., 2006. Increased oxidation and degradation of cytosolic proteins in alcohol-exposed mouse liver and hepatoma cells. *Protemics.* 6, 1250-1260.
- Kitayama, J., Carr, M.W., Roth, S.J., Buccola, J., Springer, T.A., 1997. Contrasting responses of multiple chemotactic stimuli in transendothelial migration: heterologous desensitization in neutrophils and augmentation of migration in eosinophils. *J.Immunol.* 158, 2340-2349.
- Klassen, L.W., Tuma, D., Sorrell, M.F., Immune mechanisms of alcohol-induced liver disease. *Hepatology.* 22, 335-357.
- Kono, H., Nakagami, M., Rusyn, I., Connor, H.D., Stefanovic, B., Brenner, D.A., Mason, R.P., Arteel, G.E., Thurman, R.G., 2001b. Diphenyleneiodonium sulfate, an NADPH oxidase inhibitor, prevents early alcohol-induced liver injury in the rat. *Am. J. Physio. Gastrointest. Liver. Physiol.* 280, G1178-G1186.

- Kono, H., Uesugi, T., Froh, M., Rusyn, I., Bradford, B.U., Thurman, R.G., 2001a. ICAM-1 is involved in the mechanism of alcohol-induced liver injury: studies with knockout mice. *Am. J. Physiol. Gastrointest. Liver Physiol.* 280, G1289-G1295.
- Kono, H., Wheeler, M.D., Rusyn, I., Lin, M., Seabre, V., Rivera, C.A., Bradford, B.U., Forman, D.T., Thurman, R.G., 2000. Gender differences in early alcohol-induced liver injury: role of CD- 14, NF-kappaB, and TNF-alpha. *Am. J. Physiol. Gastrointest. Liver Physiol.* 278, G652-G661.
- Korourian, S., Hakkak, S., Ronis, R., Shelnutt, M.J., Waldron, S.R., Ingelman-Sundberg, J., Badger, T.M., 1999. Diet and risk of ethanol-induced hepatotoxicity: carbohydrate-fat relationships in rats. *Toxicol. Sci.* 47, 110–117.
- Kovalovich, K., Li, W., DeAngelis, R., Greenbaum, L.E., Ciliberto, G., Taub, R., 2001. Interlukin-6 protects against Fas-mediated death by establishing a critical level of anti-apoptotic hepatic proteins FLIP, Bcl-2 and Bcl-xL. *J. Biol.Chem.* 276, 26606-26613.
- Krause, S.W., Rehli, M., Kreutz, M., Schwarzfischer, L., Paulauskis, J.D., Andreesen, R., 1996. Differential screening identified genetic markers of monocyte to macrophage maturation. *J. Leukoc. Biol.* 60, 540-545.
- Kubes, P., Jutila, M., Payne, D., 1995. Therapeutic potencial of inhibiting leukocyte rolling in ischemia/reperfusion. *J. Clin. Invest.* 95, 2510-2519.

- Kwo, P.Y., Ramchandani, V.A., O'Connor, S., Amann, D., Carr, L.G., Sandrasegaran, K., Kopecky, K.K., Li, T.K., 1998. Gender differences in alcohol metabolism: relationship to liver volume and effect of adjusting for body mass. *Gastroenterology*. 115, 1552-1557.
- Lasa, M., Chang, P.L., Prince, C.W., Pinna, L.A., 1997. Phosphorylation of osteopontin by golgi apparatus casein kinase. *Biochem. Biophys. Res. Commun.* 240, 602-605.
- Lasa-Benito, M., Marin, O., Meggio, F., Pinna, L.A., 1996. Golgi apparatus mammary gland casein kinase: monitoring by a specific peptide substrate and definition of specificity determinants. *FEBS Lett.* 382, 149-152.
- Lawson, J.A., Burns, A.R., Farhood, A., Lynn Bajt, M., Collins, R.G., Smith, C.W., Jaeschke, H., 2000. Pathophysiologic importance of E- and L-selectin for neutrophil-induced liver injury during endotoxemia in mice. *Hepatology.* 32, 990-998.
- Lawson, J.A., Fisher, M.A., Simmons, C.A., Farhood, A., Jaeschke, H., 1998. Parenchymal cell apoptosis as a signal for sinusoidal sequestration and transendothelial migration of neutrophils in murine models of endotoxin and Fas-antibody-induced liver injury. *Hepatology* 28, 761-767.
- Leo, M.A., Lieber, C.S., 1983. Hepatic fibrosis alter long-term administration of ethanol and moderate vitamin A supplementation in the rat. *Hepatology* 3, 1-11.
- Lieber, C.S., 1963. Pathogenesis of hepatic steatosis. *Gastroenterology.* 45, 760-764.

- Lieber, C.S., 1990. Alcoholism: a disease of internal medicine. *J Stud Alcohol.* 51, 101-103.
- Lieber, C.S., 1993. Aetiology and pathogenesis of alcoholic liver disease. *Baillieres Clin. Gastroenterol.* 7, 581-608.
- Lieber, C.S., 2000. Hepatic, metabolic, and nutritional disorders of alcoholism: from pathogenesis to therapy. *Crit. Rev. Clin. Lab. Sci.* 37, 551-584.
- Lieber, C.S., 2005. Pathogenesis and treatment of alcoholic liver disease: progress over the last 50years. *Rock. Akad. Med. Bioalymst.* 50, 7-20.
- Lieber, C.S., DeCarli, L.M., 1970. Quantitative relationship between amount of dietary fat and severity of alcoholic fatty liver. *Am J Clin Nutr.* 23, 474-478.
- Lieber, C.S., DeCarli, L.M., 1982. The feeding of alcohol in liquid diets: two decades of application and 1982 update. *Alcohol.: Clin. Exp. Res.* 6, 523-531.
- Lieber, C.S., DeCarli, L.M., 1986. The feeding of ethanol in liquid diets. *Alcohol Clin Exp. Res.* 10, 550-553.
- Lieber, C.S., DeCarli, L.M., 1989. Liquid diet technique of ethanol administration: 1989 update. *Alcohol Alcohol* 24, 197-211.
- Loft, S., Olesen, K.L., Dossing, M., 1987. Increased susceptibility to liver disease in relation to alcohol consumption in women. *Scand. J. Gastroenterol.* 22, 1251-1256.
- Long, J.A., Evans, H.M., 1922. The oestrus cycle in the rat and its associated phenomena. *Mem. Univ. Calif.* 6, 1-143.

- Ma, X., Baraona, E., Goozner, B.G., Lieber, C.S., 1999. Gender differences in medium-chain dicarboxylic aciduria in alcoholic men and women. *Am. J. Med.* 106, 70-75.
- Ma, X., Baraona, E., Lieber, C.S., 1993. Alcohol consumption enhances fatty acid omega-oxidation, with a greater increase in male than in female rats. *Hepatology.* 18, 1247-1253.
- MacSween, R.N., Burt, A.D., 1986. Histological spectrum of alcoholic liver disease. *Semin Liver Dis.* 6, 21-232.
- Maher, J.J., 2002. Alcoholic steatosis and steatohepatitis. *Semin.Gastrointest. Dis.* 13, 31-39.
- Maher, J.J., Scott, M.K., Saito, J.M., Burton, M.C., 1997. Adenovirus-mediated expression of cytokine-induced neutrophils chemoattractant in rat liver induces a neutrophilic hepatitis. *Hepatology* 25, 624-630.
- Malyankar, U.M., Hanson, R., Schwartz, S.M., Ridall, A.L., Giachelli, C.M. 1999. Upstream stimulatory factor 1 regulates osteopontin expression in smooth muscle cells. *Exp. Cell Res.* 250, 535-547.
- Mandayam, S., Jamal, M. M., Morgam, T.R., 2004. Epidemiology of alcoholic liver disease. *Semin. Liver Dis.* 24, 217-232.
- Manevich, Y., Feinstein, S.I., Fisher, A.B., 2004. Activation of antioxidant enzyme 1-CYS peroxiredoxin requires glutathionylation mediated by heterodimerization with pi GST. *Proc. Natl. Acad. Sci. USA.* 101, 3780-3785.

- Mann, R.E., Suurvali, H.M., Smart, R.G. 2001. The relationship between alcohol use and mortality rates from injuries: a comparison of measures. *Am J Drug Alcohol Abuse* 27, 737-747.
- McGehee, R.E., Ronis, M.J., Badger, T.M., 1997. Regulation of the hepatic CYP2E1 gene during chronic alcohol exposure: lack of an ethanol response element in the proximal 5'-flanking sequence. *DNA Cell Biol.* 16, 725-736.
- Meggio, F., Pinna, L., A. 2003. One-thousand –and-one-substrates of protein kinase CK2? *Faseb J.* 17, 349-368.
- Moore, M.A., Gotoh, Y., Rafidi, K., Gerstenfels, L.D. 1991. Characterization of a cDNA for chicken osteopontin: expression during bone development, osteoblast differentiation, and tissue distribution. *Biochemistry* 30, 2501-2508.
- Murohisa, G., Kobayashi, Y., Kawasaki, T., Nakimura, S., Nakimura, H., 2002. Involvement of platelet activating factor in hepatic apoptosis and necrosis in chronic ethanol-fed rats given endotoxin. *Liver* 22, 394-403.
- Nagendra, A.R., Mickelson, J.K., Smith, C.W. 1997. CD18 integrin and CD54-dependent neutrophil adhesion to cytokine-stimulated human hepatocytes. *Am J Physiol.* 272, G408-G416.
- Nanji, A., 2002. Alcoholic liver disease. In: Zakim, D., Boyer, T.D. (Eds.), *A Text Book of Liver Disease*. Saunders, Philadelphia, pp. 839–922.
- Nanji, A.A., Jokelainen, K., Fotouhinia, M., Rahemtulla, A., Thomas, P., Tipoe, G.L., Su, G.L., Dannenberg, A.J., 2001. Increased severity of alcoholic liver injury in

- female rats: role of oxidative stress, endotoxin and chemokines. *Am. J. Physiol. Gastro. Liver Physiol.* 2001. 281, G1348-1356.
- Nanji, A.A., Su, G.L., Laposata, M., French, S.W., 2002. Pathogenesis of alcoholic liver disease-recent advances. *Alcohol Clin. Exp. Res.* 26, 731-736.
- Nanji, A. A., Tsukamoto, H., French, S.W., 1989. Relationship between fatty liver and subsequent development of necrosis, inflammation and fibrosis in experimental alcoholic liver disease. *Exp. Mol.Pathol.* 51, 141-148.
- National Institute on Alcohol Abuse and Alcoholism, 2001. *Alcohol Alert* 51, 1-2.
- Niemela, O. 2001. Distribution of ethanol-induced protein adducts in vivo: relationship to tissue injury. *Free Radic Biol Med.* 31, 1533-1538.
- Noda, M., Yoon, K., Prince, C.W., Butler, W.T., Rodan, G.A., 1988. Transcriptional regulation of osteopontin production in rat osteosarcoma cells by type beta transforming growth factor. *J.Biol. Chem.* 263, 13916-13921.
- Nystrom, T., Duner, P., Hultgarh-nilsson, A., 2007. A constitutive endogenous osteopontin production is important for macrophage function and differentiation. *Exp. Cell Res.* 313, 1149-1160.
- O'Regan, A., Berman, J.S., 2000, Osteopontin: a key cytokine in cell mediated and granulomatous inflammation. *Int. J. Exp. Pathol.* 81, 373-390.
- Okaya, T., Lentsch, A.B., 2003. Cytokine cascades and the hepatic inflammatory response to ischemia and reperfusion. *J. Invest. Surg.* 16, 141-147.
- Omary, M.B., Ku, N.O., Toivola, D.M., 2002. Keratins: guardians of the liver. *Hepatology* 35, 251-257.

- Oneta, C.M., Lieber, C.S., Li, J., Ruttimann, S., Schmid, B., Lattmann, J., Rosman, A.S., Seitz, H.K., 2002. Dynamics of cytochrome P4502E1 activity in man: induction by ethanol and disappearance during withdrawal phase. *J. Hepatol.* 36, 47-52.
- Otsu, M., Urade, R., Kito, M., Omura, F., Kikuchi, M., 1995. A possible role of ER-60 protease in the degradation of misfolded proteins in the endoplasmic reticulum. *J. Biol.Chem.* 270, 14958–14961.
- Pei, R.J., Danbara, N., Tsujita-Kyutoku, M., Yuri, T., Tsubara, A., 2004. Immunohistochemical profiles of Mallory body by a panel of anti-cytokeratin antibodies. *Med. Electron. Microsc.* 37, 114-118.
- Piec, I., Listrat, A., Alliot, J., Chambon, C., Taylor, R.G., Bechat, D., 2005. Differential proteome analysis of aging in rat skeletal muscle. *Faseb. J.* 19, 1143-1145.
- Pozzato, G., Moretti, M., Franzin, F., Croce, L.S., Lacchin, T., Benedetti, G., Stebel, M., Campanacci, L. 1995. Ethanol metabolism and aging: the role of “first pass metabolism: and gastric alcohol dehydrogenase activity. *J Gerontol A Biol Med Sci.* 50, B135-B141.
- Prince, C.W., Butler, W.T., 1987. 1,25-Dihydroxyvitamin D3 regulates the biosynthesis of osteopontin, a bone-derived cell attachment protein, in clonal osteoblast-like osteosarcoma cells. *Coll. Relat. Res.* 7, 305-313.
- Pugin, J., Schurer-Maly, C.C., Leturcq, D., Moriarty, A., Ulevitch, R.J., Tobias, P.S. 1993. Lipopolysaccharide activation of human endothelial and epithelial cells is mediated by lipopolysaccharide-binding protein and soluble CD14. *Proc Natl Acad Sci USA.* 90, 2744-2748.

- Qin, C., Baba, O., Butler, W.T. 2004. Post-translational modification of sibling proteins and their roles in osteogenesis and dentinogenesis. *Crit Rev Oral Biol Med.* 15, 126-136.
- Rajaratnam, K., Sykes, B., Kay, C., Dewald, B., Geiser, T., Baggiolini, M., Clark-Lewis, I., 1994. Neutrophil activation by monomeric interleukin-8. *Science.* 264, 90-92.
- Ramaiah, S.K., Jaeschke, H., 2007. Role of neutrophils in the pathogenesis of acute inflammatory liver injury. *Toxicol. Pathol.* 35, 757-766.
- Ramaiah, S.K., Rittling, S., 2007. Role of osteopontin in regulating hepatic inflammatory responses and toxic liver injury. *Expert. Opin. Drug. Metab. Toxicol.* 3, 519-526.
- Ramaiah, S.K., Rivera, C., Arteel, G.E., 2004. Early-phase Alcoholic Liver Disease: An update on animal models, pathology and pathogenesis. *Int. J. Toxicol.* 23, 217-231.
- Reddy, J.K., Hasimoto, T., 2001. Peroxisomal beta-oxidation and peroxisome proliferator-activated receptor alpha: an adaptive metabolic system. *Annu. Rev. Nutr.* 21, 193-230.
- Reinhardt, P.H., Ward, C.A., Giles, W.R., Kubes, P., 1997. Emigrated rat neutrophils adhere to cardiac myocytes via alpha 4 integrin. *Circ. Res.* 81, 196-201.
- Reinke, L.A., Lai, E.K., DuBose, C.M., McCay, P.B. 1987. Reactive free radical generation in vivo in heart and liver of ethanol-fed rats: correlation with radical formation in vitro. *Proc Natl Acad Sci USA.* 84, 9223-9227.

- Rittling, S.R., Denhardt, D.T., 1999. Osteopontin function in pathology: lessons from osteopontin-deficient mice. *Exp. Nephrol.* 7, 103-113.
- Rivera, C.A., Bradford, B.U., Seabra, V., Thurman, R.G., 1998. Role of endotoxin in the hypermetabolic state after acute ethanol exposure. *Am. J. Physiol.* 275, G1252-G1258.
- Roberts, B.J., Shoaf, S.E., Song, B.J., 1995. Rapid changes in cytochrome P4502E1 (CYP2E1) activity and other P450 isozymes following ethanol withdrawal in rats. *Biochem. Pharmacol.* 49, 1665-1673.
- Roll, F.J., Bissell, D.M., Perez, H.D., 1986. Human hepatocytes metabolizing ethanol generate a nonpolar chemotactic factor for human neutrophils. *Biochem. Biophys. Res. Commun.* 137, 688-694.
- Rose, R., Banerjee, A., Ramaiah, S.K., 2006. Calpain inhibition attenuates iNOS production and midzonal hepatic necrosis in a repeat dose model of endotoxemia in rats. *Toxicol. Pathol.* 34, 785-794.
- Rose, R., Banerjee, A., Ramaiah, S.K., 2007. Characterization of a lipopolysaccharide mediated neutrophilic hepatitis model in Sprague Dawley rats. *J. Appl. Toxicol.* 27, 602-611.
- Sahai, A., Malladi, P., Melin-Aldana, H., Green, R.M., Whittington, P.F., 2004. Upregulation of osteopontin expression is involved in the development of Nonalcoholic Steatohepatitis in a dietary murine model. *Am. J. Physiol. Gastrointest. Liver Physiol.* 287, G264-G273.

- Schenker, S., 1997. Medical consequences of alcohol abuse: is gender a factor? *Alcohol Clin. Exp. Res.* 21, 179-181.
- Schumann, R.R., Leong, S.R., Flaggs, G.W., Gray, P.W., Wright, S.D., Mathison, J.C., Tobias, P.S., Ulevitch, R.J., 1990. Structure and function of lipopolysaccharide binding protein. *Science.* 249, 1429-1431.
- Scott, M.J., Cheadle, W.G., Hoth, J.J., Peyton, J.C., Subbarao, K., Shao, W.H., Haribabu, B., 2004. Leukotriene B4 receptor (BLT-1) modulates Neutrophil influx into the peritoneum but not the lung and liver during surgically induced bacterial peritonitis in mice. *Clin. Diagn. Lab. Immunol.* 11, 936-941.
- Seitz, H.K., Egerer, G., Simanowski, U.A., Waldherr, R., Agarwal, D.P., Goedde, H.W., von Wartburg, J.P., 1993, Human gastric alcohol dehydrogenase activity: effect of age, sex and alcoholism. *Gut* 34, 1433-1437.
- Shang, T., Yednock, T., Issekutz, A.C. 1999. Alpha9beta1 integrin is expressed on human neutrophils and contributes to neutrophil migration through human lung and synovial fibroblast barriers. *J. Leukoc. Biol.* 66, 809-816.
- Shaw, S. E., Jayatilleke, E., Ross, W.A., Gordon, E.R., Lieber, S., 1981. Ethanol induced lipid peroxidation: Potentiation by long-term alcohol feeding and attenuation by methionine. *J. Lab Clin. Med.* 98, 417-424.
- Shevchuk, O., Baraona, E., Ma, X.L., Pignon, J.P., Lieber, C.S. 1991. Gender differenced in the response of hepatic fatty acids and cytosolic fatty acid-binding capacity to alcohol consumption in rats. *Proc. Soc. Exp. Biol. Med.* 198, 584-590.

- Shimano, H., Horton, J.D., Hammer, R.E., Shimomura, I., Brown, M.S., Glodstein, J.L., 1996. Overproduction of cholesterol and fatty acids causes massive liver enlargement in transgenic mice expressing truncated SREBP-1a. *J. Clin. Invest.* 98, 1575-1584.
- Shiraga, H., Min, W., Vandusen, W.J., Clayman, M.D., Miner, D., Terrell, C.H., Sherbotie, J.R., Foreman, J.W., Przysiecki, C., Nelson, E.G., Hoyer, J.R. 1992. Inhibition of calcium oxalate crystal growth in vitro by uropontin; Another member of the aspartic acid-rich protein superfamily. *Proc. Natl. Acad. Sci. USA.* 89, 426-430.
- Singh, R.P., Patarca, R., Schwartz, J., Singh, P., Cantor, H., 1990. Definition of a specific interaction between the early T lymphocyte activation (Eta-1) protein and murine macrophages in vitro and its effect upon macrophages in vivo. *J. Exp. Med.* 171, 1931-1942.
- Smith, L.L., Giachelli, C.M., 1998. Structural requirements for alpha 9 beta 1 mediated adhesion and migration to thrombin-cleaved osteopontin. *Exp. Cell. Res.* 242, 351-360.
- Sodek, J., Ganss, B., McKee, M.D., 2000. Osteopontin. *Crit. Rev. Oral. Biol. Med.* 11, 279-303.
- Sorensen, E.S., Hojrup, P., Petersen, T.E., 1995. Posttranslational modifications of bovine osteopontin: identification of twenty –eight phosphorylation and three O-glycosylation sites. *Protein Sci.* 4, 2040-2049.

- Spahr, L., Garcia, I., Bresson-Hadni, S., Rubbia-Brandt, L., Guler, R., Olleros, M., Chvatcko, Y., Hadenbue, A., 2004. Circulating concentrations of interleukin-18, interleukin 18 binding protein, and g-interferon in patients with alcoholic hepatitis. *Liver Int.* 24, 582-587.
- Spitzer, J.A., Zhang, P. Mayer, A.M., 1994. Functional characterization of peripheral circulating and liver recruited neutrophils in endotoxic rats. *J Leukoc. Biol.* 56, 66-173.
- Tacchini, L., Pogliaghi, G., Radice, L., Anzon, E., Bernelli-Zazzera, A., 1995. Differential activation of heat-shock and oxidation-specific stress genes in chemically induced oxidative stress. *Biochem. J.* 309, 453-459.
- Tamai, H., Horie, Y., Kato, S., Yokoyama, H., Ishii, H., 2002. Long-term ethanol feeding enhances susceptibility of the liver to orally administered lipopolysaccharides in rats. *Alcohol.: Clin. Exp. Res.* 26, 75S–80S.
- Teli, M.R., Day, C.P., Burt, A.D., Bennett, M.K., James, O.F.W., 1995. Determinants of progression to cirrhosis or fibrosis in pure alcoholic fatty liver. *Lancet* 346, 987–990.
- Tezuka, K., Sato, T., Kamoika, H., Nijweide, P.J., Tanaka, K., Matsuo, T., Ohta, M., Kurihara, N., Hakeda, Y., Kumegawa, M. 1992. Identification of osteopontin in isolated rabbit osteoclasts. *Biochem. Biophys. Res. Commun.* 186, 911-917.
- Thiele, G.M., Worrall, S., Tuma, D.J., Klassen, L.W., Wyatt, T.A., Nagata, N. 2001. The chemistry and biological effects of malondialdehyde-acetaldehyde adducts. *Alcohol Clin. Exp. Res.* 25, 218S-224S.

- Thurman, R.G., 1998. II. Alcoholic liver injury involves activation of Kupffer cells by endotoxin. *Am. J. Physiol.* 275, G605-611.
- Torti, F.M., Torti, S.V., 2002. Regulation of ferritin genes and protein. *Blood* 99, 3505-16.
- Torti, S.V., Kwak, E.L., Miller, S.C., Miller, L.L., Ringold, G.M., Muambo, K.B., Young, A.P., Torti, F.M., 1988. The molecular cloning and characterization of murine ferritin heavy chain, a tumor necrosis factor-inducible gene. *J. Biol. Chem.* 263, 12638-12644.
- Tsukamoto, H., French, S.W., Benson, N., Delgado, G, Rao, G.A., Larkin, E.C., Largman, C., 1985a. Severe and progressive steatosis and focal necrosis in rat liver induced by continuous intragastric infusion of ethanol and low fat diet. *Hepatology* 5, 224-232.
- Tsukamoto, H., French, S.W., Reidelberger, R.D., Largman, C., 1985b. Cyclical pattern of blood alcohol levels during continuous intragastric ethanol infusion in rats. *Alcohol Clin. Exp. Res.* 9, 31-37.
- Tsukamoto, H., 2007. Conceptual importance of identifying alcoholic liver disease as a lifestyle disease. *J. Gastroenterol.* 42, 603-609.
- Tuck, A.B., Chambers, A.F., Allan, A.L., 2007. Osteopontin overexpression in breast cancer: Knowledge gained and possible implication for clinical management. *J. Cell Biochem.* 102, 859-868.

- Uesugi, T., Yin, M., Bradford, B.U., Wheeler, M.D., Uesugi, T., Froh, M., Goyert, S.M., Thurman, R.G., 2001. Toll-like receptor 4 is involved in the mechanism of early alcohol-induced liver injury in mice. *Hepatology* 34, 101–108.
- Ulyanova, T., Priestley, G.V., Banerjee, E.R., Papayannopoulou, T., 2007. Unique and redundant roles of alpha4 and beta 2 integrins in kinetics of recruitment of lymphoid vs myeloid cell subsets to the inflamed peritoneum revealed by studies of genetically deficient mice. *Exp. Hematol.* 35, 1256-1265.
- VanEyken, P., 2000. Cytokeratin immunohistochemistry in liver histopathology. *Adv. Clin. Path.* 4, 201-211.
- Wada, T., McKee M.D., Steitz, S., Giachelli, C.M. 1999. Calcification of vascular smooth muscle cell cultures: inhibition by osteopontin. *Circ. Res.* 84, 166-178.
- Weber, G.F., Zawaideh, S., Hikita, S., Kumar, V.A., Cantor, H., Ashkar, S. 2002. Phosphorylation-dependent interaction of osteopontin with its receptors regulates macrophage migration and activation. *J. Leukoc. Biol.* 72, 752-761.
- Wei, Y., Miller, S.C., Tsuji, Y., Torti, S.V., Torti, F.M., 1990. Interlukin-1 induces ferritin heavy chain in human muscle cells. *Biochem. Biophys. Res Commun.* 169, 289-296.
- Wheeler, M.D., Kono, M.D., Yin, H., Nakagami, M., Uesugi, M., Arteel, G.E., Gabele, E., Rusyn, I., Yamashina, S., Froh, M., Adachi, Y., Iimuro, Y., Bradford, B.U., Smutney, O.M., Connor, H.D., Mason, R.P., Goyert, S.M., Peters, J.M., Gonzalez, F.J., Samulski, R.J., Thurman, R.G., 2001. The role of Kupffer cell

- oxidant production in early ethanol-induced liver disease. *Free Radical Biol. Med.* 31, 1544–1549.
- Wisse, E., 1977. Ultrastructure and function of Kupffer cells and other sinusoidal cells in the liver. *Med. Chir. Dig.* 6, 409-418.
- Witthaut, R., Farhood, A., Smith, C.W., Jaeschke, H., 1994. Complement and tumor necrosis factor- α contribute to Mac-1 (CD11b-CD18) up-regulation and systemic neutrophil activation during endotoxemia in vivo. *J. Leukoc. Biol.* 55, 105-111.
- Wong, J., Johnston, B., Lee, S.S., Bullard, D.C., Smith, C.W., Beaudet, A.L., Kubes, P., 1997. A minimal role for selectins in the recruitment of leukocytes in to the inflamed liver microvasculature. *J. Clin. Invest.* 99, 2782-2790.
- Xu, Q., Kleindienst, R., Waitz, W., Dietrich, H., Wick, G., 1993. Increased expression of heat shock protein 65 coincides with a population of infiltrating T lymphocytes in atherosclerotic lesions of rabbits specifically responding to heat shock protein 65. *J. Clin. Invest.* 91, 2693-2702.
- Yamaguchi, Y., Ohshiro, H., Nagao, Y., Odawara, K., Okabe, K., Hidaka, H., Ishihara, K., Uchino, S., Furuhashi, T., Yamada, S., Mori, K., Ogawa, M., 2000. Urinary trypsin inhibitor reduces C-X-C chemokine production in rat liver ischemia/reperfusion. *J. Surg. Res.* 94, 107-115.
- Yamamoto, N., Sakai, F., Kon, S., Morimoto, J., Kimura, C., Yamazaki, H., Okazaki, I., Seki, N., Fujii, T., Uede, T., 2003. Essential role of the cryptic epitope

- SLAYGLR within OPN in a murine model of rheumatoid arthritis. *J. Clin. Invest.* 112, 181-188.
- Yang, S.Q., Lin, H.Z., Lane, M.D., Clemens, M., Diehl, A.M., 1997. Obesity increases sensitivity to endotoxin liver injury: implications for the pathogenesis of steatohepatitis. *Proc. Natl. Acad. Sci. USA* 94, 2557–2562.
- Yao, V., McCauley, R., Cooper, D., Platell, C., Hall, J.C., 2003. Myeloperoxidase response to peritonitis in an experimental model. *ANZ. J. Surg.* 73, 1052-1056.
- Yin, M., Ikejima, K., Wheeler, M.D., Bradford, B.U., Seabra, V., Forman, D.T., Sato, N., Thurman, R.G., 2000. Estrogen is involved in early alcohol-induced liver injury in a rat enteral feeding model. *Hepatology* 31, 117-123.
- Yin, M., Wheeler, M.D., Kono, H., Bradford, B.U., Gallucci, R.M., Luster, M. I., Thurman, R.G., 1999. Essential role of tumor necrosis factor alpha in alcohol-induced liver injury in mice. *Gastroenterology* 117, 942-952.
- Yokosaki, Y., Matsuura, N., Sasaki, T., Murakami, I., Schneider, H., Higashiyama, S., Saitoh, Y., Yamakido, M., Taooka, Y., Sheppard, D., 1999. The integrin alpha 9 beta 1 binds to a novel recognition sequence (SVVLYGR) in the thrombin-cleaved amino-terminal fragment of osteopontin. *J. Biol. Chem.* 274, 36328-36334.
- Yokosaki, Y., Tanaka, K., Higashikawa, F., Yamashita, K., Eboshida, A. 2005. Distinct structural requirements for binding of the integrins $\alpha_v\beta_6$, $\alpha_v\beta_5$, $\alpha_5\beta_1$ and $\alpha_9\beta_1$ to osteopontin. *Matrix Biology* 24, 418-427.

- Zakhari, S. 2006. Overview: how is alcohol metabolized by the body? *Alcohol Res. Health* 29, 245-254.
- Zhao, P., Slattery, J.T., 2002. Effects of ethanol dose and ethanol withdrawal on rat liver mitochondrial glutathione: implication of potentiated acetaminophen toxicity in alcoholics. *Drug Metab. Dispos.* 30, 1413-1417.
- Zhu, R., Diem, S., Araujo, L.M., Aumeunier, A., Denizeau, J., Philadelphie, E., Damotte, D., Samson, M., Gourdy, P., Dy, M., Schenider, E., Herbelin, A. 2007. The Pro-Th1 cytokine IL-12 enhances IL-4 production by invariant NKT cells: relevance for T cell mediated hepatitis. *J. Immunol.* 178, 5435-5442.
- Ziol, M., Tepper, M., Lohez, M., Arcangeli, G., Ganne, N., Christidis, C., Trinchet, J.C., Beaugrand, M., Guillet, J.G., Guettier, C., 2001. Clinical and biological relevance of hepatocyte apoptosis in alcoholic hepatitis. *J. Hepatol.* 34, 254-260.

VITA

Name: Atrayee Banerjee

Permanent Address: Department of Toxicology
c/o Dr. Shashi K. Ramaiah
Texas A&M University, MS 4467
College Station, TX 77843-4467

Email Address: atrayee_15@rediffmail.com

Education: B.S. (Zoology), August 1997
University of Calcutta, India.

M.S. (Environmental Science), August 1999
University of Calcutta, India.

Ph.D. (Toxicology), May 2008
Texas A&M University, College Station, Texas.